The Effect of Obesogenic and Inflammatory Factors In Regulating Adipocytes Lipid Chaperone Proteins

Hazulin Mohd Radzuan, MBBS, MMDSc

Thesis submitted to

the University of Nottingham

for the degree of Doctor of Philosophy

October 2019

ABSTRACT

It has been increasingly clear that adipose tissue (AT) actively secretes lipid chaperone proteins (LCPs) into circulatory system without preceding tissue injury or cell death event. Among them are fatty acid binding protein 4 (FABP4), which is known to be increased in inflammatory condition despite of absence of any secretion-directed signals; and lipocalin2 (LCN2), which function is still debatable since there are evidences supporting its role in both pro and anti-inflammatory states.

This study intended to investigate (i)regulation of adipocyte-derived LCPs in response towards various cellular environment states (e.g. hyperglycaemia and hypoxia), (ii)changes in LCN2 and FABP4 signalling as a result of calcium flux, mediated by transient receptor potential vanilloid 4 (TRPV4) ligands; and (iii)interaction effect of multiple cellular factors upon adipocyte genes expression. These experiments involved cells treated in normal glucose media (NG), supplemented with 5.5mMol/l glucose; and high glucose media (HG), supplemented with 17.7mMol/l glucose.

Initially, this study showed cells that were given aforementioned media, displayed similar morphological appearance and cells viability in all groups. When concomitant obesogenic factors were applied, such as HG and hypoxia, LCN2 secretion mainly upregulated by the former factor, while FABP4 secretion was induced by the latter. Apart from these two factors, duration of adipogenesis also play a role in

regulating LCN2 and FABP4, since the former was released abundantly at early stage of adipogenesis and the latter was secreted by mature adipocytes.

Next, this study reported downregulation of LCN2 attributed by GSK101, a potent TRPV4 agonist, which manifests as pro-inflammatory mediator. Whereas inhibition of TRPV4 channel by HC067 caused reduction in FABP4 signalling. Chemical activation of TRPV4 channel may compromise adipocytes differentiation as evidence by reduced expression of *pparγ* and *pgc1a*. It is also presumed to induce inflammatory response due to high expression of *ccl2* in cells treated with GSK101.

Hence, the interaction of main effects of HG and TRPV4 treatments showed that these 2 factors concomitantly affects the regulation of LCN2. However, the latter was the main factor that influenced adipocyte genes expression such as *fabp4* and *pparγ*. Therefore, verifying the regulatory mechanism and interaction of factors that modify adipocyte-derived LCPs signalling could help us to understand its role in inflammatory response, whether it will further promote or suppress development of metabolic diseases.

We hypothesize that nuclear factor of activated T cell (NFAT) presumably play a role, either direct or indirectly, via an as yet unidentified mechanism in LCN2 and FABP4 regulation. Thus, extended research is required to further explore the means.

ACKNOWLEDGMENT

All praises to Allah for His blessing, on whom I ultimately depend for sustenance and guidance in completing this thesis.

My heartfelt gratitude goes to my supervisor, Assoc. Prof. Dr Andrew Bennett, who was abundantly helpful and offered invaluable support and encouragement throughout my PhD journey. My deepest appreciation also to Dr Mark Cole, my co-supervisors.

My sincere thanks to the members of FRAME laboratory, especially Monika, Nikki, Elke, Rachel, and also to Paul Smith, who rendered their help and timely assistance during my research. Special thanks to my colleagues: Razan, Rawan, Wafa, Amer, Tara, Fatima, Nada, Nahed, Robbie, Wichitra, Syeeda, Fadly and Noraihan for invaluable help and discussions. Special tribute also goes to my employer, International Islamic University Malaysia, to my sponsor, the Malaysia Ministry of Education, and also to the School of Life Sciences and SLIM Unit, University of Nottingham for the facilities and support. To those who indirectly contributed in this research, your kindness means a lot to me.

Finally, yet importantly, I would like to express my heartfelt thanks to my beloved parents for their blessings and prayers. To my soulmate and my children, thank you for your love, patience and encouragement. You all with your support, made this achievement joyful and an excellent experience for me.

TABLE OF CONTENT

LIST OF FIGURES

LIST OF TABLES

ABBREVIATIONS

ADMs	Adipocytes-derived microvesicles
Akt	Protein kinase B
ASCs	Adipocyte mesenchymal stem cells
AT	Adipose tissues
ATGL	Adipose triglyceride lipase
ATMs	Adipose tissue macrophages
BAT	Brown adipose tissue
BMDMs	Bone marrow–derived macrophages
BMI	Body mass index
CaMKK2	Calcium/calmodulin-dependent protein kinase II
C/EBP	CCAAT enhancer binding protein
ChREBP	Carbohydrate-responsive element-binding protein
CM	Conditioned media
CREB	cAMP response element-binding protein
DAG	Diacylglyceride
ER	Endoplasmic reticulum
EVs	Extracellular vesicles
FABPpm	Fatty acid binding protein plasma membrane
FABPs	Fatty acid binding proteins
FATP	Fatty acid transport protein
FAS	Fatty acid synthase
FBS	Fetal bovine serum
FetA	Fetuin A
FFAs	Free fatty acids
GAPDH	Glyceraldehyde-3-phosphate dehydrogenase
GLUT4	Glucose transporter 4
GPCRs	G-protein-coupled receptors
HFD	High fat diet
HG	High glucose
HIF	Hypoxic- induced factor
HSL	Hormone sensitive lipase
IFNγ	Interferon γ
IKK	IκB kinase
ILVs	Intraluminal vesicles
IL-1β	Interleukin 1β
IL-6	Interleukin 6
IRβ	Insulin receptor β-subunit
IRS-1	Insulin receptor substrate 1
JNK	c-Jun N-terminal kinases
LCN2	Lipocalin2
LCPs	Lipid chaperone proteins
LPL	Lipoprotein lipase
LPS	Lipopolysaccharides
MAG	Monoacylglyceride
MAP	Mitogen-activated protein
MCE	Mitotic clonal expansion

MCP1/CCL2	Monocyte chemoattractant protein 1/chemokine (C-C motif) ligand 2
MIP1α	Macrophage inflammatory protein 1-alpha
MSCs	Mesenchymal stem cells
MVBs	Multivesicular bodies
MVEs	Multivesicular endosomes
NFAT	Nuclear factor of activated T-cells
NF-κB	Nuclear factor kappa-light-chain-enhancer of activated B cells
NG	Normal glucose
OSA	Obstructive sleep apnea
PAI-1	Plasminogen activator inhibitor-1
PGC1α	Peroxisome proliferator-activated receptor gamma coactivator 1-alpha
PI-3	Phosphatidylinositol-3 kinase
PM	Plating media
Polr2	RNA polymerase II
PPARγ	Peroxisome proliferator-activated receptor-γ
Pref-1	Preadipocyte factor 1
qRT-PCR	Quantitative real-time polymerase chain reaction
RBC	Red blood cells
RBP4	Retinol binding protein 4
RIPA	Radio-ImmunoPrecipitation Assay buffer
ROS	Reactive oxygen species
SAT	Subcutaneous adipose tissue
SEM	Scanning electron microscopy
SFM	Serum free media
SOCE	Store operated calcium entry
STAT	Signal transducer and activator of transcription
SVF	Stromal vascular fraction
TCA	Trichloroacetic acid
TGs	Triglycerides
TLR4	Toll-like receptor 4
TNFα	Tumor necrosis factor α
TRP	Transient receptor potential
TRPVs	Transient receptor potential vanilloids
UCP1	Uncoupling protein-1
VAT	Visceral adipose tissue
v/v	volume/volume
WAT	White adipose tissue
wt	Wild type
w/v	weight/volume
$[Ca^{2+}]i$	Intracellular calcium
$[Ca^{2+}]e$	Extracellular calcium

DECLARATION

I hereby declare that this thesis is the result of my own investigations, except where otherwise stated. I also declare that it has not been previously or concurrently submitted as a whole for any other degrees, at this, or any other institutions. The work was carried out primarily in FRAME laboratory, School of Life Sciences, Queen's Medical Centre, University of Nottingham, United Kingdom.

Dr Hazulin Mohd Radzuan

CHAPTER 1: GENERAL INTRODUCTION

1) Introduction

Obesity is currently acknowledged as a pandemic and is linked with metabolic diseases, such as diabetes mellitus, atherosclerosis and cardiovascular disease (A. Xu et al., 2006). A chronic low grade inflammatory condition, known as meta-inflammation, which occurs in obese person as a result at least in part, of discordant release of biologically active molecules from adipocytes (Furuhashi et al., 2011).

Adipocytes are not only act as an energy storage component of the body, but also as an endocrine organ that produces bioactive substances to be secreted into the circulation such as adipokines and free fatty acids (FFAs). These substances include pro-inflammatory mediators such as tumor necrosis factor α (TNFα), interleukin 1β (IL-1β), and anti-inflammatory proteins, such as adiponectin (A. Xu et al., 2006). It is believed that adipose tissue hypertrophy leads to hypoxia, as oxygen and blood supply to cells are compromised due to increase tissue mass. This triggers changes in adipose tissue genes expression and up-regulation of inflammatory factors such as plasminogen activator inhibitor-1 (PAI-1) and interleukin 6 (IL-6) (Trayhurn, 2013).

Besides regulating the meta-inflammatory cascade through the above mediators, adipocyte-derived substances can also initiate intracellular insult, leading to endoplasmic reticulum (ER) stress, increased production of reactive oxygen species (ROS) by mitochondria, and expression of lipid chaperone proteins (LCPs), for example fatty acid binding proteins (FABPs) and fetuin (Furuhashi et al., 2011). Therefore, function of LCPs in fat metabolism is crucial in regulating inflammatory and metabolic response.

1.1) Fundamentals of Adipose Tissue

Adipose tissue (AT) is proven to play a role in regulating bodily function and metabolism by secreting adipokines/cytokines in endocrine, autocrine or paracrine manner, which are involved in inflammation, recruitment of immune cells, angiogenesis and remodelling of extracellular matrix (Greenberg & Obin, 2006; Sun, Kusminski, & Scherer, 2011). AT is known for its ability to over expand in size in order to store excess nutrient. Once its limit is surpassed, fats will accumulate and mound in other organs. This, in part, is believed to result in metabolic disruption in our body (Ravussin & Smith, 2002).

AT can be divided according to its colour and function; in which high number of mitochondria and blood supply give a brown hue to brown adipose tissue (BAT), which is important in thermogenesis. Whereas

white AT (WAT) mainly consists of lipids and acts as energy storage (Cinti, 2005). Energy storage in WAT is more efficient as compared to skeletal muscle since the former has substantial caloric value, whereas the latter stores mainly carbohydrate (Rezaee & Dashty, 2013).

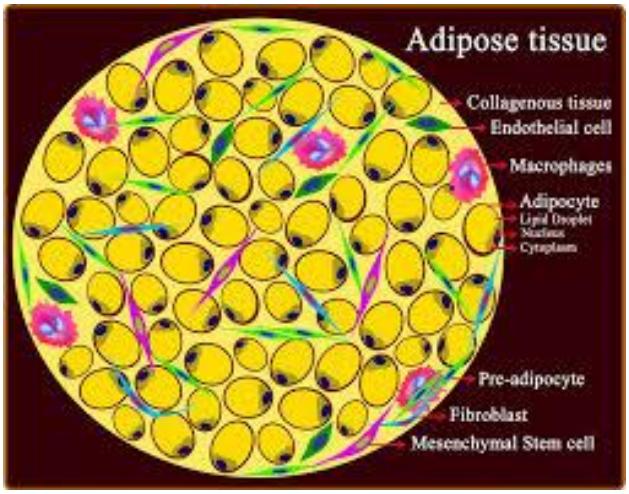

Figure 1.1: Adipocytes are the major constituent cells of adipose tissue (AT) and the main site for the storage and release of cytokines and chemokines. Preadipocytes are the most abundant cells and the linker between adipocytes (metabolic cells) and macrophages (immune cells). Lipid droplets (fat organelle) cannot be detected in preadipocytes. Other cells of AT are fibroblasts, mesenchymal stem cells and endothelial cells and each AT-cell has an important role in different pathways including the metabolic, coagulation and inflammatory systems [adapted from (Rezaee & Dashty, 2013)].

WAT is present in various depots such as subcutaneous, visceral (namely omental, retroperitoneal and epididymal fat pads) and ectopic such as intrahepatic and intramuscular fats (Wajchenberg, 2000). Mature white adipocytes dominate WAT; whereas stromal vascular fraction (SVF) occupies a small portion in WAT, although it can go up to 50% of total cellular content (see Figure 1.1). SVF

consists of adipose tissue matrix such as collagen and blood vessels, immune cells including macrophages and lymphocytes, as well as endothelial cells and adipocyte mesenchymal stem cells (ASCs) (Trayhurn, 2007). These cells can be parted from mature white adipocytes after incubation with collagenase and low speed centrifugation (Hausman, Park, & Hausman, 2008).

Apart from WAT and BAT, recent studies have discovered the presence of 'beige' or 'brite' adipocytes, formation of brown-in-white adipocytes population. Kleiner *et al*. in his study showed that fibroblast growth factor 21 (FGF21) significantly increased thermogenic gene expression, such as uncoupling protein 1 (UCP1), in BAT and in inguinal WAT (Kleiner et al., 2012). It is also reported that inguinal WAT from mice subjected to cold acclimation showed similar UCP1 protein density as compared to BAT (Shabalina et al., 2013). Others suggest that 'brite' adipocytes is a transitional condition whereby it can transform itself to either WAT or BAT (Giordano, Frontini, & Cinti, 2016). To date, it is unclear whether these observations signify its physiological role other than energy expenditure, hence extensive evaluation needed to be done.

1.1.1) Adipose tissue distribution

Among subcutaneous adipose tissue (SAT) and visceral adipose tissue (VAT), the former constitutes about 80% of total AT, whereas the latter comprises around 10% of total body fat (Arner, 2001). As the largest body fat storage, SAT has the ability to expand its size as a result of FFAs uptake from circulation, thus playing a protective role from metabolic complications. SAT is thought to have higher turnover rate, resulting in abundance of new adipocytes that presumably function more effectively, when compared to VAT, which comprises of more 'matured' adipocytes (Berry, Stenesen, Zeve, & Graff, 2013).

Known as peripheral adiposity, excess fat that has accumulated around thigh, hips and buttocks are believed to be benign as compared to central obesity, which is highly associated with metabolic and cardiovascular diseases, particularly as the extra fat is stored in visceral (Tan & Vidal-Puig, 2008). High level of FFAs in plasma of obese individuals is associated to the fact that VAT has higher lipolytic activities as compared to SAT, hence proving that accumulation of visceral fats is detrimental to bodily function. Adipokines secreted from VAT get direct access to hepatic system as it drained to portal system, causing harmful effects towards liver metabolism, especially in inflammatory state (Frayn, Karpe, Fielding, Macdonald, & Coppack, 2003).

Variation in adipokines secretion from each depot also shows distinct features that differentiates them from one another. For instance, raised leptin and adiponectin expression and secretion seen in SAT, while VAT significantly produces IL-6 and PAI-1 higher than its counterpart (Fontana, Eagon, Trujillo, Scherer, & Klein, 2007). Taking into account all of the above; low turnover rate of adipocytes, higher lipolytic activity, release of FFAs and inflammatory cytokines into circulation from VAT; results in accumulation of fat masses among other viscerae such as liver, heart, skeletal muscle, causing lipotoxicity and initiation of insulin resistance.

1.1.2) Lipogenesis and lipolysis

The energy reserve in adipocytes is stored in triglycerides (TGs) form and modulated by balance between lipogenesis and lipolysis (Coelho, Oliveira, & Fernandes, 2013). In energy surplus condition, uptake of lipids into adipocytes is initiated by lipoprotein lipase (LPL) by release of FFAs from chylomicron in capillary lumen, migrate through endothelial cells, and then enter adipocytes with assistance from fatty acid translocase (CD63) (Lindstad, 2010). Apart from CD63, other proposed mechanism is by passive diffusion and facilitated-transport system via fatty acid transporter protein, such as fatty acid transport protein (FATP) (Stahl, Gimeno, Tartaglia, & Lodish, 2001)

and fatty acid binding protein plasma membrane (FABPpm) (J. F. Glatz, Luiken, Van Bilsen, & Van Der Vusse, 2002).

It is said that during adipocytes differentiation, FATP1 and FATP4 are highly expressed, causing an increase in FAs uptake intracellularly by this mechanism (Stahl, Evans, Pattel, Hirsch, & Lodish, 2002). Besides that, increase translocation of these fatty acid transporters from intracellular membrane to plasma membrane are exerted by insulin, which further promote FAs uptake by adipocytes (Czech, 2002). Once they pass through adipocytes' plasma membrane, FABPs bind to FAs to facilitate their cytosolic transport in the cells as they are lipophilic in nature. This protein-ligand complex is carried within intracellular compartment or then converted to fatty acyl CoA and undergo β-oxidation in mitochondria (Beylot, 2014).

Other than lipids, glucose (a non-lipid precursor) is also used as a substrate in *de novo* lipogenesis (DNL), particularly in *in vitro* studies, whereby cells receive its nutrient via culture media (Collins et al., 2011). However, DNL mechanism in adipocytes, especially in human, remains elusive; unlike those reported in liver lipogenesis. It is believed that in liver, sterol regulatory element-binding protein 1c (SREBP-1c) and liver X receptor (LXR) stimulate activation of insulin, with concomitant presence of glucose, in inducing expression of lipogenic gene such as fatty acid synthase (FAS) (Beylot, 2014).

Glucose may also induce translocation of carbohydrate-responsive element-binding protein (ChREBP), a lipogenic transcription factor, into nucleus, probably by dephosphorylation of the phospho-Ser196 of ChREBP. As it enters nucleus, activation of ChREBP may lead to transcription of L-type pyruvate kinase (LPK), a regulatory enzyme of glycolysis and lipogenesis (Uyeda, Yamashita, & Kawaguchi, 2002). In adipocytes, increased ChREBP expression was previously documented, only to be induced by unphysiological, extreme level of glucose (He, Jiang, Wang, Levi, & Li, 2004).

Meanwhile, lipolysis which is represented by sequential hydrolysis of TGs to form diacylglycerol (DAG), followed by monoacylglycerol (MAG); with liberation of a FA at each step. In negative energy state, increased transcription of adipose triglyceride lipase (ATGL), an enzyme responsible in mobilizing TGs stores, is due to elevated glucocorticoids. While catecholamines binds to β-adrenergic receptors (β-AR), which caused activation of adenylate cyclase (AC) and leads to induction of cyclic AMP (cAMP) and protein kinase A (PKA) (Dinel, Kolditz, & Langin, 2010; Martin & Parton, 2006).

PKA phosphorylates perilipin, a lipid droplet-associated protein that is responsible in maintaining TGs storage in a single unilocular lipid droplets. It also phosphorylates hormone-sensitive lipase (HSL), allowing it to be translocated from cytosol into lipid droplet where it

can hydrolyse DAG. HSL acts as rate-limiting enzyme as it is subjected to reversible phosphorylation due to its responsiveness to hormones such as insulin and catecholamines (Brasaemle, 2007).

Other than these two hormones, adipose-specific phospholipase A_2 (AdPLA), a calcium-dependent PLA_2, is also involved in adiposity and lipolysis regulation (Duncan, Sarkadi-Nagy, Jaworski, Ahmadian, & Sul, 2008). Using *Adpla* null mice, lipolysis was more enhanced, relative to wild type (*wt)* mice, as evidence by increased TGs turnover. Given the inverse relationship between PLA activity and lipolysis in *Adpla* null mice, treatment of prostaglandin E_2 (PGE_2) able to suppress the latter and restore the level of cAMP comparable to *wt* mice (Jaworski et al., 2009).

As the result of lipolysis, FAs are released and bind to LCPs such as FABP4 for intracellular transport and cross plasma membrane into circulation. Glycerol, a byproduct of hydrolysis, is also secreted into systemic circulation for usage of other tissues, such as liver for gluconeogenesis, since glycerol kinase activity is very low in AT (Beylot, 2014).

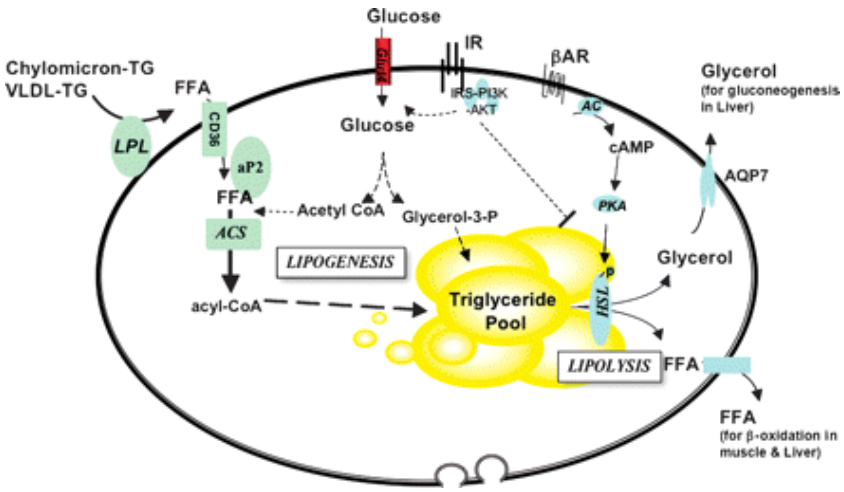

Figure 1.2: Lipid metabolism in adipocytes. Adipocytes are equipped with the biochemical machinery to function effectively as the body's fuel store. To do this, it must mediate lipogenesis [conversion of FFA to triglycerides (TG) for storage] and lipolysis (breakdown of triglycerides to FFA and glycerol). AC, adenylate cyclase; ACS, acyl-CoA synthase; AKT, AKR mouse thymoma viral proto-oncogene; AR, adrenergic receptor; HSL, hormone sensitive lipase; IR, insulin receptor; PI3K, phosphatidylinositol 3-kinase; PKA, protein kinase A [adapted from (Sethi & Vidal-Puig, 2007)].

1.1.3) Adipokine secretion

Adipokines are proteins secreted from and synthesised by AT. These cytokines are responsible in regulation of insulin, glucose homeostasis, energy balance, lipid metabolism and inflammation, to name a few (Blüher, 2016). Although numerous factors are released from AT, not all of them fulfil the features as adipokines, since response produced by other cells, such as macrophage within AT, although exhibits functional importance, prompt misperception and lack of secreted protein specificity (Trayhurn & Wood, 2004). Among all, leptin, adiponectin, IL-6, TNFα, resistin, adipsin and visfatin are

classified as true adipokines and are secreted by adipocytes primarily (Frühbeck, 2007).

Leptin is exclusively but not specifically expressed by AT since other tissues such as placenta, skeletal muscle and brain are also noted to exhibit it minimally (Coelho et al., 2013). It is responsible for energy reserve as it acts on hypothalamic cells and target tissue in regulating food intake and reduced energy utilization. Reduced concentration of leptin in a caloric restriction condition, followed by stimulation of appetite and decline in energy consumption, since its function mainly for conserving adequacy of energy (Kershaw & Flier, 2004). Meanwhile, adiponectin acts as anti-inflammatory molecule which exert insulin-sensitizing effect. High expression level of adiponectin showed to ameliorate insulin resistance and inversely correlates with TNFα expression (Kern, Di Gregorio, Lu, Rassouli, & Ranganathan, 2003). Its expression is upregulated by insulin growth factor-1 (IGF-1) and peroxisome proliferator-activated receptor gamma (PPARγ) agonist, while downregulated by glucocorticoids and inflammatory cytokine such as IL-6 (Kadowaki & Yamauchi, 2005).

Increased IL-6 and TNFα are consistently reported as associated with obesity. Increased IL-6 also mediates rise in C-reactive protein, an acute-phase protein, typically observed among obese individuals

(Fantuzzi, 2005). TNFα exhibits insulin sensitivity, causing impairment of insulin signalling via serine phosphorylation of insulin receptor (Gokhan S Hotamisligil, Murray, Choy, & Spiegelman, 1994).

Apart from the above examples, FABP4 recently is proposed as another novel adipokines. Role of FABP4 has been implicated in glucose and lipid metabolism, regulation of insulin and inflammation [as described in 1.3.1 (i)] (Kralisch & Fasshauer, 2013).

1.2) **Adipose Tissue in Insulin Signalling and Inflammation**

Mature adipocytes are thought to derive from ASCs that undergo adipogenesis, in which the cells committed into adipocytes lineage, forming a precursor cells known as preadipocytes. Preadipocytes differentiate into adipocytes after going through 4 phases, involving growth arrest, mitotic clonal expansion (MCE), early and terminal differentiation (Vigouroux, Caron-Debarle, Le Dour, Magré, & Capeau, 2011). These phases are regulated by interplay of various transcriptional factors such as PPARγ and CCAAT/enhancer binding protein (C/EBP) (Lefterova & Lazar, 2009). C/EBPβ involved in early stage of adipogenesis, since a study using 3T3-L1-*C/EBPβ* knockdown preadipocytes, did not undergo MCE and showed halted adipocytes differentiation (Y.-Y. Zhang et al., 2011). It is also responsible to induce PPARγ and C/EBPα that are essential in

regulating terminal adipocytes differentiation (Moseti, Regassa, & Kim, 2016).

Insulin plays a major role in lipid and carbohydrate metabolism. Normally, insulin binds to insulin receptor, causing tyrosine phosphorylation of insulin receptor substrate-1 (IRS-1). It then leads to activation of phosphatidylinositol-3 kinase (PI-3) and subsequently Akt (protein kinase B) (Laviola, Perrini, Cignarelli, & Giorgino, 2006). Akt signalling enhances adipogenic effect of insulin by promoting translocation of glucose transporter 4 (GLUT4) vesicles to plasma membrane, thus increasing glucose uptake from circulation into the cells (Watson, Kanzaki, & Pessin, 2004). Apart from that, Akt promotes SREBP-1 activation, which is involved in regulating adipogenesis and mediates FABP4 transcription (White & Stephens, 2010). Akt also stimulates FATPs translocation that play a role in facilitating FAs influx through cell membrane (Stahl et al., 2002).

Initially, expansion of AT mass is a physiological response to store excess nutrient. But, as it surpasses its threshold, adipocytes could not accommodate all FFAs from the increased amount of nutrient with concurrent release from liver and muscle (Schenk, Saberi, & Olefsky, 2008). Obesity results from increased AT mass by enlargement of adipocytes size, known as hypertrophy, and raised

in number of adipocytes, termed as hyperplasia. Subsequently it leads to raise in FFAs and TGs level intracellularly, exhibited as ER oxidative stress (Osborn & Olefsky, 2012). Concomitantly, it caused enlargement of adipocytes size, followed by hypoxia as oxygen and blood supply is compromised (Trayhurn & Wood, 2004). These changes not only prompt pro-inflammatory signalling including IκB kinase (IKK) and related kinases activation, they also impair insulin signalling as a result of IRS serine/threonine phosphorylation. Hypertrophied adipocytes also release high level of immune cells chemoattractant and inflammatory cytokines such as monocyte chemoattractant protein-1 (MCP-1/CCL2) and TNFα (Lee et al., 2008). CCL2 stimulates recruitment of AT macrophages (ATMs) via paracrine signalling as it induces influx of macrophage with increasing adiposity (Weisberg et al., 2003).

Apart from regulatory factors that have been aforementioned, adipocytes also secrete LCPs (loosely termed as adipokines as well), as a physiological response such as in adipogenesis, or pathological condition such as in metabolic diseases. There are still considerable gaps in our knowledge despite a great deal of data concerning the function of LCPs being generated in recent years. Given the well described link between metabolic diseases, obesity and inflammation; the role of LCPs in these regulations have become the subject of increased attention.

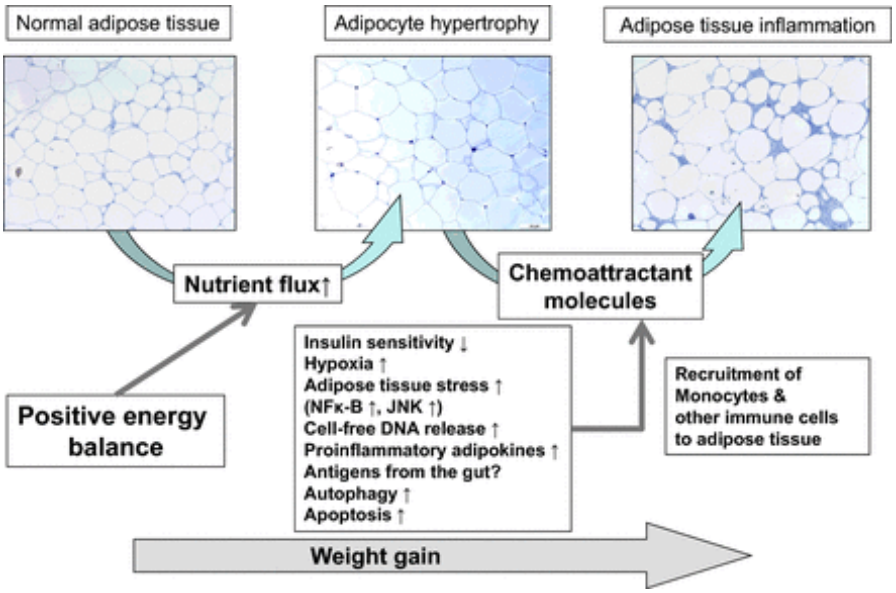

Figure 1.3: Potential mechanisms for the development of adipose tissue inflammation [adapted from (Blüher, 2016)].

1.3) **Lipid Chaperone Proteins**

Lipids play a crucial role in multiple biological cellular processes as they create a basic foundation in formation of biological membranes known as phospholipid, source of metabolic fuels production using long-chain fatty acid, and acts as signalling molecules through fatty acid compound. However, the hydrophobic nature of lipid impedes its distribution and transportation across the cells and cellular environment. To ensure bioavailability of lipids to carry out bodily functions, they need protein chaperone that is capable to reversely bind and form non-covalent bond to lipids in aqueous condition such as cytosolic region, interstitial space and blood plasma (J. F. C. Glatz, 2015).

Therefore, their intracellular and extracellular transport in cytoplasmic and interstitial compartments, are facilitated by specific LCPs, such as FABPs (Storch & Thumser, 2010). Apart from FABPs, other LCPs that are involved in insulin signalling and inflammation such as fetuin A (FetA) (Dasgupta et al., 2010), and lipocalin2 (LCN2) (Jun, Siddall, & Rosen, 2011).

1.3.1) Fatty acid binding proteins (FABPs)

FABPs are made up from 10 anti-parallel β strands, arranged into 2 nearly orthogonal β sheets, forming elliptical β barrel configuration (Figure 1.1). They are small cytoplasmic proteins of 14-15 kDa, which bind reversibly to hydrophobic ligands, such as saturated and unsaturated long chain fatty acids, eicosanoids and other lipids (Furuhashi et al., 2011).

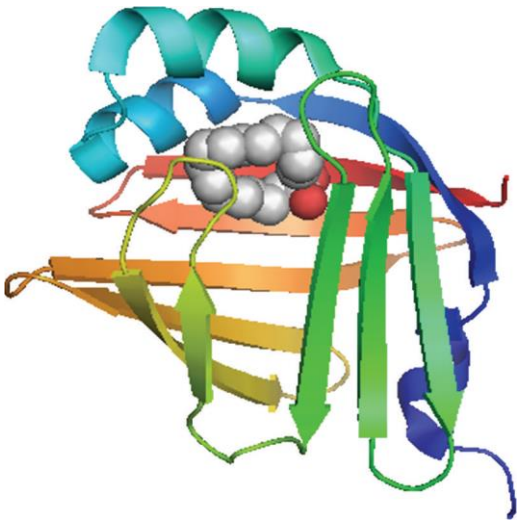

Figure 1.4: Human FABP4 binds to an endogenous fatty acid, palmitic acid, as a twisted U-shaped entity in the binding pocket [adapted from (Furuhashi, Ishimura, Ota, & Miura, 2011)].

FABPs augment transportation of FFAs to specific enzymes and cell organelles, such as the nucleus to modulate gene expression and FFAs in lipid droplets. They also facilitate oxidation of FFAs in mitochondria and peroxisomes, and re-esterification process in the ER (Krušinová & Pelikánová, 2008).

Formerly, FABPs mainly being investigated as cytoplasmic proteins and their presence in interstitium and plasma perceived as a results of cell death or tissue inflammation. This is showed by increased circulating heart-FABP (FABP3) in serum and urine among post-acute myocardiac infarction patients (Kleine, Glatz, Van Nieuwenhoven, & Van der Vusse, 1992; Tanaka, Hirota, Sohmiya, Nishimura, & Kawamura, 1991).

In contrast, current tenets proven that various tissues such as liver and adipose are capable in secreting LCPs actively into circulation. In the absence of cell injury, liver-FABP (FABP1) was noted to be present in biliary secretion (Foucaud et al., 1999). It is also reported that FABP4 is secreted in a regulated manner by adipocytes and macrophages without evidence of cell death (Cao et al., 2013; Schlottmann, Ehrhart-Bornstein, Wabitsch, Bornstein, & Lamounier-Zepter, 2014).

Table 1.1: Long-chain fatty acid–binding members of the fatty acid–binding protein (FABP) family [adapted from (Storch & Corsico, 2008)]

FABP type[a]	Gene	Expression	Phenotype of KO mice
LFABP	*fabp1*	Liver, small intestine, kidney	· Defective hepatic and intestinal β-oxidation · Decreased intestinal lipid secretion
IFABP	*fabp2*	Small intestine	· Elevated body weight · Elevated plasma TG
HFABP	*fabp3*	Cardiac and skeletal muscle, brain, ovaries, kidney, adrenals, lung, placenta, stomach, mammary tissue, testis	· Defective muscle fatty acid oxidation compensated by increased glucose utilization · No mammary phenotype
AFABP	*fabp4*	Adipocyte, macrophages	· Protection against diet-induced atherosclerosis · Modest decreases in plasma glucose, insulin · Double KO with KFABP shows strong protection against insulin insensitivity and hepatic steatosis
KFABP	*fabp5*	Epidermis, adipocyte, macrophages, tongue, mammary tissue, lung, testis, liver, brain, heart and skeletal muscle, retina, kidney	· Defective transepidermal water loss · Double KO with AFABP shows strong protection against insulin insensitivity and hepatic steatosis
BFABP	*fabp7*	Central nervous system, retina	Increased anxiety and fear memory
MFABP	*fabp8*	Peripheral nerve myelin	
TFABP	*fabp9*	Testis	

[a]Other members of the FABP gene family include FABP6, which encodes the ileal bile acid–binding protein, and genes for the cellular retinol-binding proteins and cellular retinoic acid–binding proteins, which bind retinol/retinaldehyde and retinoic acid, respectively.

Abbreviations: AFABP, adipocyte-type fatty acid–binding protein; BFABP, brain-type fatty acid–binding protein; HFABP, heart-type fatty acid–binding protein; IFABP, intestine-type fatty acid–binding protein; KFABP, keratinocyte-type fatty acid–binding protein; KO, knockout; LFABP, liver-type fatty acid–binding protein; MFABP, myelin-type fatty acid–binding protein; TFABP, testis-type fatty acid–binding protein.

i. FABP4 and FABP5 in insulin signalling and inflammation

Among all the types of FABPs that have been listed in Table 1.1, FABP4 and FABP5 are the main proteins of interest in studying insulin signalling in fat metabolism. These are the only 2 types of FAPBs that are expressed abundantly in adipocytes and macrophages and are also implicated in the pathogenesis of metabolic diseases (Furuhashi & Hotamisligil, 2008; Krušinová & Pelikánová, 2008; Makowski et al., 2001). FABP4 comprises about 1% of all soluble protein in AT, whereas FABP5 is 100-fold less prevalent. Meanwhile, the level of *fabp4* mRNA expression is noted to be much lower in THP-1 monocytes as compared to human adipocytes, since the former exhibit 10 000 fold less *fabp4* than the latter (Furuhashi et al., 2011).

Previously, in *in vivo* study, *fabp4*$^{-/-}$ mice showed modest improvement in insulin sensitivity despite of increased total body adiposity, as compared to wild type (*fabp4*$^{+/+}$) and heterozygous type (*fabp4*$^{+/-}$) mice after being fed with high fat diet (HFD). Lack of total protection from obesity was linked to the presence of FABP5, which was noted to be upregulated in order to counter the reduction of FABP4 action (G. S. Hotamisligil et al., 1996). This was supported by increased *fabp5* expression by 40 fold at the mRNA level and 13 fold at the protein level among *fabp4*$^{-/-}$ mice (Coe, Simpson, & Bernlohr, 1999). However, *fabp5* compensation in *fabp4* knockouts

was not observed in macrophages. But both cell types showed a reduction of inflammatory mediators such as IL-1β, IL-6 and TNFα in *fabp4*$^{-/-}$ mice (Makowski et al., 2001).

Besides *fabp4*$^{-/-}$ mice model, a targeted null mutation of *fabp5* mice model also was developed and investigated. It showed increased insulin sensitivity, evidenced by elevated GLUT4 protein level with decreased TGs and cholesterol level in plasma of obese *fabp5*$^{-/-}$ mice. Despite of low level of *fabp5* expression as compared to *fabp4* in adipocytes, *fabp5*$^{-/-}$ mice displayed significant systemic metabolic improvement. However, the author could not refute other cells affecting the final phenotype since there are other alternatives site (such as liver, heart, skeletal muscle) expressing *fabp5* that could be involved in influencing the outcome (Maeda et al., 2003).

Thus, a model of *fabp4/fabp5*-null mice was developed and investigated for its role in metabolic and inflammatory response. As a result, *fabp4/fabp5*-null mice demonstrated changes in tissue lipid profiles, such as protection against diet-induced obesity and hyperglycaemia, and improvement in insulin sensitivity (Maeda et al., 2005). It was evidenced by low concentration of blood glucose and insulin level among *fabp4/fabp5*-null mice, when compared to *wt* mice, after being given HFD. Therefore, FABP4 and FABP5 denote significant role in diet-induced obesity as their involvement is

essential in modulating lipid metabolism, inflammation and insulin sensitivity (Furuhashi & Hotamisligil, 2008).

Studies in *in vivo* and *in vitro* also have discovered a marked reduction in lipolysis in adipocytes taken from *fabp4* deficient mice (Coe et al., 1999; Scheja et al., 1999). The deletion of *fabp4,* causes reduction in adipocyte fatty acid release up to 2 to 3-fold. This indicates role of FABP4 in facilitating lipolysis by activating HSL, and further enhanced fatty acid efflux from adipocytes (Baar et al., 2005; Furuhashi, Saitoh, Shimamoto, & Miura, 2014).

Apart from gene deletion, inhibitors for FABP4 and FABP5 are used in order to study pharmacological method in attenuating insulin resistance. A promising study by Furuhashi *et al*. showed improvement of glucose level in *ob/ob* and diet-induced obese mice with the administration of BMS309403, a specific FABP4 inhibitor. This was evidenced by raised concentration of adiponectin associated with low level of insulin and TGs in plasma. Inflammatory chemokines such as CCL2, IL-1β and IL-6 demonstrated low expression level among *ob/ob* mice post-BMS309403 treatment as compared to vehicle-treated control (Furuhashi et al., 2007).

Besides that, the expression of LCPs is also investigated in humans. The *fabp4* expression noted to be higher in VAT as compared to SAT,

supported the evidence that FABP4 is partly responsible in development of metabolic diseases (Garin-Shkolnik, Rudich, Hotamisligil, & Rubinstein, 2014). FABP4 also abundantly present in patients' serum that are positively correlated with metabolic syndrome indicators, such as increased body mass index (BMI), waist to hip ratio, blood pressure and TGs level (A. Xu et al., 2006).

1.3.2) Lipocalin

Lipocalins are a family of diverse, small, mostly extracellular proteins that bind to small hydrophobic molecules such as retinoids, arachidonic acid and steroids. They are capable of binding to specific cell-surface receptors and forming soluble macromolecule complexes. Therefore, they are able to play a role in prostaglandin synthesis, immune response modulation and cancer cell interactions (I. K. M. Law et al., 2010).

ii. Lipocalin 2 (LCN2) in insulin signalling and inflammation

Apart from liver and bone, LCN2 is secreted by adipocytes and its production is raised abruptly in preadipocyte culture once they undergo differentiation. Many studies agreed upon the role of LCN2 in pro-inflammatory states since its expression is found to be increased with other pro-inflammatory cytokines such as IL-1β in human A549 (ATCC CCL-185) cells, and induced by TNFα in 3T3-L1 adipocytes (Cowland, Muta, & Borregaard, 2006; Yan et al., 2007).

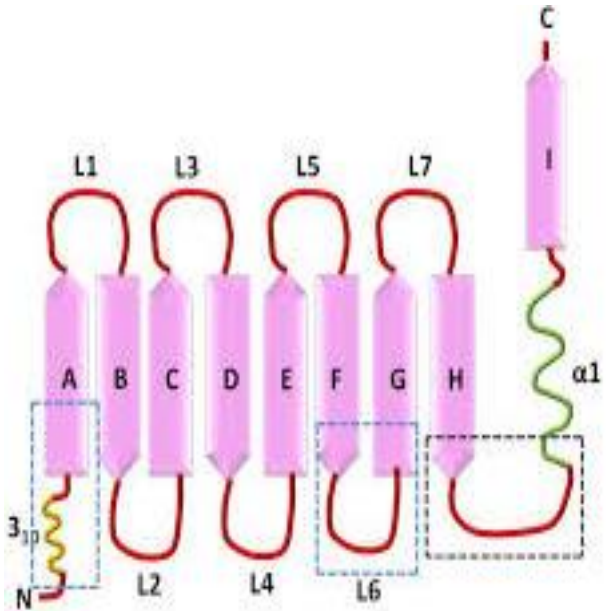

Figure 1.5: Lipocalin fold comprises of an N-terminal 3-10 helix followed by eight beta sheets (A-I). They are connected to an alpha helix (α1), which in turn connected to a C-terminal β sheet. The β sheets are connected by loops (L1-L7), forming the open end of the molecule. This eight-stranded hydrogen-bonded antiparallel β-barrel acts an internal ligand-binding site. The portion that are structurally conserved between different lipocalins shown by the blue boxes, while the region that shows significant conservation in amino acid sequence is indicated by the black box [adapted from (Chakraborty, Kaur, Tong, Batra, & Guha, 2011)].

Apart from that, increase in LCN2 secretion is also presumed to be associated with the development of metabolic disease and obesity. This has been observed by various experimental models and human studies (van Dam & Hu, 2007; Y. Wang et al., 2007; Yan et al., 2007). In human, concentration of LCN2 in serum is noted to be high, in correlation with patients that presented with risk factors for metabolic disease such as increased BMI, waist circumference and fat percentage. Wang *et al.* also discovered that the level of serum LCN2 is raised in *db/db* mouse due to increase expression in hepatocytes and AT (Y. Wang et al., 2007).

Interestingly, Zhang *et al.* reported a contrary result, demonstrating an anti-inflammatory effect of LCN2. They found that adipocytes treated with LCN2 significantly induced mRNA and protein expression of PPARγ and adiponectin. These findings were further supported by the attenuation of TNFα inhibitory effects upon PPARγ when the cells were co-treated with LCN2 (J. Zhang et al., 2008). Since TNFα is a strong inducer of nuclear factor kappa-light-chain-enhancer of activated B cells (NF-κB) signalling, LCN2 may reduce TNFα action via PPARγ regulation through direct or indirect antagonistic effects upon NF-κB pathway (J. Zhang et al., 2008).

Additionally, in HFD *lcn2*$^{-/-}$ mice, there is an increased in pro-inflammatory M1-macrophage marker expression and decreased in anti-inflammatory M2-macrophage markers observed in adipose and liver tissues. Guo *et al*. demonstrated in his study as shown in Fig. 1.6, *IL-1β* and *IL-6* were the target genes of NF-κB and signal transducer and activator of transcription 3 (STAT3) in bone marrow–derived macrophages (BMDMs). BMDMs treated with lipopolysaccharides (LPS) induced expression of both cytokines, and this stimulation was more enhanced in *lcn2*$^{-/-}$ BMDMs. This indicates that LCN2 plays an anti-inflammatory role through inhibition of the NF-κB-STAT3 feed-forward activation loop (Guo et al., 2014). Presumably, LCN2 could be the result of inflammatory response, but its action may have rate-limiting threshold.

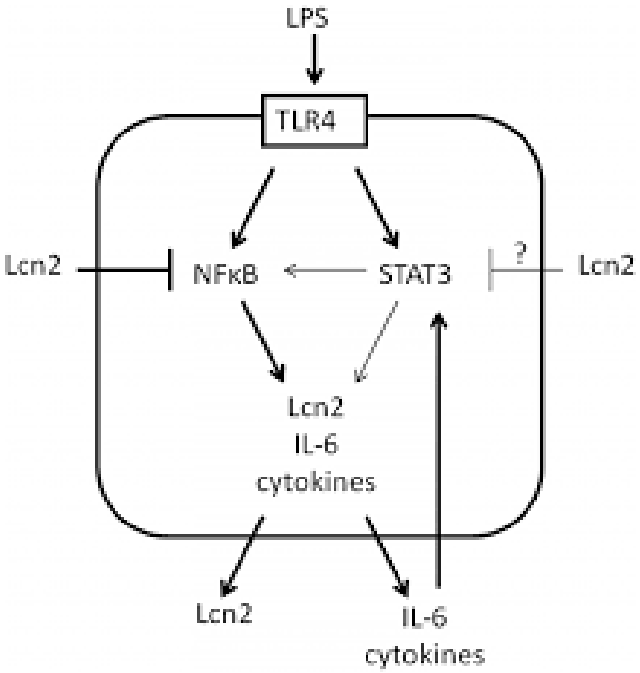

Figure 1.6: LCN2 role as a negative regulator in NF-κB-STAT3 loop activation in macrophages. Upon LPS stimulation, NF-κB is rapidly activated, leading to the secretion of cytokines. IL-6 and other molecules stimulate STAT3 phosphorylation which further activates NF-κB, forming a feed-forward loop. LCN2 breaks the NF-κB-STAT3 loop to limit the magnitude of inflammatory response by inhibiting NF-κB activation. In the absence of LCN2, NF-κB-STAT3 loop activation and inflammation will persist [adapted from (Guo, Jin, & Chen, 2014)].

1.3.3) Fetuins

Fetuins are glycoproteins belong to cystatin superfamily, that are mainly synthesized by hepatocytes. *fetA* and its recently identified fetuin family member, fetuin B (*fetB*), were noted to be closely linked at the genomic level (Denecke et al., 2003). Extensive research has been conducted to explore the functions of fetuins in metabolism, such as their role in systemic inflammation and regulation of insulin signalling (Mori, Emoto, & Inaba, 2011).

iii. Fetuin A (fetA) in insulin signalling and inflammation

Initially, it was presumed that there was a direct link between FFAs and AT inflammation through activation of toll-like receptor 4 (TLR4), leading to insulin resistance (Nguyen et al., 2007). However, a recent study showed that FFAs needs LCPs to allow direct interaction with TLR4. FetA is believed to affect inflammation by acting as an endogenous ligand for TLR4. It has been shown that FetA-TLR4 interaction leads to a raise *IL-6*, *tnfa* and *tlr4* expression levels in adipocytes of diabetic patients (Pal et al., 2012).

FetA production also noted to be increased in diabetic obese patients and its secretion could be stimulated by FAs via activation of NF-κB pathway (Dasgupta et al., 2010; Stefan et al., 2008). In this study, HepG2 cells were treated with palmitate, causing increased secretion of FetA. When HepG2 cells were given inhibitors of NF-κB signalling, the effect of palmitate-induced FetA secretion was reduced (Dasgupta et al., 2010).

Most studies done in relation to FetA revealed that this protein is secreted by hepatocytes, but Chatterjee *et al.* demonstrated alternative sites of tissue expression. They have shown that there were no significant changes in the level of circulating FetA in partial hepatectomized HFD mice, supporting their hypothesis that

adipocytes may be the source of FetA secretion. Increased circulating FAs may stimulate the expression of FetA by adipocytes, thus may then act as a chemoattractant for macrophages to be recruited into AT. It has been suggested that FetA is responsible for polarization of M2 anti-inflammatory ATMs into M1 pro-inflammatory (Chatterjee et al., 2013).

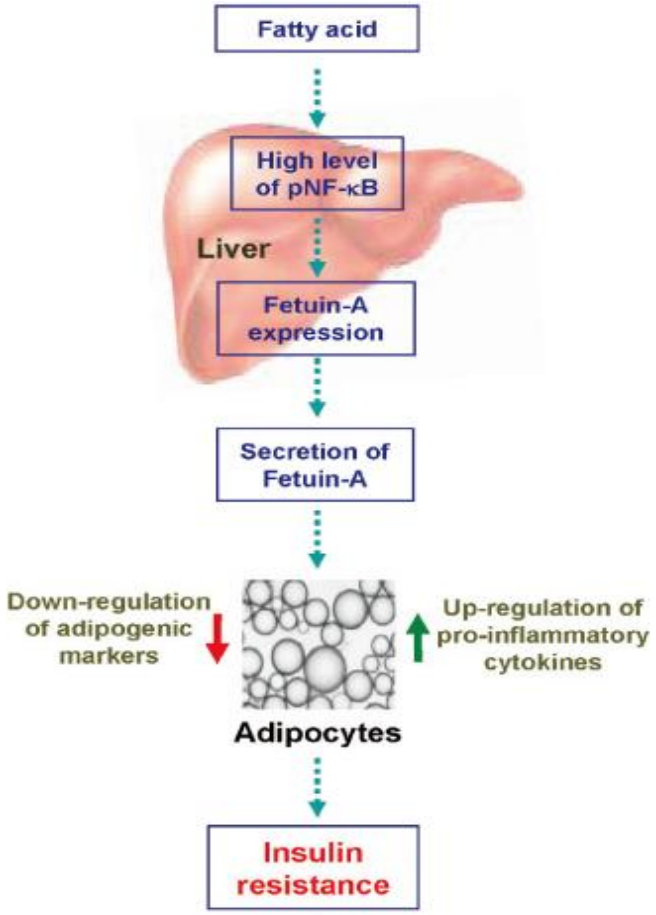

Figure 1.7: Fatty acid induced expression of *fetA* is mediated through NF-κB. Increased of pNF-κB level can enhance the expression of *fetA*. Since FetA is a secretory protein, it immediately released into the circulation and reaches adipocytes. This causes adipocyte dysfunction as determined by increased production of inflammatory cytokines and suppression of adipogenic factors, leading to insulin resistance [adapted from (Bhattacharya, Kundu, Dasgupta, & Bhattacharya, 2012)].

1.4) **Calcium-induced adipocytes LCPs signalling**

Calcium signalling is important as all cell types and tissues requires calcium to survive or perform cellular activities, such as muscle contraction (Kuo & Ehrlich, 2015), neuron excitability (Dunn, Hill-Eubanks, Liedtke, & Nelson, 2013) and bone metabolism (van der Eerden et al., 2016). There are many facets of calcium modulation within the cells, including store-operated calcium entry (SOCE) (Hogan & Rao, 2015), sequestration of calcium into intracellular store using sarco/endoplasmic reticulum Ca^{2+}-ATPase (SERCA) or mitochondrial calcium (MiCa), calcium binding protein (Clapham, 2007) and phospholipase C pathway (PLC) (Horowitz et al., 2005).

Ligand-gated channel, such as transient receptor potential (TRP), is a transmembrane protein complex that allows selected ion to flow through its channel upon activation by its stimuli. Mammalian TRP is classified into six subgroups according to its amino acid sequence homology. One of the subgroups is TRPVs, which consists of TRPV1 to 6.

As a member of vanilloid family of TRP cation channel superfamily, TRPV4 is activated by diverse factors, including moderate heat (24-37ºC), low pH, cell swelling, endogenous and exogenous chemical ligands (such as anandamide, arachidonic acid and bisandrographolide A from Indian herbal plant), and synthetic

ligands (such as GSK1016790A and RN-1734) (Nilius & Voets, 2013). As compared to sodium, calcium permeation is six times higher via this channel (Voets et al., 2002). Hence, one of many ways, it maintains calcium homeostasis since calcium ion is known as the second messenger that facilitates intracellular signal transduction for the cell to respond accordingly.

TRPV4 is broadly expressed by many tissues such as lung (J. Li et al., 2011), skin (Sokabe, Fukumi-Tominaga, Yonemura, Mizuno, & Tominaga, 2010), bone (Masuyama et al., 2008), urinary bladder (Everaerts et al., 2010), intestine (D'Aldebert et al., 2011) and pancreas (Casas, Novials, Reimann, Gomis, & Gribble, 2008); signifying its contribution in systemic processes. Several studies have shown the association of TRPV4 to different diseases that affects multiple tissues (Colsoul, Nilius, Vennekens, & Allergy, 2009; H.-X. Deng et al., 2010; Rock et al., 2008), but not many of them have demonstrated a direct relationship between TRPV4 ligands towards LCPs that involved in inflammation or metabolic diseases.

Involvement of calcium in regulating FABP4, which is also known as biomarker of obesity and metabolic syndrome, has been reported elsewhere. Adipocytes treated with ionomycin, an ionophore that increases $[Ca^{2+}]i$, displayed elevation of FABP4 secretion. Concomitantly, adiponectin secretion is unaffected by the same

treatment, indicating that FABP4 release is an active response towards raised cytosolic calcium, rather than cell damage (Kralisch et al., 2014). High FABP4 secretion is also shown to be linked to raised cytosolic calcium, rather than as a result of an increase of gene expression, as there is no upregulation of *fabp4* mRNA expression despite of increase in FABP4 secretion (Schlottmann et al., 2014).

To date, raise in LCN2 secretion modulated by calcium signalling in adipocytes is not reported extensively. Additionally, the effects of TRPV4 in promoting calcium flux in adipocytes, which subsequently modulates adipocytes-derived LCPs secretion was also not discussed elsewhere.

1.5) **Exosome-mediated secretion**

Previously, metabolic homeostasis between local and distant cellular target facilitated by hormones and metabolites. However, this multidirectional interaction becomes dysregulated in pathological states, including obesity and inflammation. Therefore, over the last few decades, the role of extracellular vesicles (EVs) in intercellular communication gained great attention, particularly exosome (Lobb et al., 2015).

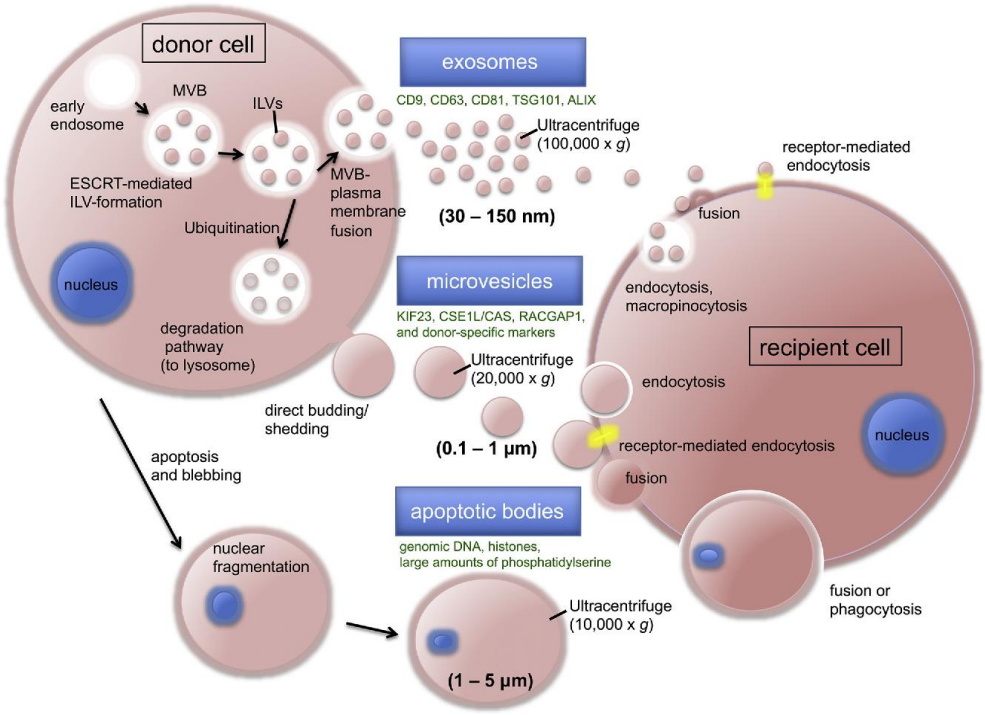

Figure 1.8: Three types of extracellular vesicles (EVs). Exosomes form in structures called multivesicular bodies (MVBs). Exosomes form inside of MVBs knowns as intraluminal vesicles (ILVs). Microvesicles (MVs) are released directly from the plasma membrane (direct shedding). Apoptotic bodies are the result of apoptosis-driven cell fragmentation, containing genomic DNA and histones. Once released into the extracellular space, EVs can cause activation of cell signaling at the surface or regulation of molecules inside the recipient cell. Recipient cells uptake vesicles via fusion, endocytosis of all types, including macropinocytosis and receptor-mediated endocytosis [adapted from (Sadovska, Eglitis, & Line, 2015)].

Exosome is a result from inward budding of multivesicular bodies (MVBs) from endosomal membrane, leads to invagination of various sizes of small vesicles to form intraluminal vesicles (ILVs), and subsequently results in late endosomes or multivesicular endosomes (MVEs). These MVEs are either fused with lysosomes or plasma membrane and cause the release of exosome extracellularly. These nano-sized vesicles measuring between 40–100nm and they are

capable in initiating physiological or pathological intercellular cross-talk as they contain DNAs, RNAs, mRNAs, miRNA, lipids and proteins (Raposo & Stoorvogel, 2013).

There are various cell types that secrete exosomes during physiological and pathological state, such as neurons (Chivet, Hemming, Fraboulet, & Sadoul, 2012), mast cells (Laulagnier et al., 2004) and cancer cells (Beach, Zhang, Ratajczak, & Kakar, 2014). It is also detected in blood (Baranyai et al., 2015), breast milk (W. Qin et al., 2016) and saliva (Gallo, Tandon, Alevizos, & Illei, 2012).

Adipocytes also known to secrete EVs, including exosome (commonly termed as small EVs) as reported by others (Sarah C Ferrante et al., 2015; J. Jin et al., 2019; Pan et al., 2019; H. Zhao et al., 2018). Conditioned media from 3T3-L1 cells was analysed and found that proteins such as CD63, CD9, CD81 and Alix were the exosomal marker in small EVs fraction, while large EVs (also known as shed MVs) were significantly enriched with caveolin-1 and flotillin-1 (Durcin et al., 2017). As FAs content in exosome was noted to be increased as adipogenesis advances, the content of adiponectin was also raised, in contrast to FABP4 level (Connolly et al., 2015).

Meanwhile, study on LCN2 in adipocyte-secreted exosome is yet to be establish, in contrast to other lipocalin family such as retinol-

binding protein 4 (RBP4). RBP4 was discovered in exosome secreted by *ob*/*ob* mice AT and it promoted activation of macrophage by stimulating the release of IL-6 and TNFα in a TLR4 dependent manner (Z.-b. Deng, Poliakov, Hardy, Clements, Liu, Liu, Wang, Xiang, Zhang, Zhuang, et al., 2009).

Due to its function as potential carrier, exosomes can be manipulated for medical purposes, such as incorporating anti-inflammatory drugs (such as doxorubicin) into purified exosomes for *in vivo* and *in vitro* usage (Lai, Yeo, Tan, & Lim, 2013; Yang, Chen, Zhang, Zhao, & Zhong, 2015). In addition, Zhuang et al. also has revealed the role of exosome in dispensing anti-inflammatory drug intranasally to the brain (Zhuang et al., 2011). By understanding how cellular milieu can influence adipocyte LCPs regulation, it can further extend their potential in therapeutic field as they are being carried by biological vectors of cellular communication and delivered to target cells or organs.

1.6) General Aims of the Research

The aims of this research were:

1. To establish a primary rat adipocytes culture model that can optimally survive and function in NG and HG media

2. To determine the pattern of LCPs signalling and formation of exosome in cultured primary rat adipocytes at different duration of adipogenesis
3. To determine the effects of obesogenic and inflammatory culture conditions (e.g: hypoxia and hyperglycaemia) on adipocyte LCPs expression and secretion
4. To determine the effects of calcium flux following TRPV4 ligands treatment on adipocyte-derived LCPs signalling
5. To verify the interaction effect of multiple independent factors (e.g: hyperglycaemia and TRPV4 ligands) towards adipocyte genes expression

CHAPTER 2: MATERIALS AND METHODS

2) Chemicals and reagents

Table 2.1: Chemicals and reagents used in this work

Chemicals/Reagents	Catalogue no.	Source
1) Cell culture		
HEPES	H4034	Sigma-Aldrich
NaCl	S7653	Sigma-Aldrich
KCl	P9641	Sigma-Aldrich
D-glucose	G8270	Sigma-Aldrich
Bovine serum albumin (BSA)	A6003	Sigma-Aldrich
$CaCl_2$ anhydrous	C4901	Sigma-Aldrich
Collagenase NB 4G	S1746503	Serva
NH_4Cl	A9434	Sigma-Aldrich
$KHCO_3$	237205	Sigma-Aldrich
EDTA	EDS	Sigma-Aldrich
Trypan blue solution	T8154	Sigma-Aldrich
3,3',5-Triiodo-L-thyronine sodium salt (T_3)	T5516	Sigma-Aldrich
Transferrin	T1428	Sigma-Aldrich
Sodium selenite	S9133	Sigma-Aldrich
Dulbecco's Modified Eagle's Medium/Nutrient Mixture F12 Ham	D6421	Sigma-Aldrich
Dulbecco's Modified Eagle's Medium - low glucose	D5546	Sigma-Aldrich
Nutrient mixture F10 Ham	N6013	Sigma-Aldrich
L-Glutamine	G7513	Sigma-Aldrich
Gentamycin sulphate	0916762J8	MP Biomedicals
Fetal bovine serum (FBS)	F9665	Sigma-Aldrich
Insulin	I9278	Sigma-Aldrich
Oil red 'O'	O0625	Sigma-Aldrich
2) Gene expression analysis		
Tri reagent	T9424	Sigma-Aldrich
1-Bromo-3-Chloro-propane	B9673	Sigma-Aldrich
Phenol:Chloroform:Isoamyl Alcohol	P3803	Sigma-Aldrich
RNAse free DNAse1	79254	Qiagen, UK
Glycogen	R0561	Thermo-Scientific
Diethylpyrocarbonate (DEPC)	D5758	Sigma-Aldrich
SuperScript™ III Reverse Transcriptase	18080051	Invitrogen, UK
10X First strand buffer	18080051	Invitrogen, UK
DTT	18080051	Invitrogen, UK

Random Primer	C1181	Promega, UK
RNaseOUT™ Recombinant Ribonuclease Inhibitor	10777-019	Invitrogen, UK
3) Protein analysis		
Trichloroacetic acid (TCA)	T9159	Sigma-Aldrich
Triton X-100	93443	Sigma-Aldrich
2-mercaptoethanol	M6250	Sigma-Aldrich
iv. Ammonium persulfate (APS)	A3678	Sigma-Aldrich
TEMED	T9281	Sigma-Aldrich
Tween 20	P1379	Sigma-Aldrich
4) Calcium imaging		
Fura2 AM	F0888	Sigma-Aldrich
ATP	A6419	Sigma-Aldrich

2.1) **Primary Rat Adipocytes Culture**

2.1.1) Materials for primary cell culture

i. Tissue collection and digestion

- HEPES solution (1.25X) for 1 litre
  - 0.125M HEPES : 29.8g
  - 0.15M NaCl : 8.78g
  - 62.5mM KCl : 4.66g
  - 6.25mM D-Glucose : 1.12g
  - 1.88% Bovine serum albumin : 18.8g
  - 1.25mM $CaCl_2$ anhydrous : 0.132g

  pH 7.3 was adjusted with NaOH and stored at -20°C in aliquots

- Collagenase solution
  - 60mg of collagenase per digestion was diluted in 1ml HPLC water (in reference: 1500 units activity/mL)

- Sterile Petri dish, sterile 30ml glass beaker, sterile 50ml Erlenmeyer flask per digest, one 0.22µM filter (Millex-GV PVDF filter unit, Millipore), syringes and sterile surgical instruments

ii. Cell separation and counting

- Red blood cell (RBC) lysis buffer
  - 155mM NH_4Cl : 0.83 g/100ml
  - 10mM $KHCO_3$: 0.1 g/100ml
  - 0.1mM EDTA : 4.45mg/100ml (or use 20ml 0.5M stock)

  Solution was sterile-filtered through 0.22µm and stored in 10ml aliquots at -20°C

- One set of sterile filter holder (25mm Swinnex; Millipore) containing 150 and 20µm mesh filters (Sefar filtration)

- Trypan blue staining solution and haemocytometer for cell counting

iii. Proliferation and differentiation of primary rat adipocytes

- 3,3',5-Triiodo-L-thyronine sodium salt (T_3) stock solution (40µg/ml or 60µM) stored at 4°C
  - 1ml of sterile 1N NaOH was swirled gently to dissolve, then 24ml of sterile culture medium was added
  - 1:30,000 dilution used in differentiation media

- Transferrin-sodium-selenite (TS) stock solution (T; 5mg/ml; S; 50µg/ml) stored at 4°C
  - 30mg Transferrin was dissolved in 5.4ml 0.1M acetic acid and 0.6ml sodium selenite was added
  - 1:1000 dilution used in differentiation medium

- Insulin stock (10 mg/mL, 1.7mM)
  - Dilute 1:2000 into differentiation medium

- Preparation of medium

Medium	Reagents/solutions	Volume/ Final concentration
Serum free media (SFM)	DMEM/F12 Ham L-Glutamine (200mM) Gentamycin (50mg/ml)	500ml 2mM 2.5mM
Plating media (PM)	DMEM/F12 Ham FBS 10% L-Glutamine (200mM) Gentamycin (50mg/ml)	500ml 50ml 2mM 2.5mM
Differentiation/ High glucose mediu (HG)	Serum free medium T3 stock solution TS stock solution Insulin (10mg/ml)	50ml 2nM T: 65µM, S: 29nM 72nM
Normal glucose mediu (NG)	DMEM-low glucose Nutrient mixture F10 Ham L-Glutamine (200mM) Gentamycin (50mg/ml) T3 stock solution TS stock solution Insulin (10mg/ml)	25ml 25ml 2mM 2.5mM 2nM T: 65µM, S: 29nM 10nM

2.1.2) Methods for primary cell culture

The method for primary cell culture was based on Hausman and colleagues (Hausman et al., 2008) with some modification and optimization throughout the experiments. This study used male Wistar rats, aged 6 to 8 weeks, weighing 200-220g that were euthanized by cervical dislocation according to the Animal Scientific Procedures Act (ASPA) and the regulation of School of Life Sciences, University of Nottingham. All rats/instruments available in our lab and School of Life Sciences, University of Nottingham (unless stated otherwise) and all reagents/chemicals purchased from Sigma-Aldrich, UK as listed in Table 2.1 (unless stated otherwise).

i. Tissue collection and digestion

A midline incision was made from hypogastric region up to epigastric region, exposing the abdominal cavity of the male Wistar rat. Epididymal and retroperitoneal fat pads were excised and pooled in sterile petri dish containing serum free media (SFM). Approximately, 2g of adipose tissue was transferred into a 30ml beaker and minced into a very fine consistency by using a sharp sterile pointed scissors. The HEPES-collagenase solution was prepared by adding 1ml aliquot of collagenase into 9ml aliquot of HEPES; this mixture was then sterile-filtered into the beaker containing minced tissue through 0.22µm filter. Then, the beaker was swirled gently to blend the mixture and transferred into a sterile 50ml conical digestion flask.

The flask was incubated for 45 to 60 minutes under constant shaking on a rotating platform (115 rpm) in 37^{o}C incubator.

ii. Cell separation and counting

After thorough digestion with collagenase, 10ml of SFM was added to digestion flask. The digested fat suspension was filtered through 150µm nylon mesh into a sterile 50ml plastic centrifuge tube. The undigested tissue was discarded. Another 10ml of SFM was added to the fat suspension, giving a total volume of 30ml, and then it was centrifuged at 50g for 5 minutes. Next, the infranatant from beneath the floating cell layer was transferred to a sterile 50ml centrifuge tube and spun again at 500g for 15 minutes to pellet the stromal vascular (SV) cells. After that, all the supernatant was discarded except 5ml was left behind to be added with 10ml of sterile RBC lysis buffer. The tube was capped; the pellet was re-suspended and incubated for 5 minutes at room temperature.

Once incubation period was completed, 15ml of plating media (PM) was added. The cell suspension was filtered again through a sterile 20µm mesh filter into a new 50ml centrifuge tube. Finally, the suspension was centrifuged for 5 minutes at 500g and the supernatant was discarded except for 2-3ml. Another 5ml of PM was added and the cell pellet was gently re-suspended again.

The isolated cells were counted by dilution of 20µl of cell suspension in 40µl of trypan blue stain solution. 20µL of the cell-dye solution was used to fill both Neubauer chambers on haemocytometer and cells were counted under phase contrast microscope (Leica) using 10x magnification. The numbers of cells in the four large outside corners were counted. AT precursor cells were visualized as rounded cells with intact outer membranes and distinct nuclei.

$$\text{Cell number/ml} = (\text{cells counted}/4) \times \text{dilution factor} \times 10^4$$

iii. Proliferation of primary rat adipocytes

The isolated primary adipocytes were seeded into cell culture plate according to Table 2.1. While plating the cells, the suspension was continuously mixed to ensure even cell numbers. Cultured cells were then incubated in PM in a humidified atmosphere of 95% air and 5% CO2 at 37°C. After 24 hours, the cells were washed with PBS twice to remove RBC and other contaminants. Then, the media was changed every other day. After 4 to 5 days, as the cells achieved 80-90% confluence, they are ready for induction of adipogenesis.

Table 2.2: Useful numbers for cell cultures in various sizes of cell culture plates

Culture plate	Surface area (cm^2)	Seeding density	Cell at confluency	Growth media (ml)
6-well	9	3×10^5	12×10^5	3-5
12-well	4	1×10^5	4×10^5	1-2
24-well	2	0.5×10^5	2×10^5	0.5-1

iv. Differentiation of primary rat adipocytes

Differentiation of pre-adipocytes was induced by replacing PM with differentiation media. The cells were washed with PBS once more before being fed with differentiation media. The media needed to be replaced after 2-3 days by removing 70 to 80% of the spent medium. After that, the cells were fed with NG/HG media and the media should be changed every other day.

2.1.3) Oil red 'O' staining

i. Materials for staining

- Sterile PBS, 10% formalin *(v/v),* 99% isopropanol *(v/v),* 60% isopropanol *(v/v),* Whatman filter paper no.1

- Oil red 'O' stock solution
    - 300mg of oil red 'O' powder was dissolved into 100ml of 99% isopropanol. Then, 3 parts of oil red 'O' solution was mixed with 2 parts of deionized water in fumed hood and allowed to sit at room temperature for 10 minutes. This working solution of oil red 'O' mixture was filtered and used within 2 hours.

ii. Method for staining

Media from differentiated cells was aspirated and gently rinsed the cells with 2ml PBS. After PBS was discarded, 2ml of 10% formalin

was added and the cells was incubated for at least 30 minutes or up to 1 hour at room temperature. The formalin was removed with a pipette into a designated waste receptacle and rinsed with 2ml of sterile water. After that, the cells were incubated for 2-5 minutes with 2ml of 60% isopropanol. The supernatant was discarded and 2ml of oil red 'O' working solution was put in each well to cover the cells completely and slowly rotated on a shaker for 5 minutes. Before the cells can be viewed, each well was rinsed with water until clear.

2.1.4) Cell viability assay

i. Materials for assay

- Trypsin/EDTA, sterile-filtered trypan blue

ii. Method for assay

Cells were treated with various concentrations of GSK101 (1nM, 10nM, 50nM, 100nM, 200nM and 500nM) for 24 hours to assess their viability. Then, media was removed and monolayer cells were washed with PBS twice. Trypsin/EDTA solution was added into the plate (0.02-0.03ml/cm^2) and trypsinisation progression was monitored at about 2-3 minutes. As rounded cells detach from culture surface, 2mls PM was added and then, cell suspension was transferred to a sterile conical tube for centrifugation at 200g for 5 minutes. Supernatant was aspirated and cell pellet was resuspended in differentiation media. After that, 20ul of sterile-filtered trypan blue

was mixed with 20ul of cell suspension in a different Eppendorf tube and cells were counted using haemocytometer (results further elaborated in Appendix A).

2.2) **Analysis of Gene Expression**

2.2.1) Total RNA extraction from primary rat adipocytes culture

i. Materials for RNA extraction

- Tri-reagent, 1-bromo-3-chloro-propane (BCP), RNAse free DNAse1, glycogen, 70% ethanol *(v/v),* isopropanol, phenol:chloroform:isoamylalcohol

- 3M DEPC sodium acetate pH 5.2
  - 24.61gm sodium acetate was added to HPLC water, making it up to 100ml by adjusting the pH as well. Then, 100µl of DEPC was added to the mixture, shake thoroughly and incubated at 37°C overnight before autoclaving.

ii. Method for RNA extraction

Culture medium was removed from the plate and the cells were lysed directly on culture dish using Tri-reagent (1ml of TRI Reagent solution per 10 cm^2 of culture dish area). The homogenates were incubated for 5 minutes at room temperature before the cells were scraped using the cell scrapper and transferred to a 1.5ml tube.

Then, 200µl of 1-bromo-3-chloropropane was added to the tube and mixed vigorously. The samples were then separated into three phases by centrifugation at 12,000g for 15 minutes at 4°C. The upper aqueous phase was transferred into a fresh tube for further usage and the remaining was kept for protein extraction later. After that, 700µl isopropanol and 1µl of glycogen was added to the aqueous and stored at -20° for 1 hour. The tube was centrifuged again at 12000g for 10 minutes at 4°C, then the supernatant was discarded. 500µl of 70% ethanol was added, vortexed for 5 seconds and centrifuged at 12000g for 10 minutes at 4°C.

Next, ethanol was discarded and the pellet was allowed to air dry for 5 minutes. The pellet was then dissolved in 200µl sterile HPLC water. 1µl RNASE free DNAse1 was also added and the tube was incubated on bench for 10 minutes. 200µl phenol:chloroform:isoamylalcohol (50:49:1) added into the tube, mixed it and vortexed for 10 seconds before centrifuged it again at 12000g for 5 minutes at room temperature. Aqueous upper layer was transferred to a fresh tube, making sure that none of the lower layer contaminates the sample. 20µl 3M DECP sodium acetate (pH 5.2) and 200µl isopropanol was added to the mixture and placed at -20°C for 1 hour. The sample tube was centrifuged at 12000g for 10 minutes at 4°C and later the supernatant was discarded. 500µl 70% ethanol was added, vortexed for 5 seconds and centrifuged 12000g for 10 minutes at 4°C. Ethanol

was removed and the pellet was allowed to air dry for 5 minutes. The pellet was dissolved in 30µl DECP HPLC water and heated to 65°C for 10 minutes. After that, the sample was calculated for total RNA concentration and it can be stored at -80°C until required. For preparation of RNA extraction using Direct-zol RNA mini-prep (Zymo Research), the total RNA was isolated from rat adipocytes using Tri reagent according to the manufacturer's instructions.

2.2.2) RNA yield and quality

The concentration of an RNA solution was verified by measuring its absorbance at 260nm via NanoDrop 2000 spectrophotometer (Thermo Scientific, USA). The A260/A280 ratio of the RNA with a ratio value of 1.8-2.2, as indication of its purity.

2.2.3) Single stranded cDNA synthesis

i. Materials for reverse transcription

- SuperScript™ III Reverse Transcriptase (200U/µl), 10X first strand buffer, 0.1M DTT, random primer (100ng/µl), 10mM dNTPs, RNaseOUT™ Recombinant Ribonuclease Inhibitor (40 U/µl)

ii. Method for reverse transcription

Total RNA (~250ng) was added to 300ng of random primers and RNase-free water to a total volume of 14.2µl. The reaction mixture

was placed into a thermocycler (MWG-Biotech Primus 69 Plus) at 65°C for 5 minutes followed by incubation on ice for 10 minutes. Then, 2µl of 10X first strand buffer (Invitrogen), 0.8µl of 100mM dNTPs mix, 2µL of 0.1M DTT, 0.5µl of RNaseOUT (40u/µL, Invitrogen) and 1µL of the reverse transcriptase (200U/µL, SuperScript™ III Reverse Transcriptase) were mixed and added to the annealed primers-RNA mixture to a final volume of 20µl. The samples were returned to the thermocycler and the reverse transcription reaction undertaken by incubation at 25°C for 10 minutes, 50°C for 60 minutes and 70°C for 15 minutes. Finally, the samples were chilled to 4°C and the cDNA stored at -20°C until required for gene expression analysis.

2.2.4) Primers design and preparation

The primers and probes were designed by using Primer Express 3 software (Applied Biosystems, USA) and synthesized commercially (Eurofins MWG Operon, Germany). They were compatible for rat *β-actin, gapdh* and *rna polymerase 2* (*polr2*) as the reference gene, *fabp4, fabp5, fetA, lcn2, trpv1, trpv4, pgc1-α, ppar-γ, glut4* (Taqman primers and probes) and *ccl2* (Sybr green primers). For Taqman qRT-PCR, the probe was labelled with a reporter fluorescent dye (FAM) at the 5'end and a fluorescent dye quencher (TAMRA) at the 3'end.

Table 2.3: Table showing primers and probes sequences for genes of interest in this study.

No	Rat gene	Sequence (5'-3') Forward/reverse/probe	Origin
1	*β-actin*	Fwd: AGCCATGTACGTAGCCATCCA Rev: TCTCCGGAGTCCATCACAATG Pro:TGTCCCTGTATGCCTCTGGTCGTACCAC	FRAME lab
2	*gapdh*	Fwd: TCTGCTCCTCCCTGTTCTAGAGA Rev: CGACCTTCACCATCTTGTCTATGA Pro: ATCTTCTTGTGCAGTGCCAGCCTCGT	FRAME lab
3	*polr2*	Fwd: TGTGTTTCATGTGGGCTTCCT Rev: CCTTAATCTTCGGGTTGTTAGAATCT Pro: CGCTGTGTCTGCTTCTTTTGCTCCAAAC	FRAME lab
4	*fabp4*	Fwd: CTTCAAACTGGGCGTGGAA Rev: CCAGGGTTATGATGCTCTTCACT Pro: TCGATGAAATCACCCCAGATGACAGGA	FRAME lab
5	*fabp5*	Fwd: TGAGGACTACATGAAGGAACTAGGAGTAG Rev: TTTTGACGGTGAGGTTGTTGTT Pro:CCAAACCAGACTGCATCATTACCCTCGA	FRAME lab
6	*fetA*	Fwd: CAGGGATTCAGGCAGATCTTG Rev: CAGCGTGTCAATTTCCAACTCA Pro: TCTCGGCGGCCCTTCGGA	Design by the author
7	*lcn2*	Fwd: CCAGAAGACCTCTGAAAACAAACA Rev: CGAATCGCTCCTTCAGTTCAT Pro: CTTCAAAGTCACCCTGTACGGAAGAACCAA	FRAME lab
8	*trpv1*	Fwd: CAGCAGCAGTGAGACCCCTAA Rev: TGTCCTGTAGGAGTCGGTTCAA Pro: CGTCATGACATGCTTCTCGTGGAACC	Design by the author
9	*trpv4*	Fwd: GAGCAAGCACATCTGGAAGCT Rev: TTGCCCACTGTCACCATCTC Pro: ACCACCATCCTGGACATCGAGCG	Design by the author
10	*pgc1-a*	Fwd: AGACAAATGTGCTTCCAAAAAGAA Rev: GTTGTTGGTTTGGCTTGAGCAT Pro: TCCCATACACAACCGCAGTCGCA	FRAME lab
11	*ppar-γ*	Fwd: TGCCAAAAATATCCCTGGTTTC Rev: TGAATCCTTGTCCCTCTGATATGA Pro: AGATCATCTACACCATGCTGGCCTCCC	FRAME lab

12	*glut-4*	Fwd: ATACCTCTACATCATCCGGAACCT Rev: GCCAGTGCATCAGACACATCA Pro: CTGCCCGAAAGAGTCTAAAGCGCCTG	FRAME lab
13	*ccl2 (sybr green)*	Fwd: ATGCAGTTAATGCCCCACTC Rev: TTCCTTATTGGGGTCAGCAC	Design by the author

2.2.5) mRNA expression by real-time quantitative PCR

The cDNA that was prepared previously was used as a template and amplified using the Taqman Universal PCR fast Master Mix Kit (Applied Biosystem, USA). Each PCR reaction was performed in a total volume of 20ul per-reaction containing 10µl of qPCRBIO Probe Mix, 0.8µl of 400pM forward and reverse primers, 0.4µl of 250pM of TaqMan probe, 6µl of DEPC treated water and 2µl of cDNA sample. For amplification using qPCRBIO SyGreen Master Mix (PCR Biosystems), each PCR reaction was performed in a total volume of 20ul per-reaction containing 10µl of qPCRBIO SyGreen Mix, 0.8µl of forward and reverse primers (final concentration 400nM), 2µl of cDNA sample and 6.4µl of DEPC treated water. 1:2 dilutions for cDNA of all samples were used to produce a standard curve. The samples for quantification were diluted in 1:8. All samples were run in triplicate and negative reverse transcriptase (-ve RT in which samples of RNA were included that had undergone the cDNA synthesis protocol in the absence of any RT enzyme) reactions were performed to assess any potential contamination of genomic DNA. The negative RT reactions had cycle threshold (Ct) values >40, and

the difference between the negative and positive reactions was >10 cycles. All samples were run in TaqMan RNase P 96-well plates (Applied Biosystem, USA) and qRT-PCR was carried out using an Applied Biosystems Step OnePlus™ Thermocycler for 40 cycles.

Assays were deemed acceptable if there was no more than 0.5 cycle threshold (Ct) difference between the values within triplicates, the slope of the standard curve was between -3.2 and -3.6 and the r2 was above 0.99 (Figure 2.2). The mRNA expression levels of specific genes were normalized to the geometric mean of the mRNA expression level of *polr2*, which was used as the reference gene for the primary rat adipocytes. Other reference genes that were validated in this study include *gapdh* and *β-actin* (see Appendix B).

2.3) **Analysis of Protein Expression (Protein Assay)**

2.3.1) Protein extraction from Tri-reagent sample

i. Materials for protein extraction

- Isopropanol, 100% ethanol, 1% SDS *(w/v)*

- 0.3M Guanidium HCl/95% ethanol
    - 6M guanidine HCl stock solution was prepared by dissolving 28.7gm of guanidine HCl in 25ml of distilled water. Once dissolved, the solution was measured upto 50ml, autoclaved and stored at room temperature.

- To use as working solution, 5ml of 6M guanidine HCl was added to 100% ethanol.

ii. Method for protein extraction

After aqueous phase (the uppermost layer) was removed for RNA extraction, the remaining interphase and lower phase was used for protein isolation. For every 1ml of Tri-reagent sample, 1.5ml of isopropanol was used and left at room temperature for 10 minutes. Then, the samples were centrifuged at 12000g for 10 minutes at 4°C. The supernatant was removed and the pellet washed with 2ml 0.3M guanidium HCl/95% ethanol for 3 times. Each washing steps required 20 minutes incubation at room temperature, followed by centrifugation at 7500g for 5 minutes at 4°C. After washing steps completed, 2 ml of 100% ethanol was added and the pellet was resuspended. The samples were incubated for 20 minutes at room temperature and centrifuged at 7500g for 5 minutes at 4°C. Subsequently, the supernatant was discarded and the protein pellet was left to dry for 5 to 10 minutes before being dissolved in 1% SDS. The protein sample was then centrifuged again at 10000g for 10 minutes at 4°C. Finally, the supernatant was transferred to a new tube for protein assay.

2.3.2) Radio-ImmunoPrecipitation Assay (RIPA) protein extraction

i. Materials for protein extraction

- Cell lysis buffer (RIPA)
  - 150mM NaCl
  - 50mM Tris-HCL pH 7.4
  - 1% sodium deoxycholate *(v/v)*
  - 1% Triton X-100 *(v/v)*
  - 0.1% SDS *(w/v)*

ii. Method for protein assay

The adherent cells were washed with cold PBS twice (500µl per well of 12-well plate). 100µl of RIPA lysis buffer with protease inhibitor (Roche) was added into a well, scraped and transferred to another well, combining 2 wells of 12-well plate into one Eppendorf tube. Each tube containing cell lysates was then sonicated 3 times for 10 seconds on ice using a small polytron probe. Then, all the tubes were placed on rotating daisy wheel in cold room for 45 minutes before centrifuged at 13000 rpm for 15 minutes at 4°C to pellet the debris. The supernatant was transferred to a new tube for protein assay.

2.3.3) Protein extraction from Directzol samples

i. Materials

- Cold acetone, 100% ethanol and 1% SDS

ii. Method

4 volumes of cold acetone was added to one volume of Tri-reagent with ethanol obtained from spin-column flow-through. The samples was incubated on ice for 30 minutes, followed by centrifugation at top speed for 10 minutes at 4°C. The supernatant was discarded and 400µl of 100% ethanol was added to the pellet and centrifuged again for 1 minute. The supernatant was removed, the pellet was air-dried for 10 minutes and resuspended in 1% SDS before being used for BCA assay.

2.4) Analysis of Protein Secretion from Conditioned Media (CM)

2.4.1) TCA precipitation

i. Materials

- 100% trichloroacetic acid (TCA) *(w/v)*, cold acetone, 2x loading buffer

ii. Method

800µl of collected CM was aliquoted and added to 200µl of 100% trichloroacetic acid (TCA) in 1.5ml tube. The tube was vortexed and incubated for 30-60 minutes at 4°C. After that, the tube was centrifuged at 13000rpm for 30 minutes. The supernatant was removed, leaving the protein pellet intact. 500µl of cold acetone was used to wash the pellet, vortexed and spun at 13000rpm for 15 minutes. This washing step using acetone was repeated for a total of 2 acetone washes and the pellet was leaved to be aired dry. Then, 100µl of 2x loading buffer (Laemmli buffer with 2-mercaptoethanol) was added and boiled in 99°C heat block for 10 minutes.

2.4.2) Acetone precipitation

i. Materials

- Cold acetone, 2x loading buffer

ii. Method

1ml CM was aliquoted in acetone-compatible tube and 4ml 100% cold acetone (-20°C) was added to it. The tube was vortexed and incubated for 60 minutes at -20°C. After that, the tube was centrifuged for 10 minutes at 13,000-15,000g. The supernatant was carefully disposed so that the protein pellet was not dislodged. The tube was left uncapped to allow acetone to evaporate at room temperature for about 30 minutes. The protein pellet was

resuspended in appropriate buffer and can be stored in -20°C or directly used for protein assay.

2.4.3) BCA protein assay

i. Materials and method for protein assay

The protein concentration for all samples were determined by Pierce BCA Protein Assay Kit (Thermo Scientific, USA) using BSA as a standard. The samples were prepared according to the manufacturer's instructions. The absorbance was read at 560nm using FLUOstar Omega spectrometer-based microplate reader (BMG Labtech, Germany).

2.5)**Immunoblotting**

2.5.1) Western blotting gel electrophoresis

i. Materials for immunoblotting

- Preparation of 2X sample buffer (10ml)
  - 1.2ml 1M Tris-HCl pH 6.8
  - 2ml 100% glycerol
  - 4ml 10% SDS *(w/v)*
  - 200µl 1% bromophenol blue (final concentration 0.02%)
  - Water up to 10ml
  - 5% 2-mercaptoethanol (to add prior to use)

- Preparation of 4X sample buffer (10ml)
  - 2.4ml 1M Tris-HCl pH 6.8
  - 4ml 100% glycerol
  - 0.8gm SDS
  - 4mg bromophenol blue
  - Water up to 10ml
  - 1/10th volume of 2-mercaptoethanol (to add prior to use)
- Preparation of 6X sample buffer (10mL)
  - 1.2ml of 500mM Tris-HCl pH 6.8
  - 4.7ml 100% glycerol
  - 1.2gm SDS
  - 6mg bromophenol blue
  - Water up to 10ml
  - 1/8th volume of 2-mercaptoethanol (to add prior to use)
- Preparation of 10% ammonium persulfate (APS)
  - 0.1g of APS dissolved in 1ml of distilled water prior to use
- Preparation of 4X separation gel buffer (pH 8.8)
  - 1.5M Tris Base; 0.4% (w/v) SDS pH 8.8
- Preparation of 4X stacking gel buffer (pH 6.8)
  - 0.5M Tris Base; 0.4% (w/v) SDS pH 6.8

- Preparation of 12% SDS-PAGE gel (for 1 mini gel)

Reagents/solutions	**Separating gel (10ml)**	**Stacking gel (5ml)**
30% acrylamide/bis acrylamide	4ml	0.5ml
4X separation/stacking buffer	2.5ml	1.25ml
Water	3.4ml	3.25ml
10% APS	100µl	50µl
TEMED	10µl	5µl

- Preparation of 10X running buffer (1000ml)
  - 144g Glycine; 30g Tris Base; 100ml 10% SDS *(w/v)*, made up to 1litre with HPLC water

- Preparation of 10X transfer buffer (1000ml)
  - 30g Tris Base; 144g Glycine, made up to 1litre with HPLC water

- Preparation of transfer buffer working solution (1X)
  - 80ml 10X Transfer Buffer; 160ml Methanol, made up to 800ml with HPLC water

- Preparation of 10X tris buffered saline (TBS) (1000ml)
  - 24.23g Tris Base; 80.06g Sodium Chloride (NaCl) pH 7.6 with concentrated HCl

- Preparation of 1X tris buffered saline-tween 20 (TBS-T)
    - 100ml 10X TBS with 1ml of Tween 20, made up to 1litre with HPLC water
- Preparation of blocking buffer
    - 5% (w/v) non-fat dry milk dissolved in 1X TBST

ii. Method for immunoblotting

Equivalent proteins concentration from cell lysates and equivalent sample volume from CM were loaded and separated on 12% SDS-PAGE gel in reducing condition. 5µL of protein molecular weight marker (Precision Plus Protein TM Standards, Kaleidoscope, Bio-Rad) was also loaded into each gel for target protein identification. The gel electrophoresis for protein samples was run at 150volt for 1 hour, followed by electro-transferred the protein from the gel to nitrocellulose membranes (GE Healthcare Life Sciences) at 300mA for 1 hour using Mini Trans-Blot Cell Tank (Bio-Rad, USA) according to the manufacturer's description (Bio-Rad, USA).

2.5.2) Immunodetection following western blotting

The nitrocellulose membrane was incubated in blocking buffer for one hour on a shaker. The blocking solution was discarded, followed by addition of primary antibody in blocking buffer and the membrane was incubated overnight at 4°C. Following primary antibody

incubation, the membrane was washed with TBS-T solution for 15 minutes for a total of 3 times. The secondary antibody (1:10000 dilution) was added to the blocking buffer and the membrane was incubated for one hour at room temperature. The membrane was then washed 3 times, 15 minutes each with TBS-T. Finally, the membrane was immersed in distilled water for 5 minutes prior to scanning of the membrane using the Odyssey®Infrared Image system (LICOR Biosystem, USA) using 700nm (red channel) and 800nm (green channel) with the focus offset to membrane imaging. Densitometry was performed using Odyssey® Imaging System Software (LICOR Biosystem, USA).

Table 2.4: List of primary antibodies used for western blotting in this study

Primary antibody	**Catalogue no.**	**Origin**	**MW**	**Dilution**
Rabbit polyclonal anti FABP4 antibody	ab66682	abcam, USA	15 kDa	1:500
Goat polyclonal LCN2/NGAL antibody	AF3508	R&D Systems, USA	25 kDa	1:200
Mouse monoclonal anti α-tubulin antibody	T9026	Sigma-Aldrich, USA	50 kDa	1:5000
Mouse monoclocal anti β-actin antibody	A5441	Sigma-Aldrich, USA	42 kDa	1:5000

Table 2.5: List of secondary antibodies used for western blotting in this study

Secondary antibody	Catalogue no.	Origin	Dilution
IRDye® 680LT Conjugated donkey anti-rabbit IgG	926-68023	Licor Bioscience, USA	1:10000
IRDye® 800CW Conjugated donkey anti-goat IgG	926-32214	Licor Bioscience, USA	1:10000
IRDye® 680LT Conjugated donkey anti-mouse IgG	926-68022	Licor Bioscience, USA	1:10000
IRDye® 800CW Conjugated goat Anti-Rabbit IgG	926-32211	Licor Bioscience, USA	1:10000

2.5.3) Antibody stripping from nitrocellulose membrane

i. Materials

- 15 g glycine, 1 g SDS, 10 mL Tween 20
    - All of the above were dissolved in 800 mL distilled water. pH was adjusted to 2.2 and the final volume of stripping buffer was added up to 1 L with distilled water.

ii. Method

The membrane was immersed in stripping buffer using a volume that was enough to cover and incubated at room temperature for 5 to 10 minutes on a shaker. Then, the buffer was discarded, replaced with fresh stripping buffer and incubation step was repeated. After that, the membrane washed with PBS twice for 10 minutes, followed by TBST wash twice 5 minutes each.

2.6) Exosome isolation from condition medium

2.6.1) Serial centrifugation and ultracentrifuge

i. Materials needed for centrifugation

- Phosphate-buffered saline, polyallomer tubes, refrigerated table-top centrifuge, Beckman-Coulter Optima LE-80K ultracentrifuge

ii. Methods for benchtop and ultracentrifuge

30ml CM that was attained fresh from cell culture was centrifuged at 300g for 10 minutes to remove cell suspension. The supernatant was collected and centrifuged again at 2,000g for 10 minutes to pellet apoptotic bodies and cell debris. After debris have been removed, the collected supernatant was subjected to high speed centrifuged at 10,000g for 30 minutes to separate shed microvesicles (sMVs) from the medium. The pellet formed after this step was kept for sMVs isolation later, whereas the supernatant was collected in a fresh tube for ultracentrifugation at 100,000g for 70 minutes. This was done to segregate the pellet containing extracellular vesicles including exosome from CM.

Next, we removed the supernatant and the pellet was resuspend in PBS. In this washing step, the solution was centrifuged again at 100,000g for 70 minutes. Finally, the supernatant was removed completely and the pellet containing exosome was resuspended in in

30ul PBS. The exosome can be stored up to 1 year at -80°C in small aliquots.

All centrifugations were done at 4°C and a marker was used to mark location of pellet at the end of centrifugation since the pellet was difficult to visualize. Due to that reason, few millimetres of supernatant were allowed above the pellet, except for the final pellet that need to be resuspended in PBS.

2.6.2) Protein detection via coomassie blue staining

i. Materials

- Coomassie Brilliant Blue R-250, methanol, glacial acetic acid

- Preparation of coomassie staining solution
  - 0.4g of coomassie blue was added to 200ml of 40% methanol *(v/v)* in HPLC water; the solution was stirred for 2 hours and filtered through Whatman filter paper
  - 200ml of 20% acetic acid *(v/v)* was then added to the solution and it can be reuse and store at room temperature

- Preparation of destaining solution
  - 40% of methanol *(v/v)* was added to 10% acetic acid *(v/v)* and the total volume adjusted to 1litre with HPLC water

- Preparation of storage solution
    - 5% acetic acid *(v/v)*

ii. Method

Gel was stained in coomassie staining solution for 30 minutes with gentle agitation. After that, the gel was immersed in destaining solution for overnight. The destaining solution was replenished several times until background of the gel was fully destained. The gel can be stored in the storage solution.

2.7)**Electron microscopy (EM)**

2.7.1) Materials used in EM

- 4% paraformaldehyde (PFA), phosphate-buffered saline, 1% glutaraldehyde, fomvar-carbon coated EM grid, 4% uranyl acetate pH 4.0, parafilm, forceps, glass dish, stainless steel loops, Whatman no. 1 filter paper, grid storage boxes, electron microscope

- Preparation of 4% paraformaldehyde (PFA) *(w/v)*
    - 4g of PFA powder was dissolved in 90ml 0.1M sodium phosphate buffer and heated to 65°C while stirring
    - 0.1M sodium phosphate buffer was added to a final volume of 100ml; sterile-filtered the solution and stored at -20°C in aliquot

- Preparation of 1% glutaraldehyde *(v/v)*
  - EM-grade glutaraldehyde fixative was diluted in 0.1M sodium phosphate buffer pH 7.4 to the appropriate dilution
  - It can be stored up to 6 months at -20°C or up to 4 weeks at 4°C after thawing

- Preparation of 4% uranyl acetate pH 4.0 *(w/v)*
  - 2g of uranyl acetate was dissolved in 50ml distilled water
  - The solution should be protected from light and filtered using 0.22µm filter prior to use and can be stored up to 4 months at 4°C

2.7.2) Method for EM

An equal volume of exosome-containing pellet that has been resuspended in PBS was mixed with 4% of paraformaldehyde (PFA) to make the final product of 2% PFA. 13µl of this mixture was deposited on Formvar-carbon coated EM grids and covered for 20 minutes. Then, 100µl drops of PBS were put on a sheet of Parafilm and the grid was transferred (membrane side down) to drops of PBS with clean forceps in this washing step.

After that, the grid was transferred to a 50-µl drop of 1% glutaraldehyde for 5 minutes. The washing steps were repeated for 7 times using 100µl drop of distilled water and let the grid stand for

2 minutes each. Then the grid was contrasted in a solution of 50µl drop uranyl acetate for 5 minutes

The grid was removed by stainless steel loops and the excess contrast fluid was blotted by gently pushing the loop sideways on Whatman no. 1 filter paper. The grid was air-dried for 5 to 10 minutes while still on the loop and can be stored in appropriate grid storage boxes for many years or immediately observed under the electron microscope at 80 kV that was available at the Nanoscale Magnetic Resonance Centre (NMRC), University of Nottingham.

2.8)**Calcium imaging**

2.8.1) Sub-culturing primary rat adipocytes

i. Materials

- 1X Phosphate Buffered Saline (PBS)
  - 1 tablet of PBS in 100ml of deionised water and followed by autoclaved for sterilization
- 10X Trypsin EDTA solution (Sigma, UK)
  - Dilute 1:10 with sterile PBS, aliquot into universal containers and stored at -20°C

ii. Method

When cells were 80% confluent, PM was aspirated and rinsed with 1X PBS. 5ml of trypsin- EDTA solution was added in 75cm^2 size flask and incubated for 2-3 minutes 37°C in tissue culture nonhumidified chamber. The trypsin solution was swirled around the flask to detach the cells from the flask. Then 15ml of PM was added and mixed. The cell mixture was pipetted out from the flask into a 50ml tube, followed by centrifugation at 200g for 5 min. The supernatant was aspirated and the pellet was resuspended in fresh media. The cells were diluted and were plated accordingly depending on the required number of cells needed to perform the experiment.

2.8.2) Gelatin-coated coverslip

i. Materials and method

- Cover slip 19mm diameter, 12-well cell culture plate, 0.2% gelatin solution (*w/v*)

- Preparation of gelatine solution
  - 0.5 g gelatin was dissolved in 500 mL distilled water and sterilized by autoclaving.

Table 2.6 : Suggested volume required per plate well:

Wells	0.2% gelatin (amount/well)
96	100ul
48	300ul
24	500ul
12	1ml
6	1.5-2.0ml

The appropriate amount of gelatin solution should be enough to immerse the coverslip and should be incubated for at least 1 hour at 37°. Then, gelatin solution was aspirated before adding cell suspension and media.

2.8.3) Imaging

i. Materials for calcium imaging

- Preparation of cell culture
  - Cells were seeded approximately $0.4x10^5$ cells on 0.2% gelatin-coated coverslip and subjected for proliferation about 4-5 days, followed by induction of differentiation once cells confluency reached 80-90%

- Preparation of calcium buffer

Chemical	Final concentration	g/500ml	g/1L	g/2L
NaCl	145mM	4.24	8.48	16.96
KCl	5mM	0.186	0.372	0.744
CaCl	2mM	0.147	0.294	0.588
$MgSO_4 7H_2O$	1mM	0.123	0.246	0.492
HEPES	10Mm	1.192	2.384	4.768
1% BSA stock solution	0.1%	50ml	100ml	200ml

- Preparation of buffer without calcium

Chemical	Final concentration	g/500ml	g/1L	g/2L
NaCl	145mM	4.24	8.48	16.96
KCl	5mM	0.186	0.372	0.744
$MgSO_4 7H_2O$	1mM	0.123	0.246	0.492
HEPES	10mM	1.192	2.384	4.768
0.5M EDTA stock solution	0.1mM	100ul	200ul	400ul
1% BSA stock solution	0.1%	50ml	100ml	200ml

  - calcium buffer with 5.5mM glucose concentration: add glucose 0.99g/L
  - calcium buffer with 17.5mM glucose concentration: add glucose 3.15g/L
  - pH was adjusted to 7.4 by using 10M NaOH

- Preparation of Fura2 AM stock solution (1mM)

  - Fura2 AM (Sigma F0888), 1mg, was dissolved in 1ml DMSO and aliquoted 5ul each. They were protected from light and stored at 20°C. Upon using it, 445ul of buffer was added to 5ul Fura2 AM stock (final concentration 10uM).

- Preparation of ATP stock solution (100mM)

  - ATP (Sigma A6419), 1g, was dissolved in 18.15ml distilled water and stored at -20°C. Prior using it as positive control in the calcium imaging experiment, 50ul of ATP stock solution was added to 50ml buffer to achieve final concentration 100uM.

ii. Method for calcium imaging

At day 6 or day 10 differentiation, the adipocytes-coated coverslip was transferred to a petri dish and washed for 3 times in appropriate buffer. After that, the cells were loaded with 10uM Fura2 AM for 30 minutes in the dark at 37°C. The coverslip was then washed again with buffer, placed on the coverslip holder and viewed with a Leica DMIRB inverted microscope coupled to Andor IQ Bioimaging system equipped with Hamamatsu DCAM digital camera. The cells were continuously perfused with buffer at 28°C and fluorescent images were obtained (at 510nm) upon sequential excitation with 340nm followed by 380nm light. After establishing baseliner 340/380 ratios, a selective TRPV4 agonist, GSK101 100nM and TRPV1 agonist, capsaicin 1μM were perfused onto the cells in normal/high glucose condition with the presence/absence of 2mM extracellular calcium containing buffer. The results were analysed using Excel and presented as the 340/380 fluorescent intensities ratio collected at 510nm.

2.9) **Statistical Analysis**

All statistical analyses were performed using GraphPad Prism software. Data are presented as mean ± SEM. Statistical comparisons of different groups were made using independent student t-test. Analysing the outcome of each dependent variables (*lcn2* and *fabp4*) with each independent factor (duration of

adipogenesis, glucose concentration media and TRPV4 treatments) requires one-way analysis of variance (ANOVA) and Bonferroni's multiple comparison post-hoc test. Meanwhile, the interaction of 2 independent variables (glucose concentration media and TRPV4 treatments) on the outcome of dependant variables (*lcn2, fabp4, pparγ, pgc1α and ccl2*) were analysed using two-way ANOVA. A *p* value < 0.05 was considered as statistically significant.

The images analyses for protein expression and secretion were evaluated by Image J software. The statistical outcomes were assessed by one-way ANOVA by measuring loading control protein in cell lysate samples as reference. All effects were statistically significant when *p* value <0.05.

CHAPTER 3:

CELLULAR ENVIRONMENT THAT AFFECT ADIPOCYTE LIPID CHAPERONE PROTEINS SIGNALLING

3) Introduction

Over the past decade, a wide spectrum of human tissues has been identified to secrete LCPs into the circulatory system. Among them, the most notable examples are fatty acid binding proteins (FABPs)(Furuhashi & Hotamisligil, 2008), lipocalin2 (LCN2) (Yan et al., 2007) and fetuin A (FetA) (Stefan & Häring, 2013). Whilst the presence of these intracellular proteins in the circulation was initially assumed to occur due to their release following tissue injury and cell death, numerous studies have shown that a variety of tissues, including liver and adipose tissues, actively secrete these proteins (Cao et al., 2013; Foucaud et al., 1999; Schlottmann et al., 2014).

These LCPs can influence metabolic and inflammatory processes as they possess the capability to activate cellular signalling pathways, such as FABP4 and 5 that are involved in the activation of immune cells, namely macrophages (Furuhashi et al., 2008; Hui et al., 2010). While FetA has been presumed as an endogenous ligand for TLR4 and controversially, saturated FAs may induce insulin resistance when bound to FetA by activating TLR4 (Pal et al., 2012). Despite serving as clinical biomarker in certain diseases, such as acute

pancreatitis (Chakraborty, Kaur, Guha, & Batra, 2012), multiple sclerosis (L. et al., 2012) and cardiovascular disease (Lindberg et al., 2014), the function of LCN2 in obesity-induced insulin resistance still remains elusive, for it acts either as pro or anti-inflammatory factor (Guo et al., 2010; Y. Wang et al., 2007; Yan et al., 2007; J. Zhang et al., 2008).

Hyperglycaemia and hypoxia, among others, are known as factors implicated in pathogenesis of metabolic diseases. Hyperglycaemia induced *fabp4* gene expression observed among rats treated with fructose rich diet (B. Qin & Anderson, 2011); whereas *fabp4*$^{-/-}$ mice exhibited improvement in systemic glucose homeostasis, and protection against insulin resistance, dyslipidaemia and atherosclerosis (Makowski et al., 2001). As for LCN2, increased glucose concentration, together with presence of high insulin, induced its secretion (Y. Zhang et al., 2014). In conjunction to that, *lcn2*$^{-/-}$ mice were able to impede obesity-associated insulin resistance, hyperglycemia and hyperinsulinemia (I. K. Law et al., 2010).

In the human body, blood supply and cardiac output to AT are not increased in obese individuals, despite increased AT mass (Trayhurn, Wang, & Wood, 2008). Therefore, certain local areas of AT may receive less oxygen due to this limitation (Lolmede, de Saint Front,

Galitzky, Lafontan, & Bouloumie, 2003). This leads to increment of hypoxia inducible factor 1α (HIF-1α) activity in AT (He et al., 2011). FABP4 secretion is also reported to be upregulated in hypoxic state (B. Wang, Wood, & Trayhurn, 2008; Wu et al., 2014), but reports of hypoxic effect on LCN2 is limited.

Apart from the factors that affect their secretion in the entire body circulation, the mode of secretion of these LCPs has yet to be elucidated.

FABP4 protein was believed to be secreted via non-classical pathway since its secretion was unaffected despite treatment of brefeldin A and monensin A; endoplasmic reticulum-Golgi apparatus inhibitors (Garay-Rojas, Harper, Hraba-Renevey, & Kress, 1996; Kralisch et al., 2014; Schlottmann et al., 2014). Although the secretion was released via exosomes and microvesicles (MVs), the production was scarce, in comparison to that of non-exosomes and MVs fractions (Mita et al., 2015).

Mode of secretion for LCN2, on the other hand, has not been documented elsewhere, to date. Its other isoform, which is also in the lipocalin family, RBP4 is secreted via exosome-like vesicles (Z.-b. Deng, Poliakov, Hardy, Clements, Liu, Liu, Wang, Xiang, Zhang, & Zhuang, 2009). Since both share a common tertiary structure

known as 'lipocalin fold', which facilitates binding of hydrophobic small molecules, such as lipids, it is presumed that LCN2 is also secreted via exosome.

3.1) **Objectives**

The objectives of this study were:

1. To establish a primary rat adipocytes culture model that can optimally survive and function in NG and HG media
2. To determine the mRNA expression of LCPs, such as *fabp4*, *lcn2* and *fetA*, at different duration of adipogenesis in different glucose concentration media, as well as in normoxic and hypoxic states, using qRT-PCR
3. To determine the protein expression and secretion of LCPs in different duration of adipogenesis, glucose concentrations and oxygen levels
4. To verify the presence of exosomes from CM

3.2) **Experimental design**

In comprehending these LCPs signalling in primary rat adipocytes and in determining the effect of oxygenation and glucose concentration upon adipocyte-related LCPs gene expression (*fabp4*, *fabp5*, *lcn2* and *fetA*), the differentiated adipocytes were cultured in 12-well plates and classified into 2 groups. The first group was fed

with NG media (5.5mM/l glucose concentration) and the second group was given HG media (17.5mM/l glucose concentration). Both groups were monitored in 37°C incubator in normoxic condition with 21% oxygen (O_2). After 9 day of adipocytes differentiation, one group with NG media and one group with HG media were incubated in hypoxic chamber with 2% O_2, 5% carbon dioxide (CO_2) and 93% nitrogen (N_2) for 24 hours prior to RNA extraction. The 24-hour conditioned media (CM) of both NG and HG that received hypoxic treatment (and normoxic condition as control) were collected for protein precipitation and exosome isolation.

3.3) **Results**

3.3.1) Micrographs of primary rat adipocytes culture from WAT

The primary *in vitro* model of adiposity was performed by isolating SVF cells from WAT biopsies, as described in Chapter 2 (sub-heading 2.1). The initial purpose of this project is to observe the cells in proliferation and differentiation phases in order to estimate the duration of cell sustenance. Next, cell viability is monitored in NG and HG states.

The primary preadipocytes cultures monitored from the proliferation phase (day 1) displayed elongated flat, phase-dark and spindle-

shaped cells in DMEM/Ham F12 plating media (see Figure 3.1 a). The proliferative phase lasted for about 4 to 5 days and as the cells confluency reached 80-90%, they were incubated in differentiation media (see Figure 3.1 b). The early phase of differentiation exhibited morphological changes of the cells as they changed from elongated fibroblast-like cells into rounded cells (see arrow in Figure 3.1 c). The mature adipocytes filled with lipid droplets as evidence by well-defined rim and 'shiny' rounded surface (see Figure 3.1 d). As the cells aged, they easily detached from the plate and became suspended cluster (see arrow in Figure 3.1 e). At day 17 differentiation, the number of cells remarkably reduced, possibly due to change of media, as the cells appeared to be loosely attached to the plate. The lipid droplets grew, from multi-lobulated lipid into one central lipid droplet, which gave rise to monovacuolar appearance (see arrow in Figure 3.1 f).

Apart from those, cells treated in NG and HG media displayed similar morphological appearance after oil red 'O' staining, either at day 6 or day 10 adipocytes differentiation (Figure 3.2).

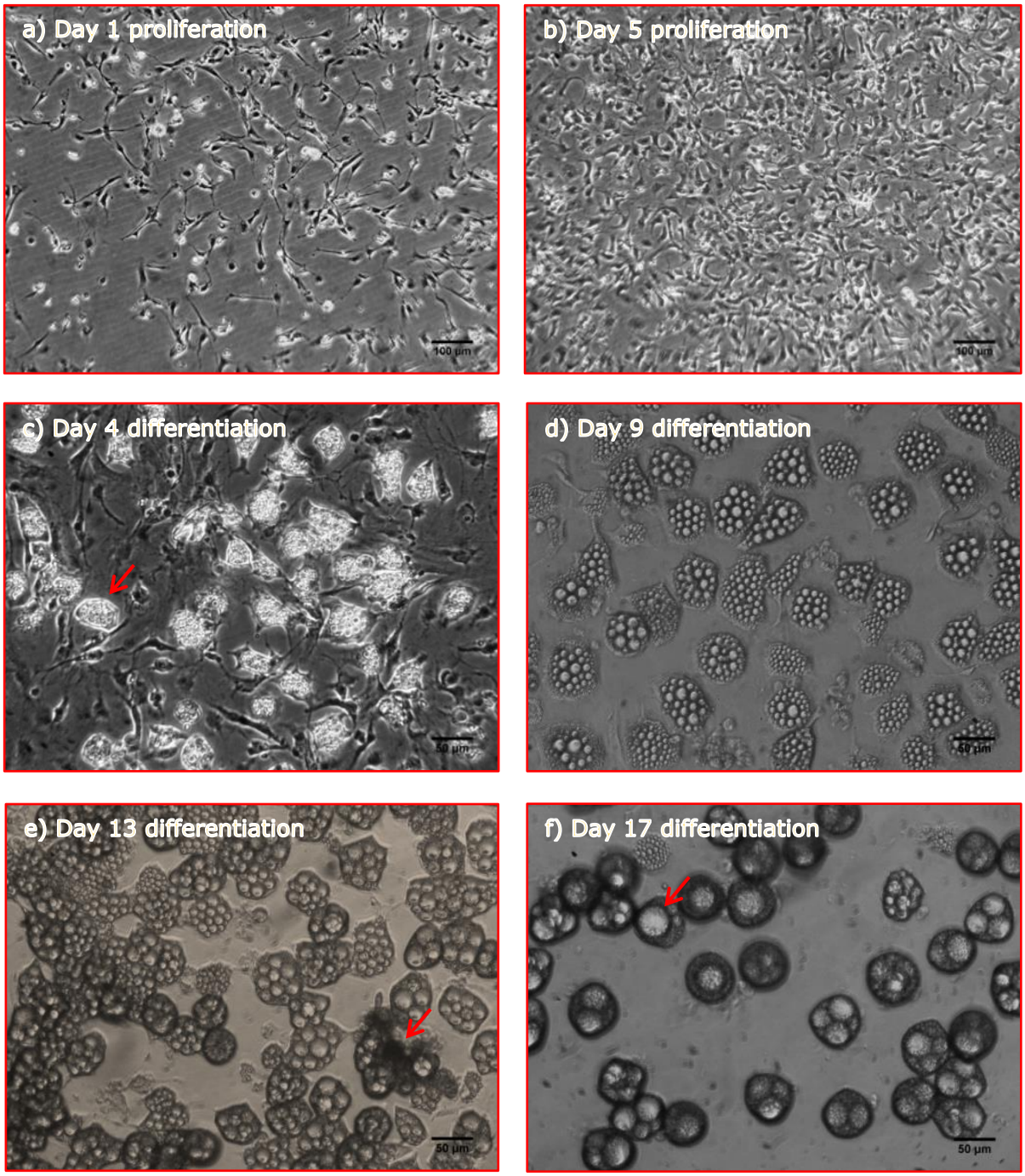

Figure 3.1: Phase contrast pictures of cultured primary rat adipocytes in proliferation and differentiation phase. (a, b) Primary adipocytes in proliferation phase maintained in DMEM/Ham F12 with 10% FBS (images acquired using phase-contrast microscope at 10x magnification (Leica). (c, d, e, f) Primary adipocytes in differentiation phase maintained in SFM. Images were captured using phase-contrast microscope at 20x magnification (Leica).

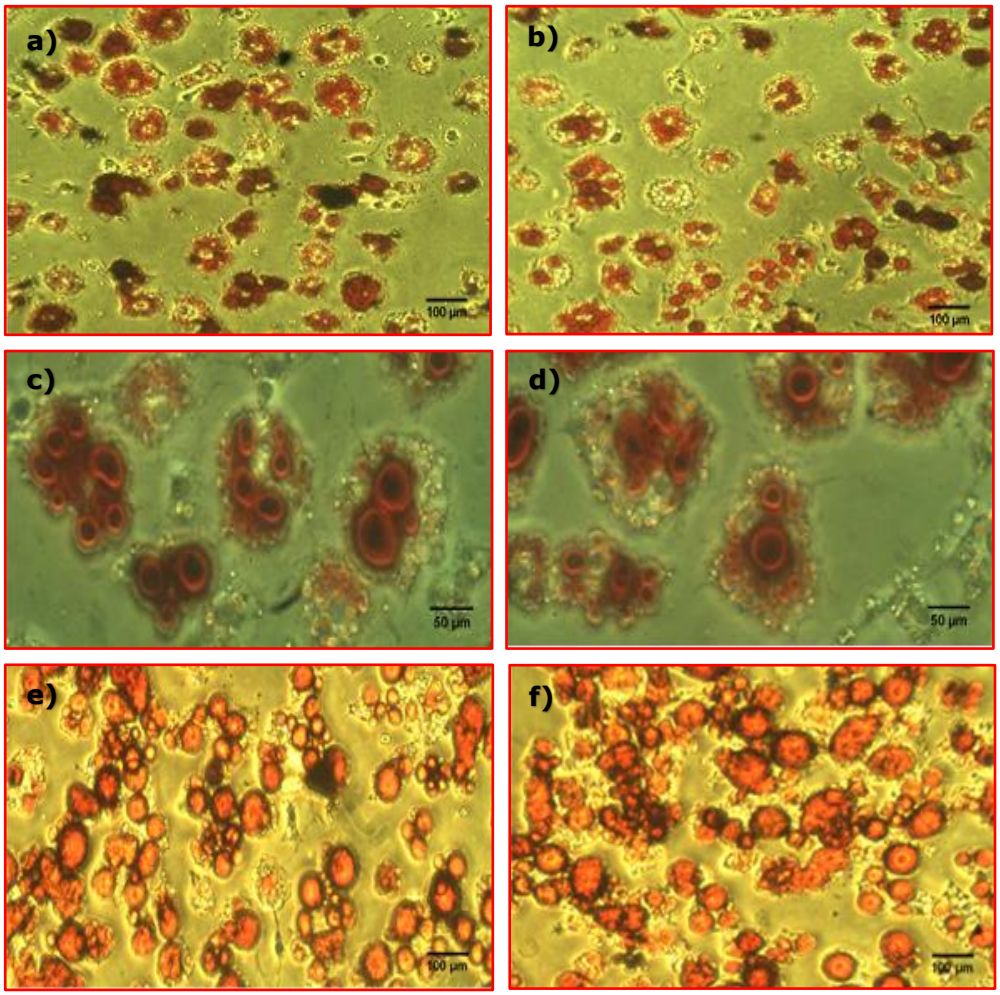

Figure 3.2: Micrographs of cultured primary rat adipocytes stained with oil red 'O' in NG and HG media. (a, b, c, d) Day 6 differentiation of primary adipocytes maintained in serum free DMEM with NG, 5.5mmol/L (left panel) and HG, 17.5mmol/L (right panel). (e, f) Primary adipocytes at day 10 differentiation maintained in the same media; left panel with NG and right panel with HG. Images were captured using phase-contrast microscope at 10x (a, b, e, f) and 20x (c, d) magnification (Leica).

3.3.2) Distinghuishing protein secretion from cell lysis

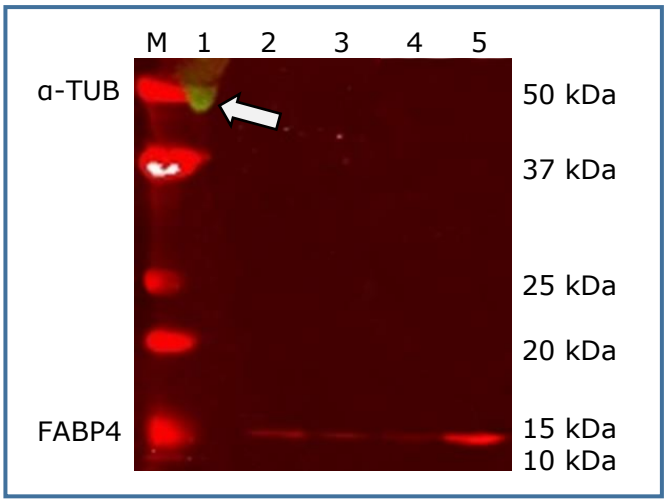

Figure 3.3: Protein extraction from skeletal muscle cell lysate served as a control to detect intracellular component in adipocytes CM. Lane 1: Green band (white arrow) represents α-tubulin (50kDa) from RIPA preparation using skeletal muscle cell lysate. Red bands at 15 kDa denote FABP4 secretion from TCA preparation using day 10 cultured adipocyte NG (lane 2-3) and HG (lane 4-5) CM. M denotes protein marker. This experiment was repeated 3 times using 1-2 independent biological replicates obtained from 3 different preparations.

FABP4 is among adipocyte-derived LCPs that is highly present intracellularly. Therefore, in order to determine that the presence of FABP4 protein in CM was not a consequence of adipocytes rupture or lysis, immunoblotting using cell lysate (CL) from skeletal muscle (lane 1) and TCA protein precipitation using CM from day 10 adipocytes differentiation in NG and HG samples (lane 2-5) had been employed. The presence of α-tubulin band in lane 1 (green band showed by white arrow in Figure 3.3), unlike those in other lanes, showed that the FABP4 protein was secreted from undamaged cells.

3.3.3) Effects of glucose and duration of adipogenesis on LCN2 expression and secretion

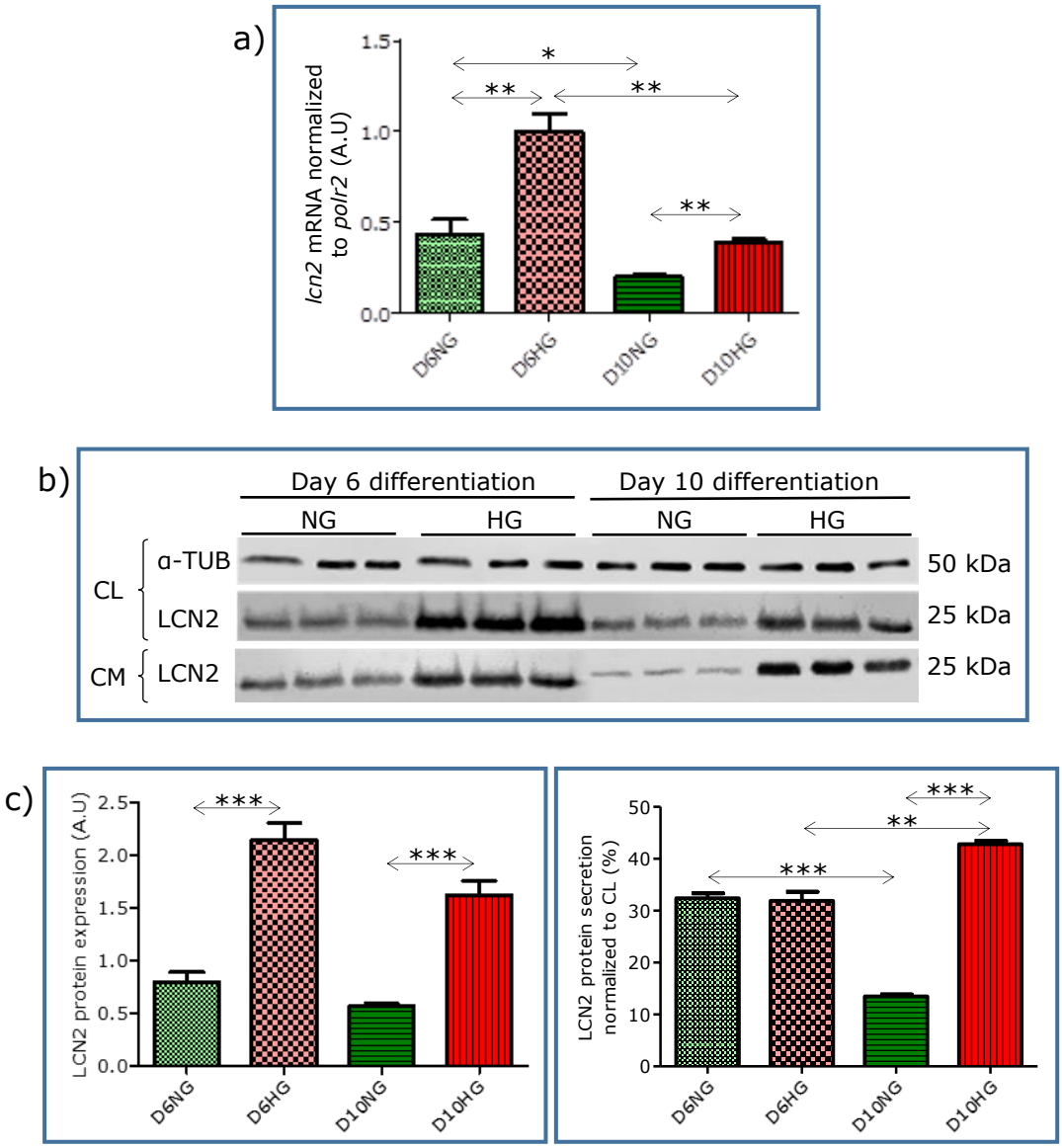

Figure 3.4: LCN2 mRNA expression, protein expression and secretion from primary rat adipocytes in different glucose concentration media and duration of adipogenesis. (a) qRT-PCR analysis of *lcn2* mRNA expression on day 6 and day 10 differentiation in NG and HG media. (b) WB results for LCN2 protein expression from cell lysate and protein secretion from CM. The results were obtained from at least three independent experiments; n=3 or 4 in each preparation. (c) Statistical analysis of LCN2 protein expression and secretion using Image J. The data for gene and protein were analysed by using one-way ANOVA, followed by Bonferroni's post-hoc test and expressed as mean ± SEM; *p<0.05, **p<0.01, ***p<0.001.

In order to understand the regulation of adipocytes LCPs in NG and HG media, the expression and secretion of LCN2 and FABP4 were monitored at day 6 and day 10 differentiation. This was done to identify and distinguish any changes occurred during progression of adipogenesis.

It was noted that day 6 differentiated cells showed an increment in *lcn2* mRNA expression as compared to their counterpart, wherein HG media also accentuated similar expression (see Figure 3.4 a).

The LCN2 protein expression and secretion were in accordance to its gene expression (see Figure 3.4 b and c).

3.3.4) Effects of glucose and duration of adipogenesis on FABP4 expression and secretion

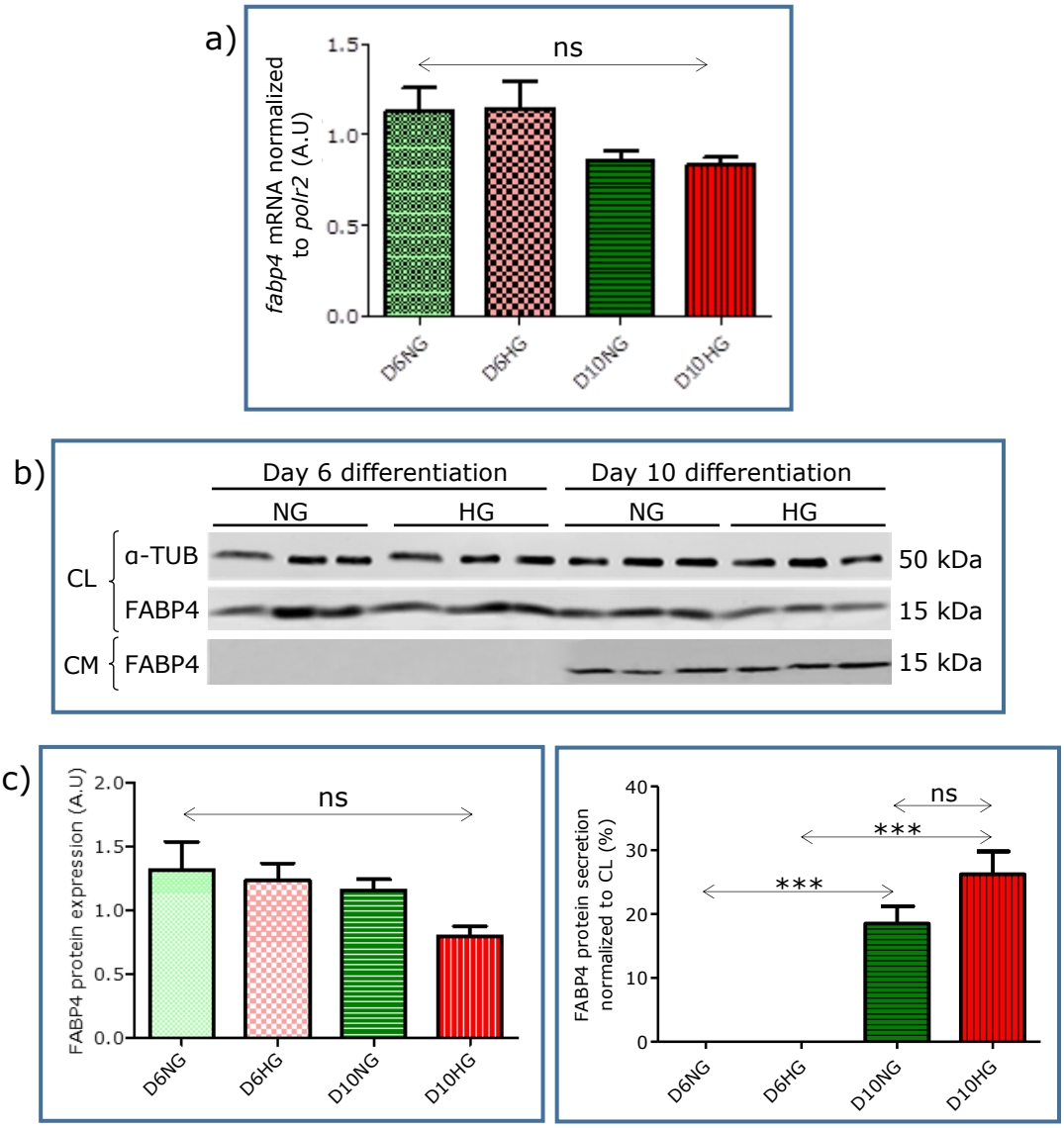

Figure 3.5: FABP4 mRNA expression, protein expression and secretion from primary rat adipocytes in different glucose concentration media and duration of adipogenesis. (a) qRT-PCR analysis of *fabp4* mRNA expression on day 6 and day 10 differentiation in NG and HG media. (b) WB results for FABP4 protein expression from cell lysate and protein secretion from CM. The results were obtained from at least three independent experiments; $n=3$ or 4 in each preparation. (c) Statistical analysis of FABP4 protein expression and secretion using Image J. The data for gene and protein were analysed by using one-way ANOVA, followed by Bonferroni's post-hoc test and expressed as mean ± SEM; ***$p<0.001$, ns=not significant.

The *fabp4* gene expression seemed higher among day 6 groups as compared to day 10, but it failed to attain its significant level. In addition, HG did not affect *fabp4* expression (see Figure 3.5 a).

Similar response was also observed in FABP4 protein expression. However, FABP4 secretion was not detected at day 6, only to be observed at day 10 with comparable protein bands between NG and HG (see Figure 3.5 b and c).

3.3.5) Effect of glucose and duration of adipogenesis on *pparγ* expression

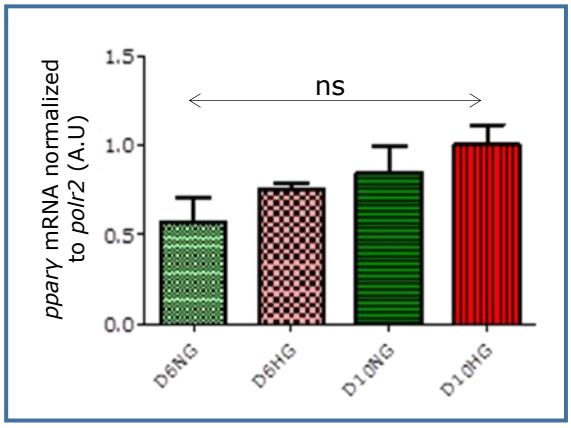

Figure 3.6: Results of *pparγ* gene expression from primary rat adipocytes treated in NG and HG media at different duration of adipogenesis. The results were obtained from three independent experiments; *n*=3 or 4 in each preparation. The data were analysed by using one-way ANOVA, followed by Bonferroni's post-hoc test and expressed as mean ± SEM, ns=not significant.

PPARγ is known as terminal adipogenesis marker and critical for adipocytes differentiation. Although its expression pattern noted as increasing in trend among HG and day 10 groups, but the level did not attain significant level.

3.3.6) Effects of glucose and oxygenation on LCN2 expression and secretion

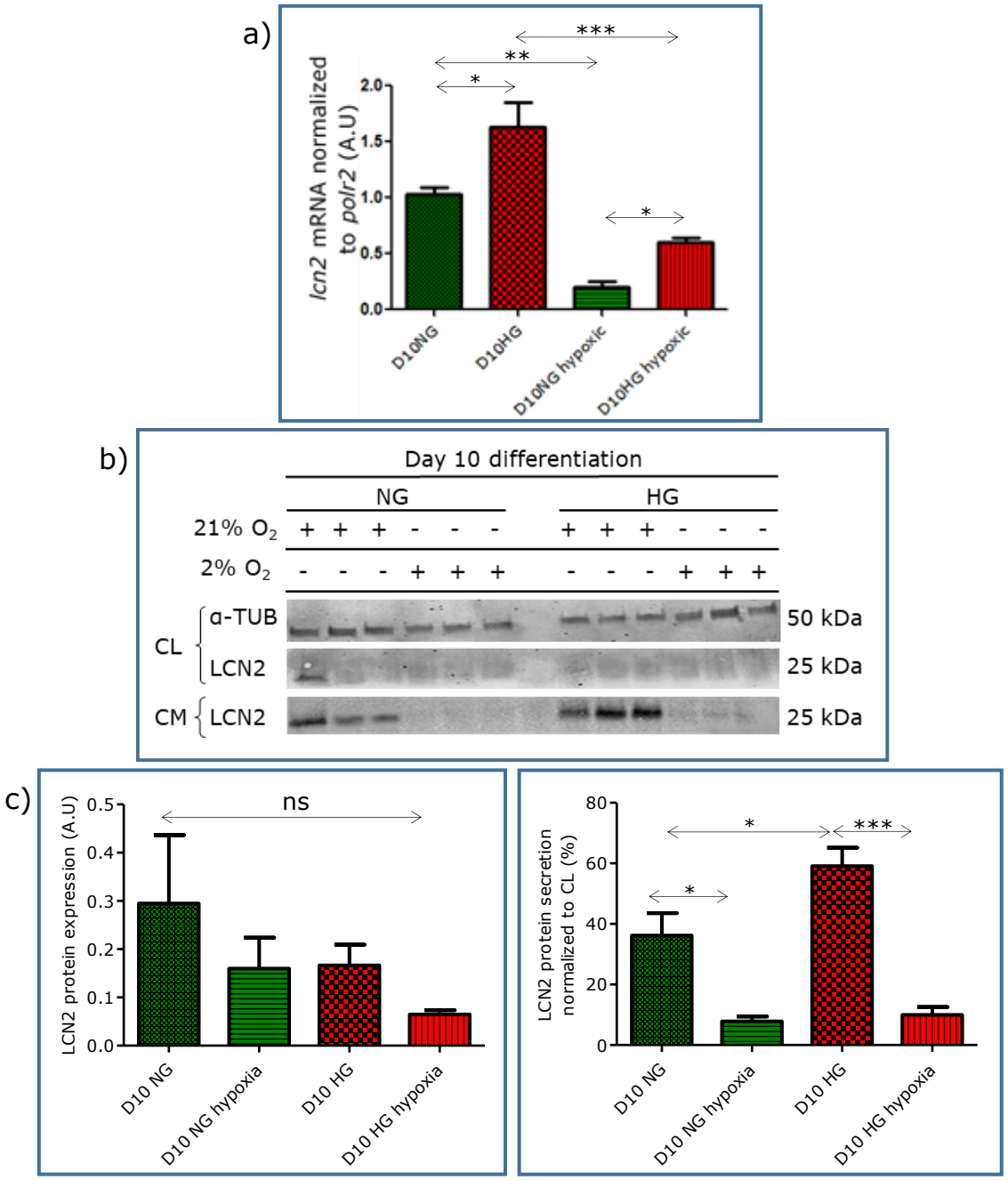

Figure 3.7: LCN2 mRNA expression, protein expression and secretion at day 10 adipocytes differentiation. (a) qRT-PCR analysis of *lcn2* mRNA expression in normoxia/hypoxia with NG/HG media. (b) WB results for LCN2 protein expression from CL and protein secretion from CM. The results were obtained from at least three independent experiments; n=3 or 4 in each preparation. (c) Statistical analysis of LCN2 protein expression and secretion using Image J. The data for gene and protein were analysed by using one-way ANOVA, followed by Bonferroni's post-hoc test and expressed as mean ± SEM; *p<0.05, **p<0.01, ***p<0.001.

In this experiment, presence of 2% oxygen level significantly caused reduction in *lcn2* mRNA expression, as compared to cells treated under 21% oxygen level; and increment of glucose concentration from 5.5mM/l to 17.5mM/l remarkably increased almost 2 fold of its expression (see Figure 3.7 a).

LCN2 protein expression showed poor signal and revealed insignificant difference between the groups. Whereas its secretion was diminished in hypoxic condition. Although HG normoxic group showed significant increase in protein secretion as compared to NG normoxic group, no significant different observed among hypoxic groups albeit difference in their glucose concentration media (see Figure 3.7 b and c).

3.3.7) Effects of glucose and oxygenation on FABP4 expression and secretion

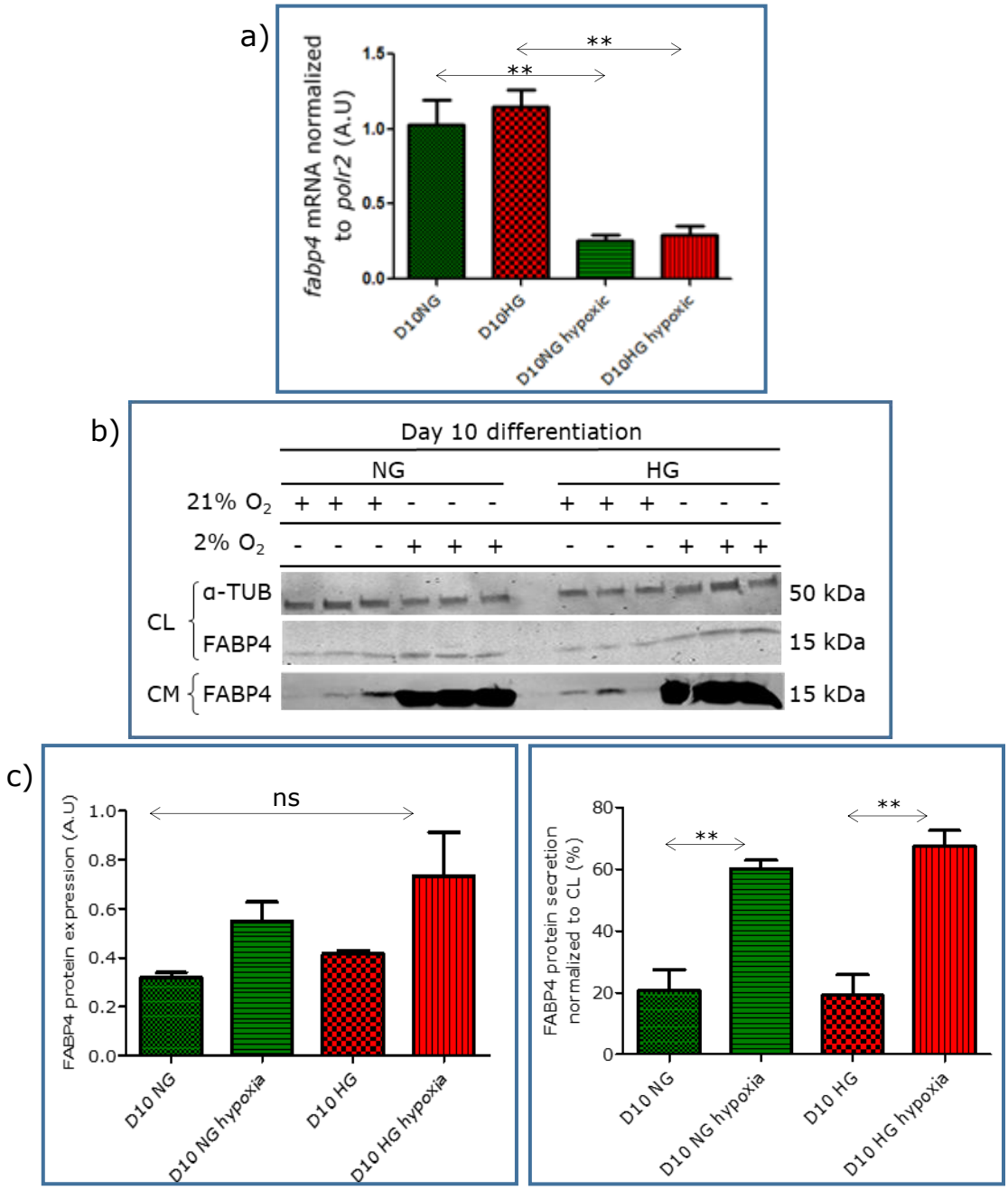

Figure 3.8 FABP4 mRNA expression, protein expression and secretion at day 10 adipocytes differentiation. (a) qRT-PCR analysis of *fabp4* mRNA expression in normoxia/hypoxia with NG/HG media. (b) WB results for FABP4 protein expression from CL and protein secretion from CM. The results were obtained from at least three independent experiments; n=3 or 4 in each preparation. (c) Statistical analysis of FABP4 protein expression and secretion using Image J. The data for gene and protein were analysed by using one-way ANOVA, followed by Bonferroni's post-hoc test and expressed as mean ± SEM; **p<0.01, ns=not significant.

Reduction of *fabp4* gene expression significantly observed among groups treated in hypoxic condition, while glucose concentration did not demonstrate similar effect as seen in *lcn2* expression (see Figure 3.8 a).

Although FABP4 protein expression showed insignificant difference between the groups, but it followed similar pattern as its secretion, whereby FABP4 was found to be highly secreted in hypoxic state. HG did not show notable effect on its expression and secretion as it did towards LCN2 (see Figure 3.8 b and c). However, FABP4 protein expression and secretion were not corresponded to its mRNA expression.

3.3.8) Effect of glucose and oxygenation on *glut4* expression

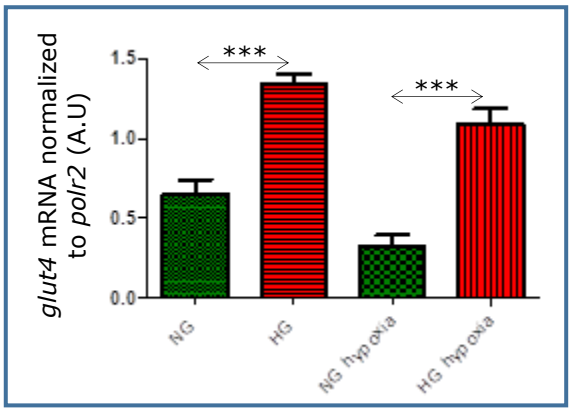

Figure 3.9: *glut4* mRNA expression at day 10 adipocytes differentiation in NG and HG media treated in normoxic and hypoxic conditions for 24 hours. The results were obtained from at least three independent experiments; n=3 or 4 in each preparation. Data were analysed using independent t-test with mean ± SD, ***p<0.001.

In order to analyse the impact of hyperglycaemia and hypoxia that were implicated in the pathogenesis of metabolic diseases, the expression of *glut4* was determined as it plays role in regulating whole body glucose homeostasis. Hyperglycaemia significantly induced *glut4* mRNA expression both in HG (M=11.39, SD=1.99) and HG hypoxic (M=9.43, SD=0.24) states; t(6)=3.6, p=0.001, t(6)=10.54, p=0.001 as compared to their counterparts. Whereas *glut4* mRNA expression in hypoxic groups did not exert any significant differences upon comparison to normoxic groups.

As for fetuin A that was mentioned earlier, there was no significant amplification observed from the samples used in all the above experiments (results further elaborated in Appendix C).

3.3.9) Protein detection from exosome isolated from HG CM

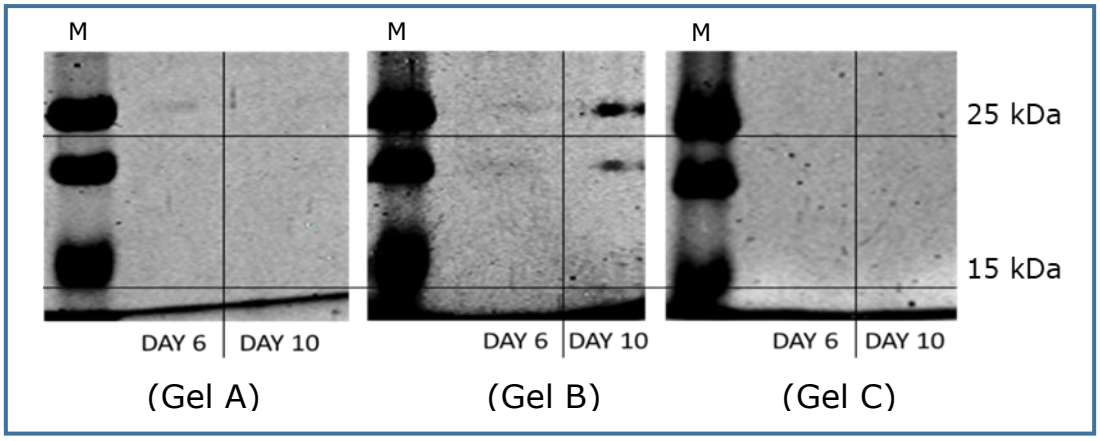

Figure 3.10: Exosomal protein was poorly visualised in coomassie blue staining and inconsistent throughout these 3 gels. This experiment was repeated 3 times (represented by Gel A, B and C) using 3 sets of biological replicates obtained from 3 different preparations. M represent protein marker, whereas 15 kDa and 25 kDa represent protein molecular weight of interest.

This experiment was intended to extract exosomal protein isolated from CM in order to investigate secretion mode of LCPs. Since the secretion pattern of LCN2 and FABP4 have been determined (see Figure 3.4 and 3.5), HG media from day 6 and day 10 preparation were used. However, the exosome samples obtained from 3 independent experiments prepared separately revealed unreliable outcomes as protein bands were poorly seen, with only one (see Figure 3.10: Gel B) out of three gels showed bands at about 20 and 25kDa.

3.3.10) LCN2 and FABP4 protein from supernatant, shed MVs and exosome

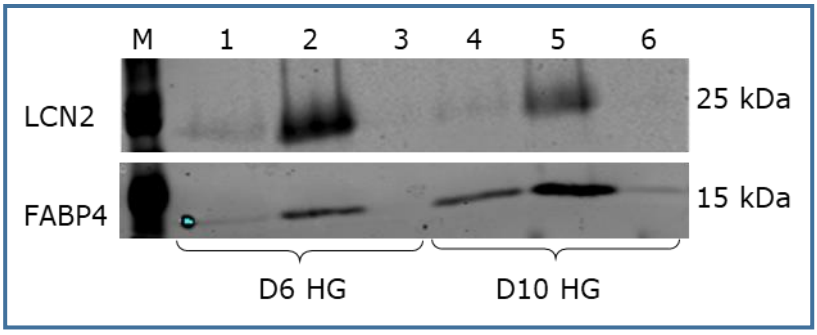

Figure 3.11: Three byproduct protein samples obtained from exosome isolation preparation. HG media from day 6 (lane 1, 2, 3) and day 10 (lane 4, 5, 6) adipocytes differentiation were used to verify the presence of LCN2 and FABP4 proteins. Protein bands from supernatant (lane 1 and 4), shed MVs from CM post ultracentrifugation (lane 2 and 5) and exosome (lane 3 and 6) were observed. M refers to protein marker. The above blot represented $n=1$ and has been repeated 3 times using 3 sets of different biological replicates obtained from 3 different preparations.

In the attempt of ascertaining the presence of LCN2 and FABP4 in exosome samples, immunoblotting using CM samples was performed. Protein precipitated from (i)supernatant post-serial centrifugation, protein from (ii)shed MVs collected post-ultracentrifugation, and lastly, (iii)exosomal protein retained in the final pellet, were compared. Samples containing protein from supernatant (lane 1 and 4) only revealed FABP4 protein at day 10 differentiation. While shed MVs protein (lane 2 and 5) in both day 6 and day 10 HG showed LCN2 and FABP4 bands prominently. Whereas LCN2 and FABP4 protein bands were not displayed among exosome samples (lane 3 and 6).

3.3.11) Identifying exosome using marker

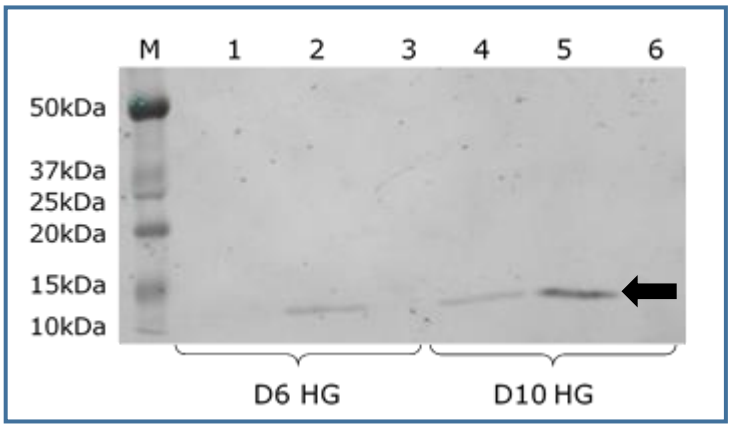

Figure 3.12: Re-blotting of the membrane performed with CD63, an exosome marker, in order to identify presence of exosome in the final product of the isolation. M refers to protein marker. The above blot represented *n*=1 and has been repeated 3 times using 3 sets of different biological replicates obtained from 3 different preparations.

Since protein band from exosome sample was not visualized via immunoblotting, an exosome marker was used and re-blotting of the same membrane, from that shown in Figure 3.11, was carried out with CD63 antibody. Since molecular weight of LCN2 and CD63 are almost similar, different channels were used to identify the protein. The expected CD63 molecular weight was 24kDa with potential glycosylation site approximately 30-50kDa. Unfortunately, no protein band was present at the expected molecular weight. The bands visualized in the membrane was FABP4 protein (see arrow in Figure 3.12).

3.3.12) EM imaging from exosomal pellet

a) b)

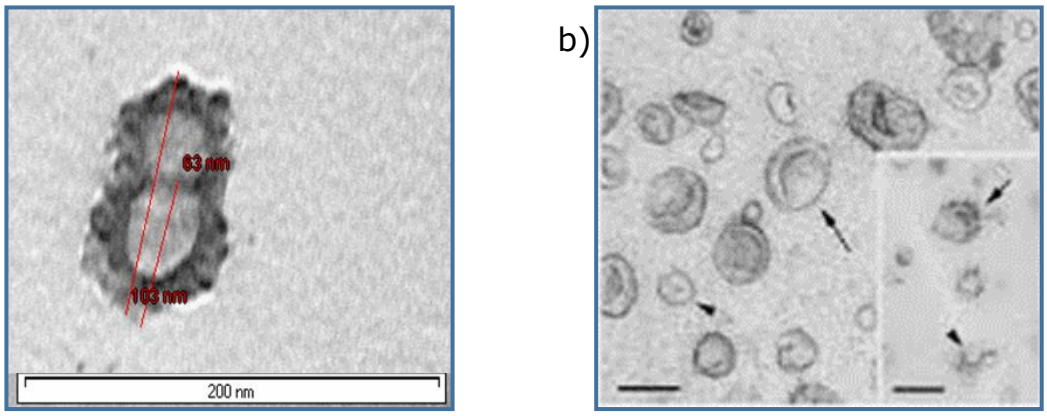

Figure 3.13: (a) Image presumed as exosome obtained from adipocytes HG CM in this experiment visualized using EM at 80 kV. (b) Electron-microscopic observation of whole-mounted exosomes purified from mouse dendritic cells taken from (Thery, Amigorena, Raposo, & Clayton, 2006). Arrows indicate exosomes, showing cup-shaped membrane vesicles of 50 to 90 nm (scale bar=100 nm).

Hence, detection of exosome from CM was continued by imaging using scanning electron microscopy (SEM), as depicted in Chapter 2 (sub-heading 2.7). Nonetheless, the image captured (see Figure 3.13 a) did not turn out as described by the others in protocols (see Figure 3.13 b), although the size measured was within the expected range, between 40 to 100nm.

3.4)**Discussion**

3.4.1) Primary rat adipocytes culture model

The initial part of the project is to establish a primary rat adipocyte culture by observing the progression of cell culture treated in varying glucose concentration media at different duration of adipogenesis

(see Figure 3.1). The cells lasted not more than 13 days in differentiation state and they were morphologically similar, either in NG or HG media. Previously, comparison of adipocyte in NG and HG media has been done using human AT by other researchers (Cheng, Hsieh, Lai, & Young, 2016; Peshdary, Gagnon, & Sorisky, 2016; Rønningen, Shah, Reiner, Collas, & Moskaug, 2015). Cheng *et al*. did not observed any morphological difference in adipocyte treated with NG and HG media, assessed by oil red 'O' dye (Cheng et al., 2016). The same finding was also observed in this study as shown in Figure 3.2. While Peshdary *et al*. investigated the intracellular TGs accumulation and adipogenic protein expression in varying glucose concentration media, and failed to observed any change in response (Peshdary et al., 2016). Both cells treated in NG and HG media seemed to demonstrate similar duration of adipocyte differentiation (Rønningen et al., 2015).

Since FABP4 is an adipogenic marker and highly present in adipocyte cytosol, it is important to ensure that protein precipitated from CM was secreted extracellularly, rather than as the result of cell disruption. Skeletal muscle was used as control cell lysate, and α-tubulin band was expected to be seen in the presence of intracellular component. Upon post-incubation with secondary antibodies, α-tubulin band was observed in the skeletal muscle sample, but not in the other lanes where protein from adipocyte CM were applied (see

Figure 3.3). This experiment showed that adipocyte treated with varying glucose concentrations in different duration of adipogenesis were intact. Skeletal muscle cell lysates functioned as negative control in this experiment since FABP4 is minimally present in skeletal muscle, only expressed amongst endurance-trained individuals (Fischer et al., 2006). Hence, it was expected that the skeletal muscle cell lysate did not exert FABP4 protein band.

3.4.2) Effects of glucose and duration of adipogenesis upon LCPs signalling

In order to understand how adipocyte bioactive molecules response towards various micro-environment factors, this study has reported for the first time, regulation of LCN2 and FABP4 mRNA expression, protein expression and secretion from day 6 and day 10 differentiation in NG and HG media.

i. LCN2 mRNA expression, protein expression and secretion

lcn2 mRNA expression was highly expressed in HG groups, in which day 6 group displayed higher expression than that at day 10. It showed that *lcn2* mRNA level was influenced by glucose concentration and duration of adipogenesis (see Figure 3.4 a). Zhang *et al*. and Yan *et al*. also reported high *lcn2* mRNA expression at early phase of adipocytes differentiation, which is similar as in this study

(Yan et al., 2007; J. Zhang et al., 2008). Albeit the outputs, the role of LCN2 in adipogenesis remains understudied.

While LCN2 protein expression showed upregulation in HG groups as compared to NG groups, observed at both day 6 and day 10. As for its secretion, as expected, corresponded to its mRNA and protein expression (see Figure 3.4 b and c). These could be mainly because of different glucose concentration and/or insulin levels. Zhang *et al.* documented similar findings in 3T3-L1 cells, as they found that LCN2 protein expression was stimulated by insulin in dose-dependent manner, which significantly increased in the presence of HG concentration, but abolished in NG media (Y. Zhang et al., 2014). They believed that glucose metabolism and NF-κB signalling activation triggered *lcn2* transcription. This was proven in the reduction of LCN2 protein expression and secretion, following inhibition of NF-κB pathway by aspirin and BAY 11-7082. The role of NF-κB pathway in *lcn2* transcription is also supported by others (Guo et al., 2014; P. Zhao, Elks, & Stephens, 2014).

ii. FABP4 mRNA expression, protein expression and secretion

fabp4 mRNA expression was high at day 6 as compared to day 10, however HG did not affect its expression. Although higher mRNA expression noted at day 6, the difference was insignificant relative to its counterpart (see Figure 3.5 a). Similarly, FABP4 cytosolic

protein corresponded to its mRNA expression and did not show significant variance among the groups (see Figure 3.5 b). Higher expression at day 6 could be explained as FABP4 was expected to serve as carrier protein in transporting FFAs to cellular compartment for intracellular use, such as oxidation, re-esterification, lipid storage and translocation into nucleus for gene expression regulation, particularly in early phase of differentiating cells (Furuhashi & Hotamisligil, 2008; Mita et al., 2015). Jessen *et al*. also reported that *fabp4* mRNA expression in adipocytes was high from day 3 to day 5, but decreased from day 7 onwards (Jessen & Stevens, 2002).

Despite of higher FABP4 mRNA and protein expression at day 6, no protein secretion was observed. Instead, FABP4 secretion was only noted at day 10 with almost equivalent band intensities between NG and HG groups (see Figure 3.5 b). FABP4 is known as an adipogenic marker secreted by mature adipocytes (Satish et al., 2015; Schlottmann et al., 2014). However, the reason for the undetected FABP4 secretion at early stage of differentiation despite of measurable mRNA expression is still obscure. This could be due to poorly identified nuclear localization signal in primary sequence of *fabp4* and lack of N-terminal secretory signal that is responsible for classical secretory (Furuhashi & Hotamisligil, 2008; Furuhashi et al., 2014). Further studies could be done to explore extensively factors that contribute to gene transcription and protein translation in early

stage of adipocytes differentiation, and possibly different mode of secretion among premature differentiating adipocytes.

PPARγ refers to as a late marker of adipogenesis, as it is responsible for terminal differentiation of adipocytes. In the outcome of this study (see Figure 3.6), *pparγ* failed to display any significant variance between day 6 and day 10, although the latter showed an increased expression pattern. Therefore, this study could not determine that day 10 differentiation was in late phase of adipogenesis, and FABP4, which served as general marker of differentiation, was released after day 6 differentiation. It is essential to verify these genes as early, late or general marker of adipogenesis as it helps researchers to identify their role throughout differentiation process (Ambele, Dessels, Durandt, & Pepper, 2016; Ullah et al., 2013).

3.4.3) Effects of glucose concentration and oxygenation upon LCPs signalling

lcn2 and *fabp4* were the genes of interest in this study as they were thought to play a role in initiation and development of obesity and inflammation in adipocytes. However, their exact function in affecting metabolic signalling and lipid metabolism are still unclear. Thus, the effects of concurrent cellular environment changes,

involving glucose concentration and oxygenation, upon these LCPs in adipocyte, had been determined since these two conditions, among others, are involved in the pathogenesis of metabolic diseases such as diabetes mellitus.

i. LCN2 mRNA expression, protein expression and secretion

Studies on *lcn2* gene expression in hypoxic adipocyte are still underdeveloped as compared to its role in fostering tumorigenesis in cancer research and inflammation in ischemic/reperfusion (I/R)-related disease (Cui, Yang, & Zhang, 2011; F. et al., 2007; Rodvold, Mahadevan, & Zanetti, 2012). In I/R study on transplanted heart, *lcn2* expression was found to be decreased after hypoxic treatment (F. et al., 2007).

Whereas others presumed that LCN2 could be enhance in low cellular oxygen level, considering that LCN2 and transferrin are both an iron-trafficking protein; and the latter showed elevation of its expression in response to hypoxia (Holden et al., 2014). In addition to that, Bricambert *et al.* discovered increment of *lcn2* mRNA expression in 3T3-L1 cells treated with 1% oxygen for 12 hours, which is different compared to findings in this experiment (see Figure 3.7 a) (Bricambert et al., 2016). They suggested that cAMP response element-binding protein (CREB) was induced by hypoxia. Upon activation, it induced activities of transcription factor 3 (ATF3) and

subsequently impeded insulin-induced glucose uptake as evidenced by decreased *glut4* expression. Concomitantly, stimulation of ATF3 also enhanced other adipokines, such as LCN2 and IL-6, but the mechanism was not explained.

LCN2 secretion was also diminished in hypoxic groups, both in NG and HG groups (see Figure 3.7 b). There are numerous studies suggested that LCN2 secretion is increased in the presence inflammatory factors, such as interferon γ (IFNγ) and TNFα (P. Zhao et al., 2014), which leads to adiposity and insulin resistance (Catalán et al., 2009; Y. Wang et al., 2007). However, studies that investigate the effect of hypoxia on LCN2 secretion are scarce.

Apart from animal studies, two clinical reports involving obstructive sleep apnea (OSA) patients revealed opposite results as Kiskac *et al*. revealed lower level of LCN2 in OSA patients' blood serum; whereas Murase *et al.* noted inverse relationship between patients' LCN2 plasma level and severity of OSA condition (Kiskac et al., 2014; Murase et al., 2013). However, both studies did not attain significant results to denote association between LCN2 and low oxygenation.

Unlike *fabp4*, hyperglycaemia clearly caused elevation of *lcn2* mRNA expression, as compared to normoglycaemic condition (see Figure 3.7 a). Its protein expression and secretion were observed among

normoxic groups, but prominently seen in HG samples (see Figure 3.7 b and c). Wang *et al.* discovered that increased level of serum LCN2 in *db/db* mouse was in accordance to its gene expression in AT and hepatocytes (Y. Wang et al., 2007). Other data also revealed increment of *lcn2* expression in *ob/ob*, *db/db* and HFD fed mice (Yan et al., 2007). It appears that HG and insulin play a role in inducing LCN2 secretion and inhibiting NF-kB pathway suppressed its secretion in adipocyte (Y. Zhang et al., 2014).

In contrast, an *in vivo* study involving *lcn2*$^{-/-}$ mice exerted anti-inflammatory properties of LCN2 as *lcn2*$^{-/-}$ mice exhibited susceptibility towards diet-induced obesity, impaired adaptive thermogenesis and cold intolerance (Guo et al., 2014). LCN2 also hampered the production of IL-6 and CCL2 when 3T3-L1 cells were co-treated with both LCN2 and TNFα. This leads to stimulation of leptin and adiponectin production (J. Zhang et al., 2008). Therefore, the exact role of LCN2 in inflammation is still debatable.

ii. FABP4 mRNA expression and secretion

Hypoxia-treated groups showed significant downregulation of *fabp4* mRNA expression, as compared to normoxic groups (see Fig. 3.8 a). Hypoxia regulates activation of hypoxic-inducible (HIF) transcription, involving *hif-1α*, *-2α*, and *-3α* (Regazzetti et al., 2009); and mediates cellular inflammatory pathways via release of pro-

inflammatory cytokines, such as IL-1β, IL-6 and TNFα, in AT of human and murine animals (Trayhurn, Wang, & Wood, 2008). Upon activation, *hif-3α* positively regulates adipogenesis, triggers a rise of *fabp4* and AMP-dependent protein kinase γ1 (*ampkγ1*) expression by 1.9 and 1.6 fold, respectively (Hatanaka et al., 2009).

Suppression of *fabp4* mRNA expression due to hypoxia (as recorded in this experiment) was also reported by others. Fehrer *et al.* claimed that decreasing the oxygen level from 20% to as low as 3% diminished adipogenic differentiating capacity of human mesenchymal stem cells (MSCs) (Fehrer et al., 2007). Hypoxia activates transforming growth factor-β/Smad (TGF-β/Smad) signalling pathway and mediates impairment of adipocyte differentiation in MSCs, as evidence by downregulation of *pparγ* (Zhou, Lechpammer, Greenberger, & Glowacki, 2005). *pparγ*, an adipogenic transcription factor, together with *c/ebpα*, are responsible in promoting *fabp4* gene expression (Ichiro, L, T, Jian-Guo, & J, 2004).

Low oxygen level inhibits adipogenic gene expression, such as *fabp4,* and reduces TGs content in differentiating adipocyte as a result of cytoskeletal tension since these cells experienced morphological transformation that caused actin reorganization. This was further supported as treatment with cytochalasin D, an actin polymerisation

inhibitor, weakens cytoskeletal tension and upregulates adipogenic marker (Schiller, Schiele, Sims, Lee, & Kuo, 2013; B. Wang et al., 2008; Zhou et al., 2005).

Hyperglycaemia, on the other hand, has no significant effect in regulating *fabp4* expression adipocytes, in contrast to other reports (see Figure 3.8 a). Qin *et al.* reported that rats supplemented with fructose-rich diet showed downregulation of adiponectin mRNA expression and secretion; while *fabp4* was noticeably overexpressed (B. Qin & Anderson, 2011). Glucose homeostasis and lipid metabolism in HFD *fabp4/fabp5* knockout mice models revealed profound improvement, which suggests that its deficiency offers protection from deterioration in diet-stimulated insulin resistance (Krušinová & Pelikánová, 2008). The significant upregulation of *fabp4* expression was also documented by others as cells treated with 25mM/l glucose also displayed high expression of TNFα and IL-1β as compared to 5mM/l media (H. Li et al., 2018). Given the data that *fabp4* expression was significantly induced in HG condition, the above-mentioned studies did not consider simultaneous effect of both oxygenation and glucose concentration upon *fabp4* gene expression from the cells.

Whereas FABP4 secretion among hypoxic groups was present abundantly as compared to normoxic groups (see Figure 3.8 b). This

increment was expected in hypoxic condition as documented by others in obese human and mice (Wu et al., 2014). Wu *et al*. have proven that hypoxia and β-3-adrenergic agonists induced FABP4 secretion from 3T3-L1 cells, in comparison to that exerted by control. Despite of comparable cytosolic FABP4 protein observed among hypoxic and normoxic groups, this expression was not reflected and directly translated into circulating secretion, possibly due to the lack of N-terminal secretory sequence (Wu et al., 2014).

Increasing glucose concentration from 5.5mM/l to 17.5mM/l did not affect FABP4 secretion in this experimental model (see Figure 3.8 b). This could be attributed by the action of high insulin supplemented in HG groups that has the capability to supress FABP4 secretion (Cao et al., 2013). It was reported among patients that received calorie loading test (e.g. oral glucose tolerance test and high fat meal loading test) that elevated insulin level post-test is associated with reduced FABP4 secretion. This is because, high level of insulin augmented anti-lipolytic response, thus supressing FABP4 release into circulation (Mita et al., 2015).

The effect of glucose concentration in normoxic and hypoxic conditions was also analysed by measuring *glut4* mRNA expression, an insulin-regulated glucose transporter that is highly expressed in adipocyte and skeletal muscle. As expected, its expression was

substantially raised among HG groups, but not among NG groups (see Fig. 3.9). The presence of insulin causes activation of insulin receptor, which leads to tyrosine phosphorylation and translocation of intracellular vesicles containing GLUT4 to the cell membrane (Sano et al., 2003). Others also have reported that *glut4* expression is induced in HG/insulin condition and increases as adipogenesis advanced (Dalen, Ulven, Bamberg, Gustafsson, & Nebb, 2003; Wu-Wong, Berg, Wang, Chiou, & Fissel, 1999).

Meanwhile, *glut4* expression in hypoxic groups was insignificant when compared to normoxic groups, as many studies have reported that *glut4* expression is unchanged in hypoxic experiment, unlike *glut1* (Stuart Wood, Wang, Lorente-Cebrián, & Trayhurn, 2007; Yin et al., 2009). However, a prior study proposed that *glut4* mRNA expression could be reduced as a consequence of diminished C/EBP activity caused by hypoxia (Kaestner, Christy, & Lane, 1990). Thus, prolonged hypoxic exposure time is suggested to verify the significant impact of hypoxia on *glut4* expression. This is because, half-life of GLUT4 in mature adipocytes was documented at exceeding 16 hours, while most of these studies performed hypoxic treatment for only 24 hours (J. Shi & Kandror, 2005; Yin et al., 2009).

Interestingly, Fain *et al*. discovered that expression of *lcn2* and *fabp4* were not correlated to their secretion in omental AT explant (Fain, 2010). Catalan *et al.* also revealed insignificant variances of LCN2 secretion between lean and obese subjects despite of increased *lcn2* mRNA expression in the latter group when compared to former (Catalan et al., 2009). These observed findings needed further explanation as there is a possibility that intracellular signalling that affects gene expression may not necessarily translate to protein secretion due to post-translational modification.

3.4.4) Determining presence of exosome from CM

In order to understand the role of LCPs in both hypoxic and hyperglycaemic states, the circulating component of LCN2 and FABP4 secretion from adipocyte have to be determined. Extracting extracellular vesicles, together with secreted proteins that adipocytes actively release into circulatory system as paracrine signalling molecules, may help to distinguish their role in physiological and pathological conditions (Gao, Salomon, & Freeman, 2017).

In this experiment, CM from HG experiment was used, as exosomal protein was anticipated to be highly isolated based on the secretory outputs (shown in Fig. 3.4 b and 3.5 b). However, no definite and

conclusive protein band was noted from gels stained with coomassie blue (see Fig. 3.10). Differentiated 3T3-L1 adipocyte treated with ionomycin induced FABP4 protein content in adipocyte-derived microvesicles (ADMs) and was secreted via non-classical ER-Golgi pathway (Kralisch et al., 2014). Since exosomal protein was not as abundant as cell lysate protein, the coomassie blue staining may be insensitive to detect low amount of protein in a sample (Prax, Vatani Shahmirzadi, & Götz, 2015).

In order to verify whether the absence of protein is definite, the byproduct proteins obtained through exosome isolation steps were precipitated and used in western blot. Protein precipitation was performed by using (1) remaining supernatant post-serial centrifugation to obtain protein released into media; (2) supernatant post-ultracentrifugation to obtain protein from shed MVs; and lastly, (3) protein from pellet-containing exosome resuspended in PBS (see Fig. 3.11).

Based on the findings, only FABP4 was detected at day 10 from sample (1). The other group (day 6) did not show any notable protein band. The protein band observed in (2) revealed remarkable presence of LCN2 and FABP4 in both day 6 and day 10 groups. This suggested that early stage of differentiating adipocyte (represented as day 6) released its secretory protein via shed MVs; in contrast to

day 10 differentiating adipocyte that was able to release its secretion directly and/or via shed MVs. Meanwhile, the exosome samples showed neither LCN2 nor FABP4 protein bands. In general, the experiment failed to prove the presence of LCN2 and FABP4 proteins in exosome, but these were abundantly observed amidst shed MVs samples.

Recent studies revealed that FABP4 was secreted via exosome (Erikci Ertunc et al., 2014; Sarah C. Ferrante et al., 2014; Mita et al., 2015). Villeneuve *et al*. found that only 5% of FABP4 released through exosome, while mostly was from secretory lysosome (Villeneuve et al., 2017). Some studies showed that FABP4 secretion was in soluble form (Kralisch et al., 2014; Lamounier-Zepter et al., 2009); which proposed that its mode of secretion varied with different types of cells, and as a consequence from various triggering factors.

Studies concerning LCN2 mode of secretion are not as many as compared to those which investigates FABP4. In a study that analysed urine exosome and its association with kidney injury post-transplant, LCN2 is secreted via exosome and extracellular fraction, however the former is secreted much lower than the latter (Alvarez et al., 2013).

The inability to detect presence of exosome containing these two LCPs needs further validation, since CD63 antibody protein band, is not observed in these current findings (see Figure 3.12). CD63 is among the first tetraspanins protein discovered, and commonly used as marker in exosome and MVs studies (Hu et al., 2016; Katsuda et al., 2013),. Its role as a specific marker, however, is undermined as recent studies noted that CD63 is actually enriched in other extracellular vesicles (EVs) fractions, instead of exosome (Pavlova, 2016). CD63 is not much present, as compare to CD9 and CD81, since the latter upregulated 10-fold higher in exosome, when compared to the former (Jørgensen et al., 2013). Furthermore, the variation in individuals' exosome tetraspanins protein expression, especially CD63, may dispute the final outcome (Kastelowitz & Yin, 2014). Other exosome biophysical assessments, such as flow cytometry, dynamic light scattering (DLS) and nanoparticle tracking analysis (NTA), were disregarded as SEM result was not promising (see Fig. 3.13), in addition to the insignificant results from immunoblotting. Multiple exosome markers should be used to verify the result, such as CD9, CD81 and CD82, and cytosolic proteins such as heat shock proteins (e.g. HSP-70 and HSP-90) since viable method to differentiate EVs of different intracellular origins is still required (Kowal et al., 2016).

In summary, presence of *lcn2* and *fabp4* mRNA expression were determined in rat adipocytes. Meanwhile, regulation of LCN2 expression and secretion was substantially affected by glucose concentration and oxygenation; while FABP4 expression and secretion was only affected by oxygenation. This study had determined that LCN2 was secreted abundantly in hyperglycaemic state at early stage of adipogenesis, while FABP4 secretion was noted from mature adipocytes. Despite the detection of LCN2 and FABP4 secretion from primary rat adipocytes, their mode of secretion via exosome was inconclusive, thus calls for further optimisation prior to arriving at a definite conclusion. Instead, there was significant amount of LCN2 and FABP4 were incorporated in shed MVs obtained from adipocytes CM.

CHAPTER 4:

EFFECTS OF TRPV4 LIGANDS ON ADIPOCYTE LIPID CHAPERONE PROTEINS SIGNALLING

4) Introduction

A further question concerning the potential activities of adipocyte-derived LCPs, such as LCN2 and FABP4, is the impacts of exogenous ligands on adipocytes receptors in regulating its LCPs signalling. LCN2 has a wide spectrum of biological functions due to its ability to bind to various ligands such as FAs, retinol and steroids (Jin et al., 2011). Meanwhile, FABPs can bind to a diverse range of biologically active lipid species, including FAs, acyl-ethanolamines and endocannabinoids (Storch & McDermott, 2009).

Studies have indicated that calcium may be involved in regulating LCPs expression and secretion. Kralisch *et al*. and Schlottman *et al*. concluded that FABP4 is significantly released by adipocyte in a calcium-dependent manner (Kralisch et al., 2014; Schlottmann, Ehrhart-Bornstein, Wabitsch, Bornstein, & Lamounier-Zepter, 2014); whereas LCN2 expression is reported to be increased in calcium-induced keratinocyte differentiation (J.-H. Lee et al., 2008).

In high extracellular calcium ($[Ca^{2+}]e$) state, differentiation of preadipocyte is affected in dose-dependent manner as evidenced by

inability of cells to transform their shapes from spindle-like into rounded-lipid shape (Jensen, Farach-Carson, Kenaley, & Akanbi, 2004). While in high intracellular calcium ($[Ca^{2+}]i$) condition, adipocyte differentiation is inhibited in early stage, but enhanced at later stage of adipogenesis (Shi, Halvorsen, Ellis, Wilkison, & Zemel, 2000).

One of the methods involved in cellular calcium signalling is via ligand-gated channels, such as transient receptor potential (TRP). TRP channel is a group of ion channels that is expressed in cell membranes of various tissues, including adipocytes. More than 30 mammalian TRP channels have been identified and divided into six subfamilies based on their amino acid sequence homology, namely TRPA, TRPC, TRPM, TRPN, TRPP and TRPV families (Bishnoi, Kiran Kondepudi, Gupta, Karmase, & Boparai, 2013).

This study main interest is TRPV4, a calcium permeable non-selective cation channel that is highly sensitive towards physical activator (such as heat, hypotonic stress and low pH) and chemical activator (such as phorbol ester (4a-PDD) and arachidonic acid metabolites) (Thorneloe et al., 2008). Unlike action of TRPV1 that is still debatable as pro or anti-inflammatory (L. L. Zhang et al., 2007), TRPV4 is responsive for positive regulation of inflammatory genes, such as *mip-1a*, *ccl2*, *Rantes* and *IL-6* (Ye et al., 2012). Gough *et al*.

has reported downregulation of pro-inflammatory gene expression in a *trpv4* knockdown adipocytes cell line. Treatment with TRPV4 antagonist also displayed similar outcomes, along with raised thermogenic gene expression and enhanced insulin sensitivity in diet-induced obese mice (Gough, 2012). Conversely, in vascular studies, TRPV4 is essential in modulating vascular tone in response to calcium influx. It is responsible for maintaining vasodilatation in response to sheer stress, while carotid arteries of *trpv4*$^{-/-}$ mice exhibited vasoconstriction upon TRPV4 agonist treatment (Hartmannsgruber et al., 2007).

As TRPV4 is correlated with pro-inflammatory cytokine, and calcium plays an important role in adipogenesis, this study probed into TRPV4 ligands action in adipocytes towards LCN2 and FABP4 signalling. Despite the evidence that links $[Ca^{2+}]i$ with LCPs expression and secretion, the role of calcium signalling via TRPV4 ligands in regulating LCN2 and FABP4 expression/secretion in different duration of adipogenesis and glucose concentration media has yet to be unravelled.

4.1) **Objectives**

The objectives of this study were:

1) To determine concomitant agonist-antagonistic effect of TRPV4 ligands on adipocytes' calcium signalling
2) To determine calcium response in the presence of TRPV4 agonist by using calcium and calcium-free media in varied glucose concentration at different duration of adipogenesis
3) To determine the effects of TRPV4 ligands upon LCN2 and FABP4 mRNA expression, protein expression and secretion in primary rat adipocytes cultured in NG and HG media
4) To determine the interaction between main effect of different glucose concentration in media and treatment of TRPV4 ligands upon *lcn2*, *fabp4* and other adipocyte genes expression

4.2) **Experimental design**

Upon depiction in Chapter 2, primary rat adipocyte culture was prepared, proliferated and differentiated. For calcium imaging, cells were seeded on 12-well plate first, instead of directly cultured onto gelatin-coated coverslip. This is to avoid contaminant, such as RBC from being embedded onto gelatin. Rigorous washing with PBS is able to remove RBC, but it may as well dislodge cells from coverslip. When cells proliferation reached 80% confluent, sub-culturing was performed and cells were counted prior to plating. The cells

underwent proliferation phase and differentiation in NG and HG media up to day 10.

On the experiment day (day 6 or day 10), coverslip was removed from the 12-well plate and calcium imaging was performed. Calcium buffer was applied with glucose concentration that mimicked NG (5.5mM/l) or HG (17.5mM/l), and cells were perfused with the same buffer containing HC067 (TRPV4 antagonist). Next, TRPV4 agonist, GSK101 (either 5nM, 10nM, 25nM, 50nM or 100nM) was added concomitantly to the same cells. The experimental work used ATP 100μM as positive control.

The cells also underwent calcium imaging that required 2 phases of perfusion. To begin with, cells were perfused with buffer supplemented with calcium ion; either with 5.5mM/l or 17.5mM/l glucose concentration. Then, GSK101 was added to the buffer upon achieving baseline level. After the agonist response was recorded, cells were perfused with calcium-free buffer with the same glucose concentration. After new baseline was achieved, GSK101 was added to the buffer to determine cell response in calcium-free condition.

As for the third and fourth objectives, SVF cells from WAT biopsies were classified into two groups, NG and HG media. Each group was further divided into two subgroups, subjected to day 5/6 and day

9/10 experiments (see Figure 4.1). Both groups were monitored in 37°C incubator in normoxic condition with 21% oxygen and media was replenished every two days.

One group from each NG and HG media that was allocated for day 5/6 experiment was further divided into 3 subgroups (including control). Treatment given at day 5 differentiation was 100nM GSK101 (TRPV4 agonist) and 500nM HC067 (TRPV4 antagonist). After 24-hour incubation, at day 6, CM was collected, while RNA extraction and cell lysate were prepared from adherent adipocytes. The second group from each NG and HG media was subjected to day 9/10 experiment with similar method and concentration of treatments.

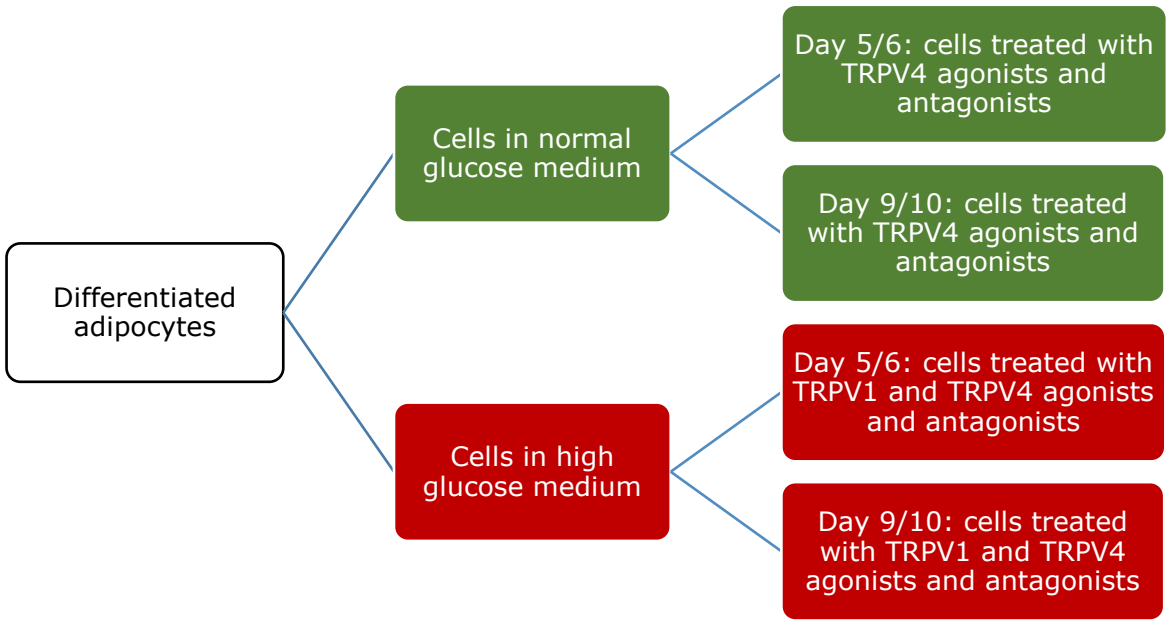

Figure 4.1: Plan of experiment used in this chapter

4.3) **Results**

4.3.1) Calcium signalling in the presence of both TRPV4 agonist and antagonist

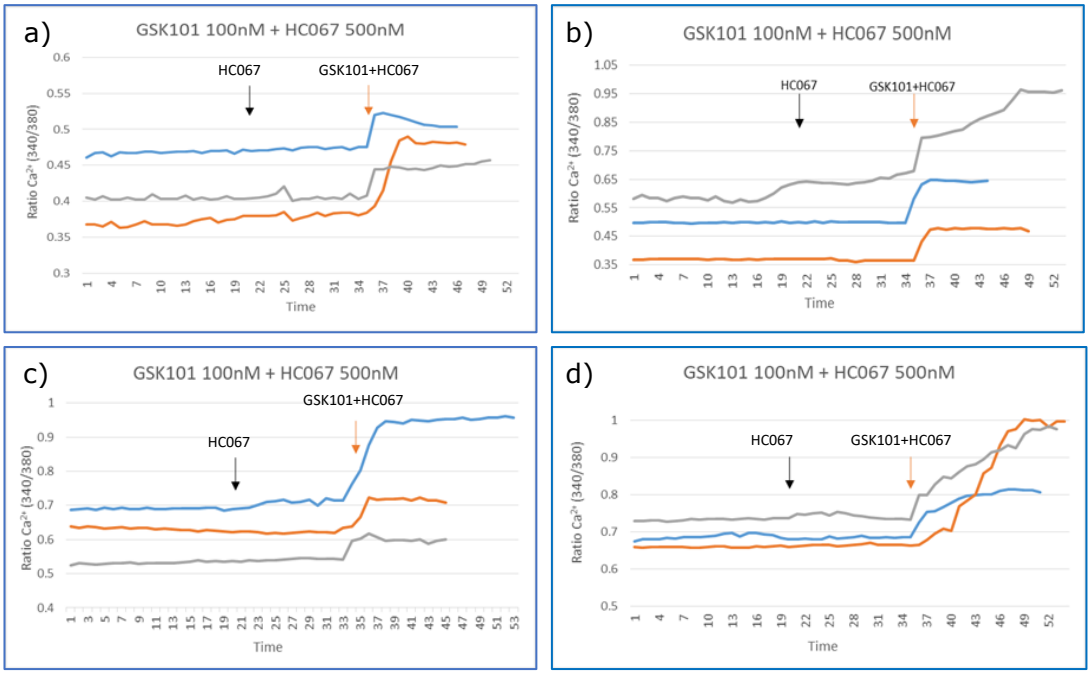

Figure 4.2: Agonist-antagonistic treatment of TRPV4 ligands on adipocytes' calcium signalling at (a) day 6 NG, (b) day 6 HG, (c) day 10 NG, and (d) day 10 HG media. The cells were perfused with HC067 500nM only prior to addition of 100nM GSK101. The experiments were repeated three times using 3 different preparation, represented by different coloured lines, with a minimum of 25 cells each. Other concentrations of GSK101 have been used in this experiment and showed in Appendix D.

By using calcium imaging, the working concentration of GSK101 in this experiment had been determined by observing the agonist-antagonistic effect of TRPV4 ligands in cells treated with different dosage of GSK101. The antagonistic action of HC067 subsided after being given GSK101 50nM (refer Appendix D: Figure 6.4 to 6.7) and further diminished in cells treated with GSK101 100nM (see Figure 4.2). As shown in Appendix D, the effect of low GSK101 dosages (5 and 10nM) were inhibited by HC067 500nM (see Figure 6.4 to 6.7).

4.3.2) Calcium signalling in the presence and absence of calcium ion in culture media

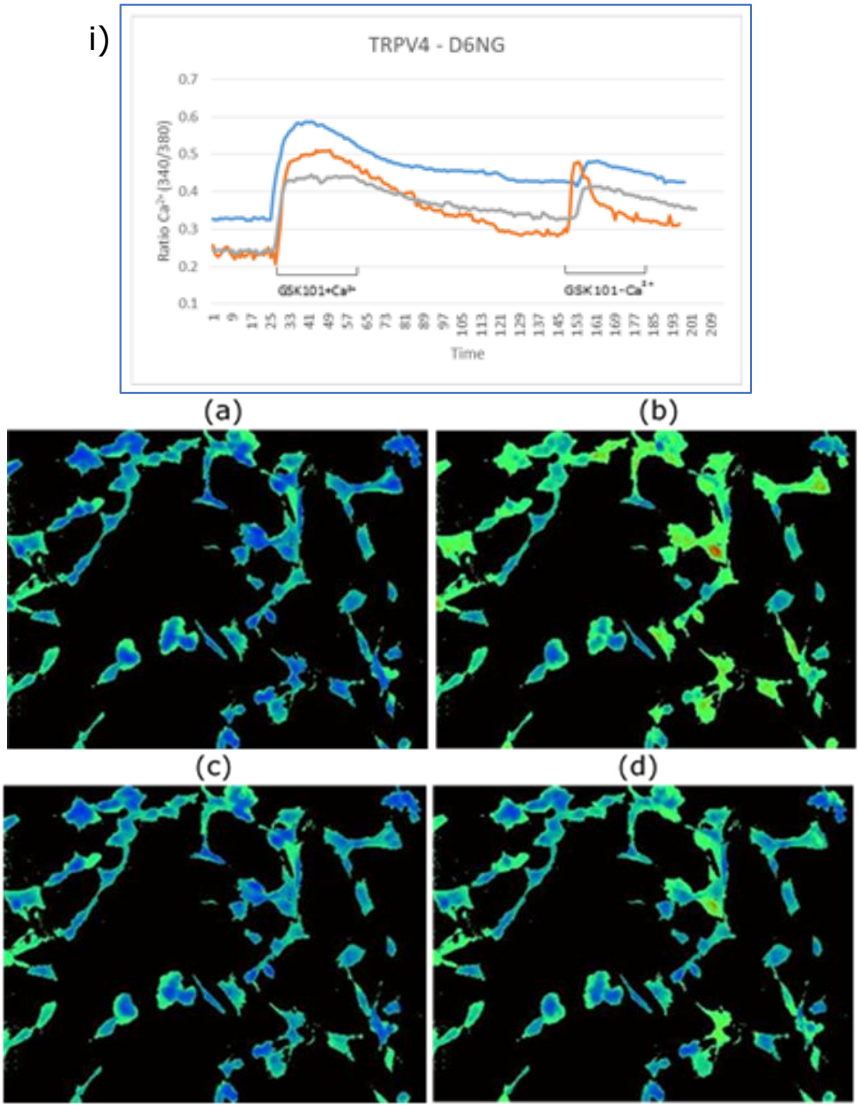

Figure 4.3: The effects of TRPV4 ligands on $[Ca^{2+}]i$ response in primary cultured rat adipocytes at day 6 differentiation in NG media. (i) Cells were loaded with Fura-2 and perfused with calcium buffer prior to addition of 100nM GSK101 for 2 minutes. Next, the cells were perfused with calcium-free buffer before the same ligands were added using the same buffer. A fura-2 dual-wavelength fluorescence imaging system was applied and the response is portrayed in the graph (upper panel). Three independent experiments, represented by different coloured lines, were carried out with a minimum of 25 cells in each preparation. Lower panel: Cell fluorescence images in pseudocolor, which changed from blue as baseline to red upon addition of agonist, indicating increased $[Ca^{2+}]i$. (a) baseline in calcium buffer; (b) treated with GSK101 in calcium buffer; (c) perfused with calcium-free buffer; (d) treated with GSK101 in calcium-free buffer. Images were captured using Leica inverted microscope and coupled with Hamamatsu DCAM digital camera at 20x magnification.

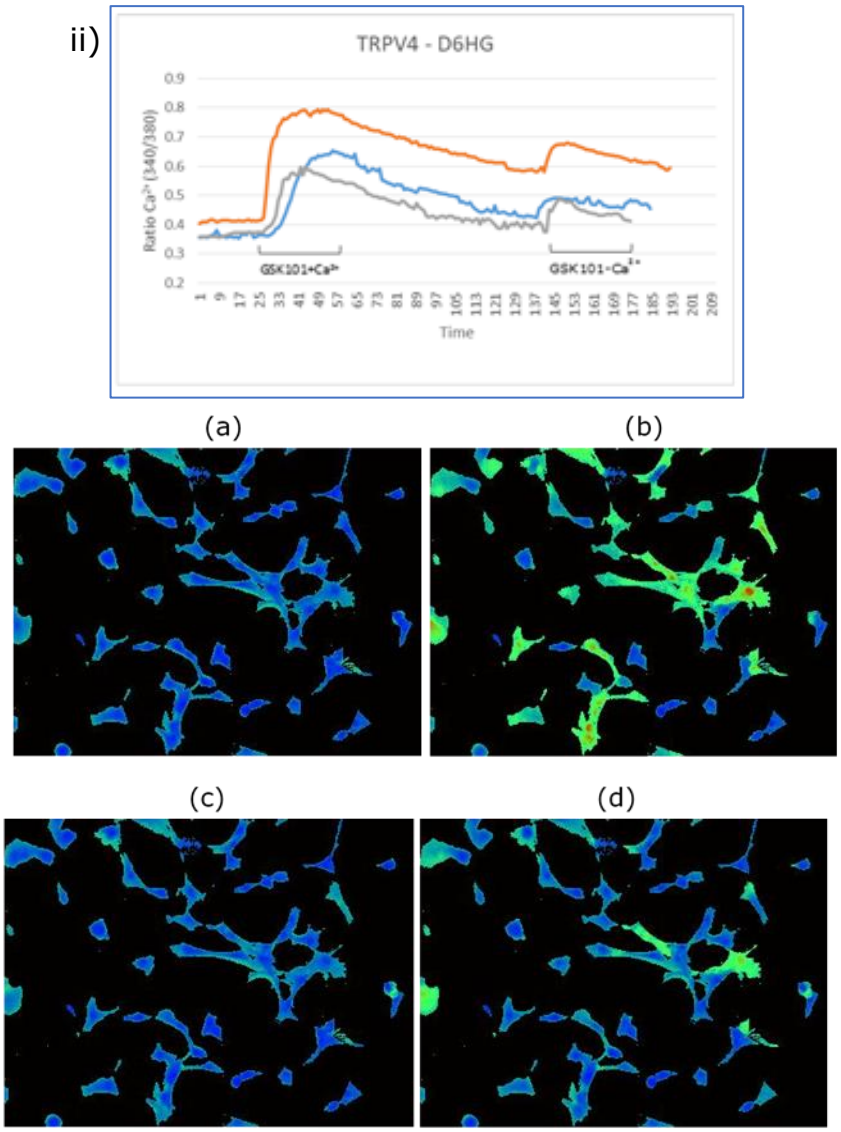

Figure 4.4: The effects of TRPV4 ligands on $[Ca^{2+}]i$ response in primary cultured rat adipocytes at day 6 differentiation in HG media. (ii) Cells were loaded with Fura-2 and perfused with calcium buffer prior to addition of 100nM GSK101 for 2 minutes. Next, the cells were perfused with calcium-free buffer before the same ligands were added using the same buffer. A fura-2 dual-wavelength fluorescence imaging system was applied and the response is portrayed in the graph (upper panel). Three independent experiments, represented by different coloured lines, were carried out with a minimum of 25 cells in each preparation. Lower panel: Cell fluorescence images in pseudocolor, which changed from blue as baseline to red upon addition of agonist, indicating increased $[Ca^{2+}]i$. (a) baseline in calcium buffer; (b) treated with GSK101 in calcium buffer; (c) perfused with calcium-free buffer; (d) treated with GSK101 in calcium-free buffer. Images were captured using Leica inverted microscope and coupled with Hamamatsu DCAM digital camera at 20x magnification.

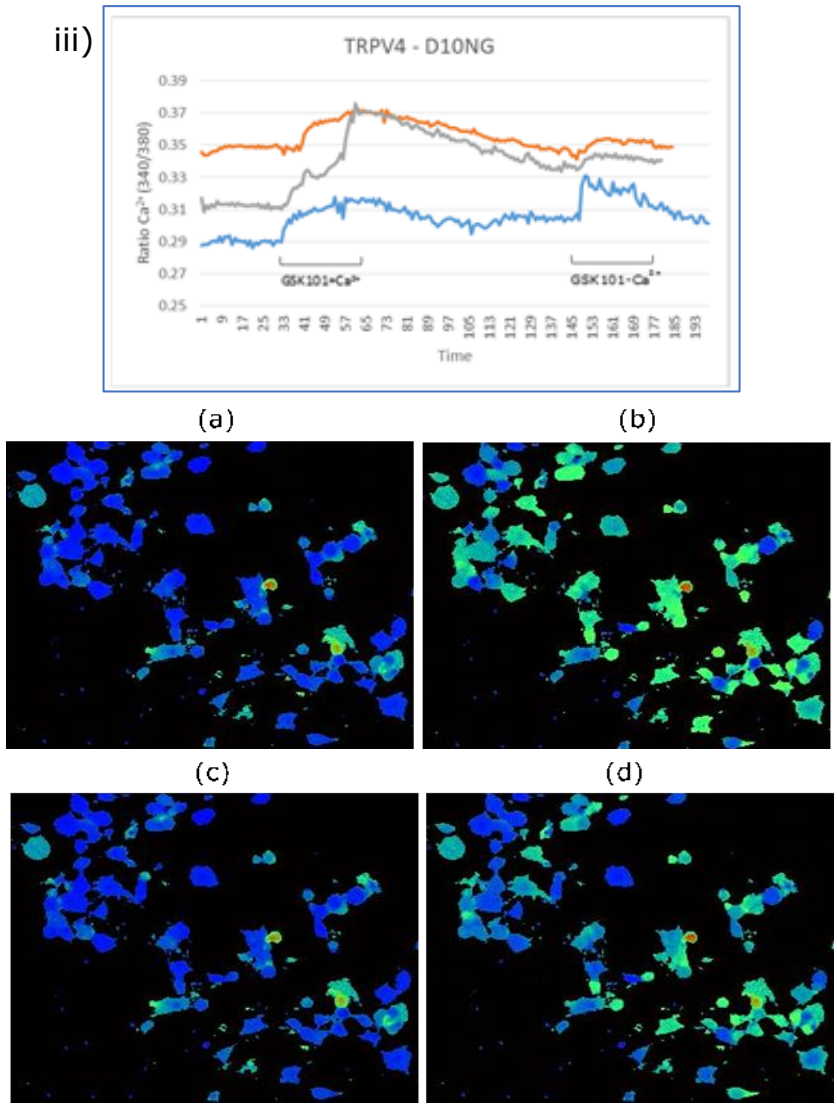

Figure 4.5: The effects of TRPV4 ligands on $[Ca^{2+}]i$ response in primary cultured rat adipocytes at day 10 differentiation in NG media. (iii) Cells were loaded with Fura-2 and perfused with calcium buffer prior to addition of 100nM GSK101 for 2 minutes. Next, the cells were perfused with calcium-free buffer before the same ligands were added using the same buffer. A fura-2 dual-wavelength fluorescence imaging system was applied and the response is portrayed in the graph (upper panel). Three independent experiments, represented by different coloured lines, were carried out with a minimum of 25 cells in each preparation. Lower panel: Cell fluorescence images in pseudocolor, which changed from blue as baseline to red upon addition of agonist, indicating increased $[Ca^{2+}]i$. (a) baseline in calcium buffer; (b) treated with GSK101 in calcium buffer; (c) perfused with calcium-free buffer; (d) treated with GSK101 in calcium-free buffer. Images were captured using Leica inverted microscope and coupled with Hamamatsu DCAM digital camera at 20x magnification.

iv)

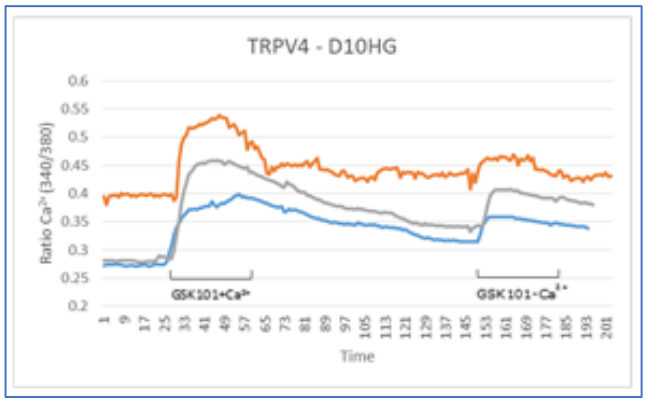

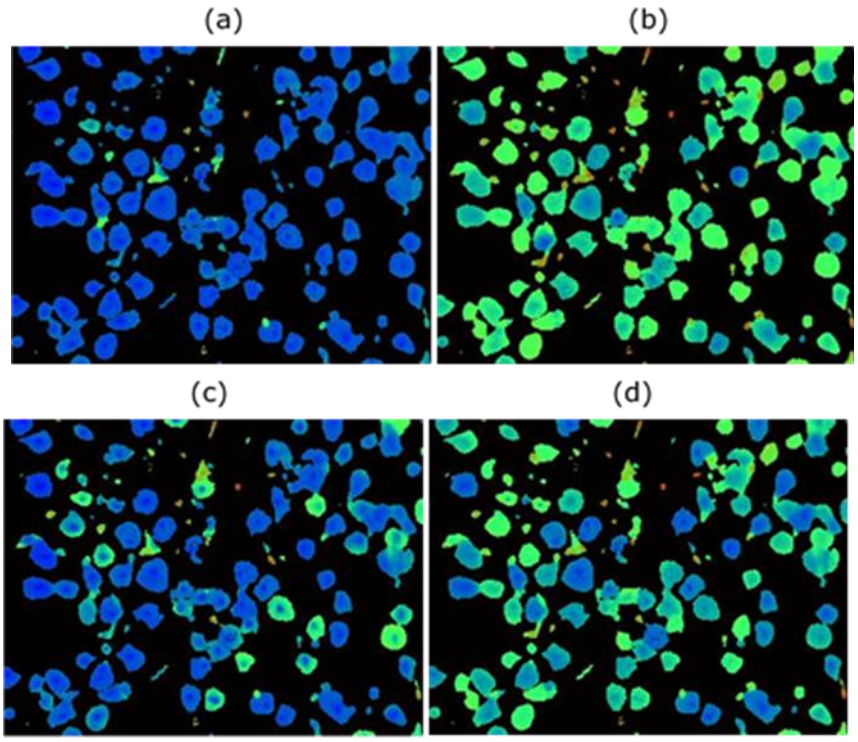

Figure 4.6: The effects of TRPV4 ligands on $[Ca^{2+}]i$ response in primary cultured rat adipocytes at day 10 differentiation in HG media. (iv) Cells were loaded with Fura-2 and perfused with calcium buffer prior to addition of 100nM GSK101 for 2 minutes. Next, the cells were perfused with calcium-free buffer before the same ligands were added using the same buffer. A fura-2 dual-wavelength fluorescence imaging system was applied and the response is portrayed in the graph (upper panel). Three independent experiments, represented by different coloured lines, were carried out with a minimum of 25 cells in each preparation. Lower panel: Cell fluorescence images in pseudocolor, which changed from blue as baseline to red upon addition of agonist, indicating increased $[Ca^{2+}]i$. (a) baseline in calcium buffer; (b) treated with GSK101 in calcium buffer; (c) perfused with calcium-free buffer; (d) treated with GSK101 in calcium-free buffer. Images were captured using Leica inverted microscope and coupled with Hamamatsu DCAM digital camera at 20x magnification.

Since this study has documented calcium response post-concurrent TRPV4 agonist/antagonist treatment, the next step is to determine if the absence of $[Ca^{2+}]e$ affects GSK101 treatment in varying glucose concentration at day 6 and day 10 differentiation. This could lead a way to further investigate and understand calcium regulatory mechanism in adipocytes.

Figure 4.3 to 4.6 showed raised $[Ca^{2+}]i$ signalling in cells treated with GSK101, either in the presence or absence of calcium in the buffer; though the latter displayed reduced response than the former. The second baseline recorded post GSK101 treatment in calcium free buffer did not return to the same level as initial baseline.

4.3.3) *trpv* gene expression in NG and HG at different duration of adipogenesis

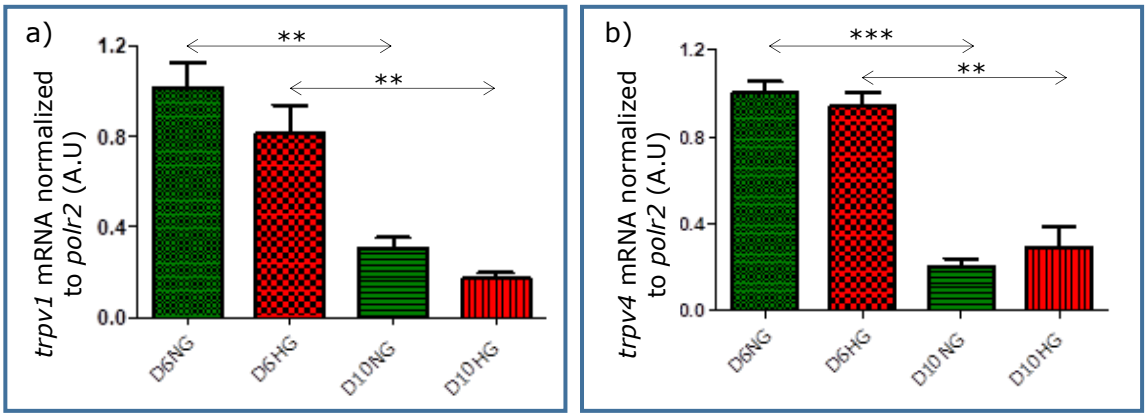

Figure 4.7: (a) *trpv1* and (b) *trpv4* gene expressions at different duration of adipocytes differentiation in NG and HG media. The data were analysed by using one-way ANOVA, followed by Bonferroni's post-hoc test and expressed as mean ± SEM, $n=3$; $^{**}p<0.01$, $^{***}p<0.001$. This experiment was repeated 3 times using 3 different preparation.

trpv1 and *trpv4* gene expression were identified in the samples and appeared to be significantly decreased among day 10 groups, when compared to day 6 [*trpv1*; D10NG (M=0.31, SD=0.04), D10HG (M=0.17, SD=0.03)], [*trpv4*; D10NG (M=0.21, SD=0.03), D10HG (M=0.29, SD=0.095)] either in NG or HG media, [t(4)=5.93, $p=0.004$, t(4)=5.05, $p=0.0072$], [t(4)=13.14, $p=0.0002$, t(4)=5.86, $p=0.0042$] respectively.

4.3.4) Effect of TRPV4 ligands upon LCN2 signalling at day6/day10 adipocytes differentiation in NG and HG media

i. Day 6 NG

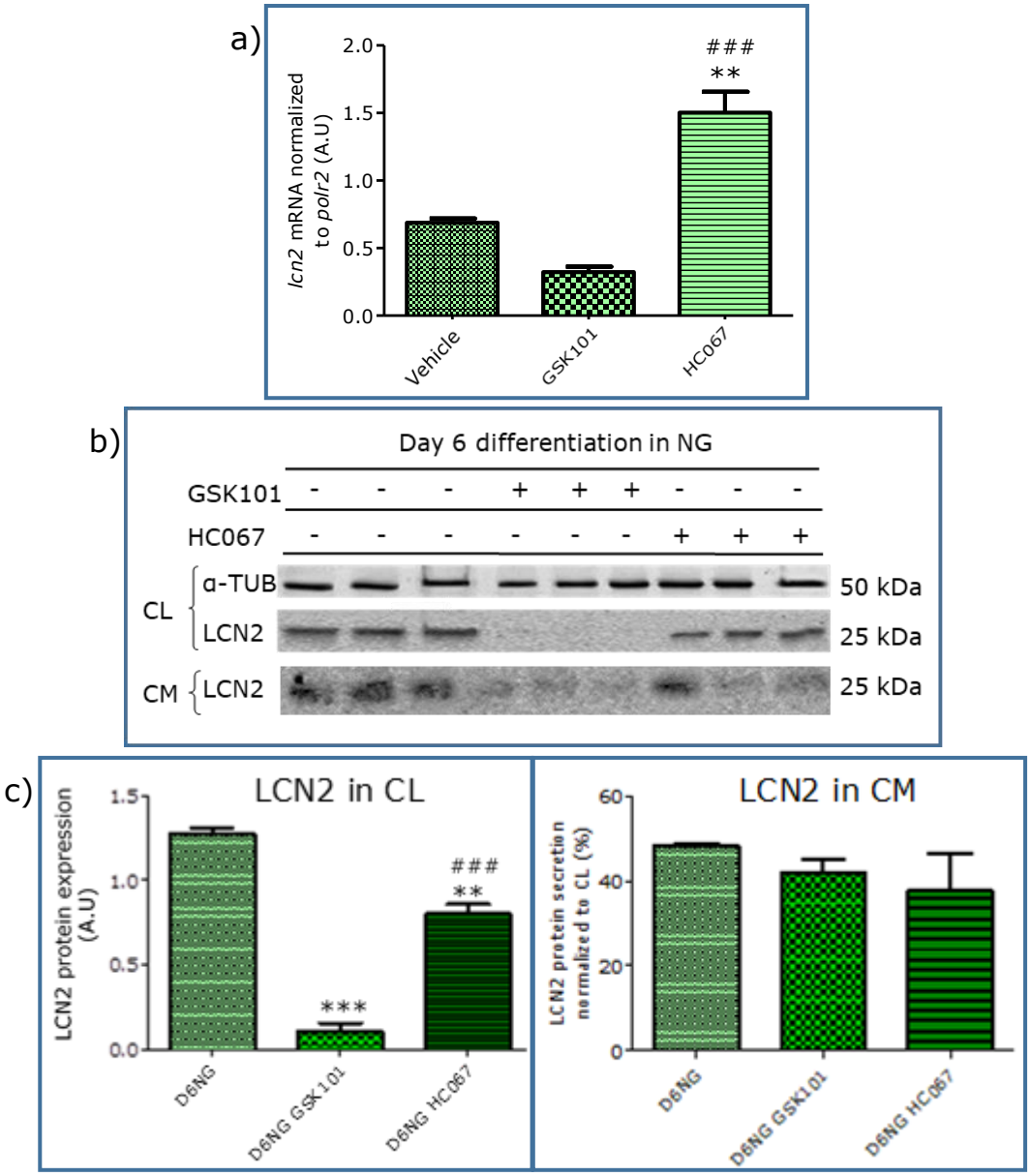

Figure 4.8: LCN2 mRNA expression, protein expression and secretion at day 6 adipocytes differentiation treated with TRPV4 ligands in NG media. (a) qRT-PCR analysis of *lcn2* mRNA expression, (b) WB results for LCN2 protein expression from CL and protein secretion from CM. The results were obtained from at least three independent experiments; n=3 or 4 in each preparation. (c) Statistical analysis of LCN2 protein expression and secretion using Image J. The data for gene and protein were analysed by using one-way ANOVA, followed by Bonferroni's post-hoc test and expressed as mean ± SEM; *p<0.05, **p<0.01, ***p<0.001; TRPV4 agonist (GSK101 100nM); TRPV4 antagonist (HC067 500nM); *=compare to control; #=compare to agonist.

ii. Day 6 HG

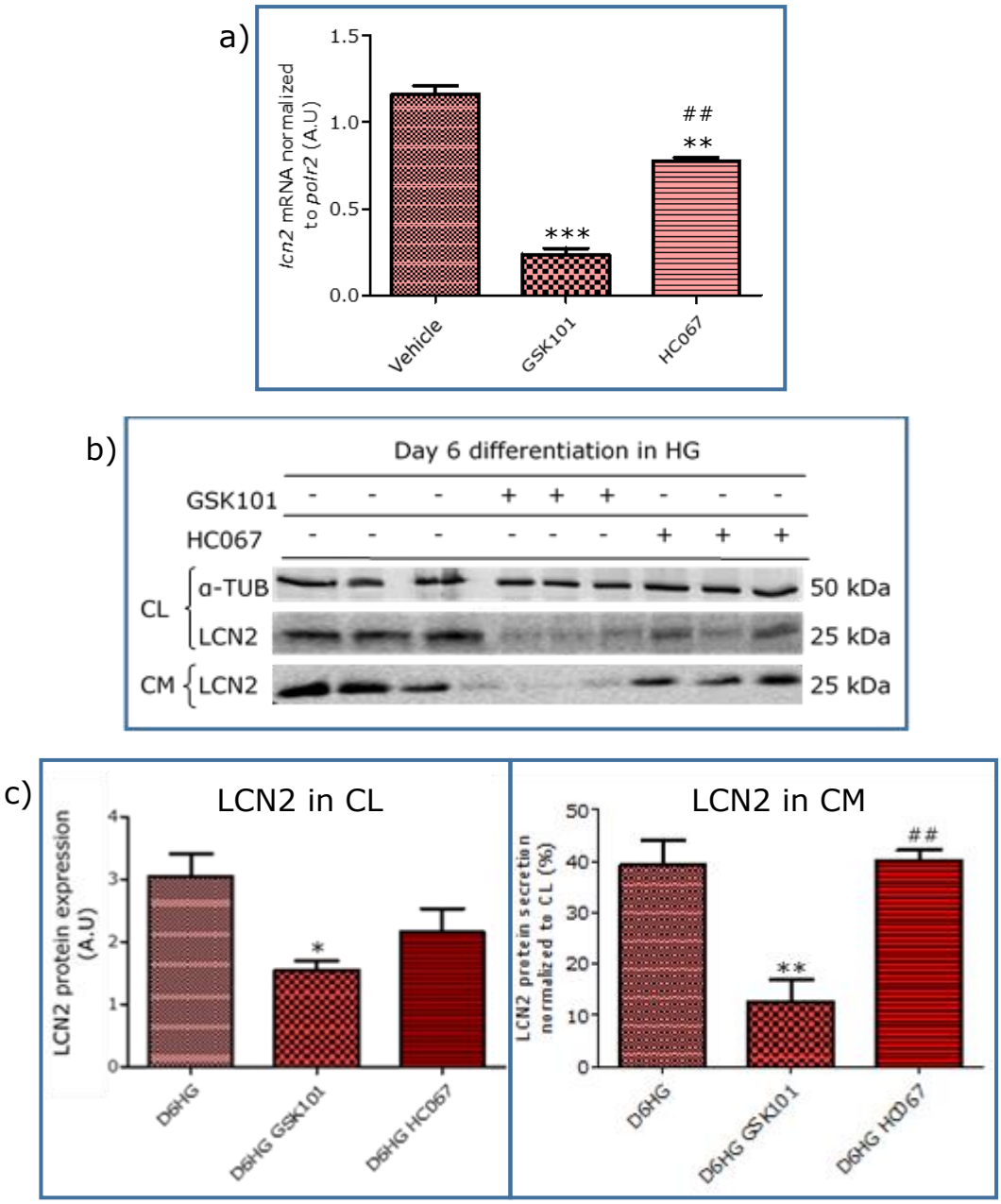

Figure 4.9: LCN2 mRNA expression, protein expression and secretion at day 6 adipocytes differentiation treated with TRPV4 ligands in HG media. (a) qRT-PCR analysis of *lcn2* mRNA expression, (b) WB results for LCN2 protein expression from CL and protein secretion from CM. The results were obtained from at least three independent experiments; n=3 or 4 in each preparation. (c) Statistical analysis of LCN2 protein expression and secretion using Image J. The data for gene and protein were analysed by using one-way ANOVA, followed by Bonferroni's post-hoc test and expressed as mean ± SEM; *p<0.05, **p<0.01, ***p<0.001; TRPV4 agonist (GSK101 100nM); TRPV4 antagonist (HC067 500nM); *=compare to control; #=compare to agonist.

iii. Day 10 NG

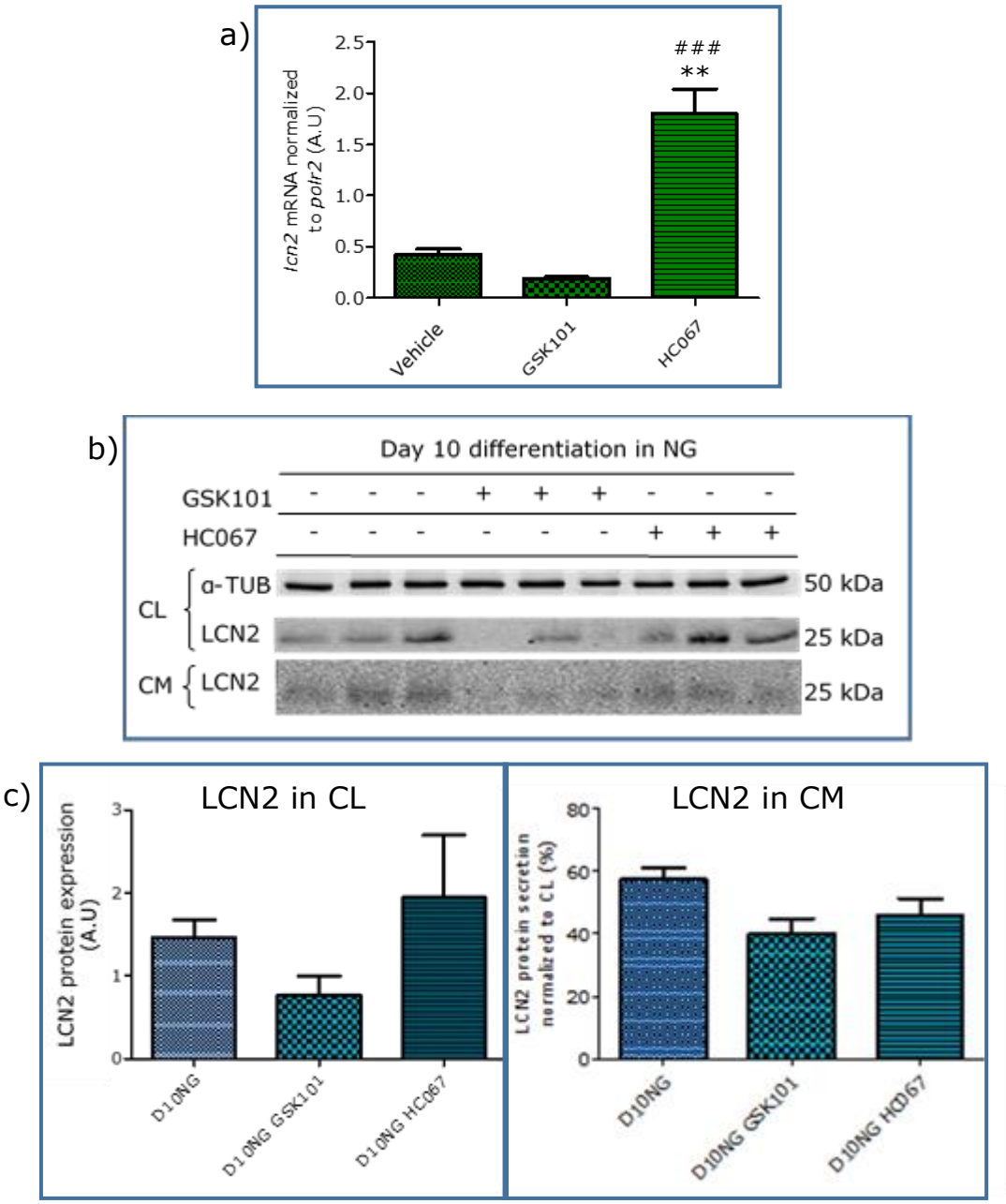

Figure 4.10: LCN2 mRNA expression, protein expression and secretion at day 10 adipocytes differentiation treated with TRPV4 ligands in NG media. (a) qRT-PCR analysis of *lcn2* mRNA expression, (b) WB results for LCN2 protein expression from CL and protein secretion from CM. The results were obtained from at least three independent experiments; *n*=3 or 4 in each preparation. (c) Statistical analysis of LCN2 protein expression and secretion using Image J. The data for gene and protein were analysed by using one-way ANOVA, followed by Bonferroni's post-hoc test and expressed as mean ± SEM; *p<0.05, **p<0.01, ***p<0.001; TRPV4 agonist (GSK101 100nM); TRPV4 antagonist (HC067 500nM); *=compare to control; #=compare to agonist.

iv. Day 10 HG

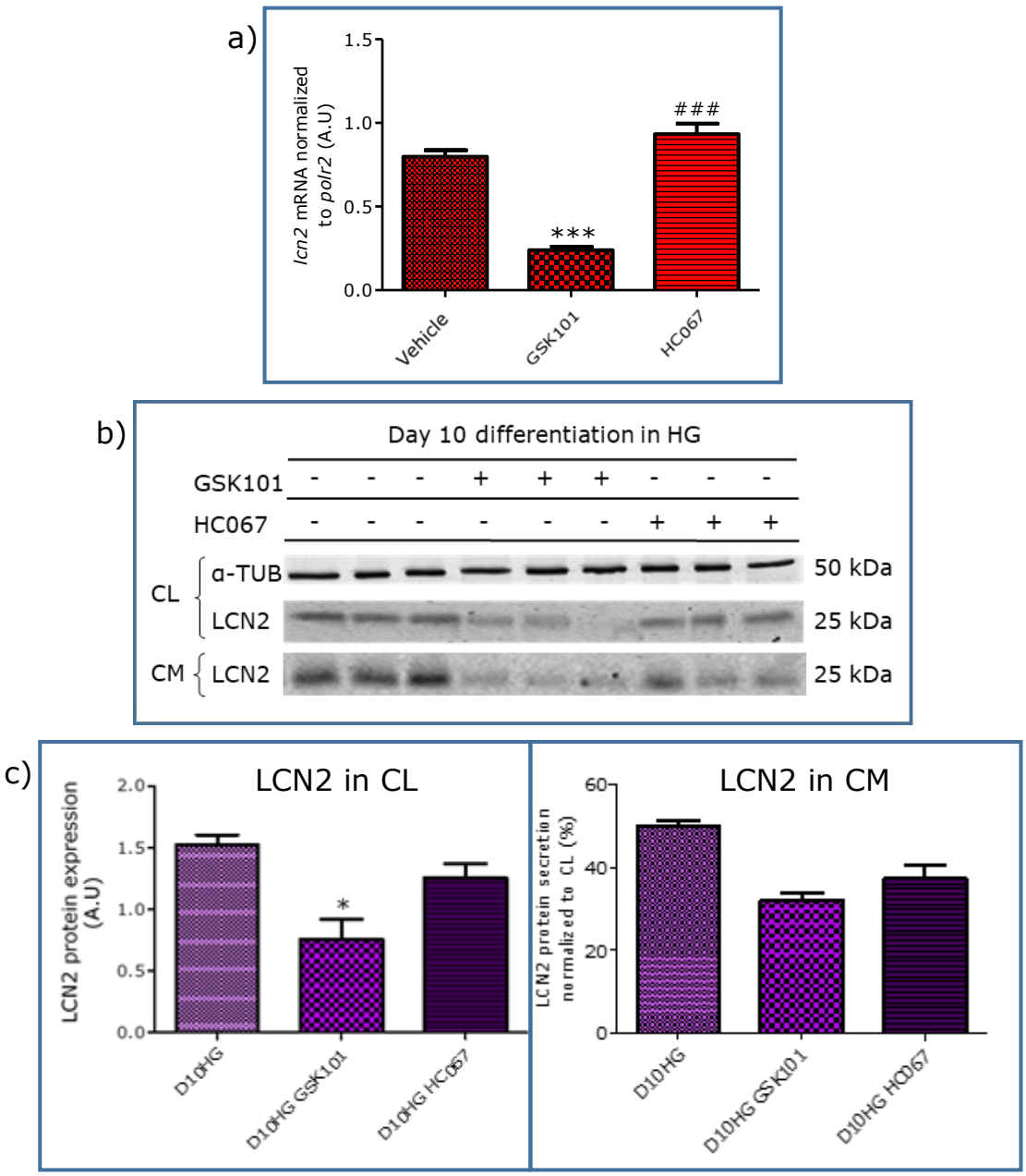

Figure 4.11: LCN2 mRNA expression, protein expression and secretion at day 10 adipocytes differentiation treated with TRPV4 ligands in HG media. (a) qRT-PCR analysis of *lcn2* mRNA expression, (b) WB results for LCN2 protein expression from CL and protein secretion from CM. The results were obtained from at least three independent experiments; n=3 or 4 in each preparation. (c) Statistical analysis of LCN2 protein expression and secretion using Image J. The data for gene and protein were analysed by using one-way ANOVA, followed by Bonferroni's post-hoc test and expressed as mean ± SEM; *p<0.05, **p<0.01, ***p<0.001; TRPV4 agonist (GSK101 100nM); TRPV4 antagonist (HC067 500nM); *=compare to control; #=compare to agonist.

The effect of TRPV4 agonist/antagonist on *lcn2* gene expression was investigated at different duration of adipogenesis at varying glucose concentration media. Administering GSK101 led to downregulation of *lcn2* gene expression in all groups. On the contrary, treatment with HC067 caused upregulation of its expression, mainly among NG groups.

Similarly, LCN2 protein expression was diminished in cells treated with GSK101, however inhibition of the channel with HC067 did not show any profound effect. Although LCN2 secretion revealed insignificant finding among the groups, but the secretion pattern was corresponded to its gene and protein expression.

4.3.5) Effect of TRPV4 ligands upon FABP4 signalling at day6/day10 adipocytes differentiation in NG and HG media

i. Day 6 NG

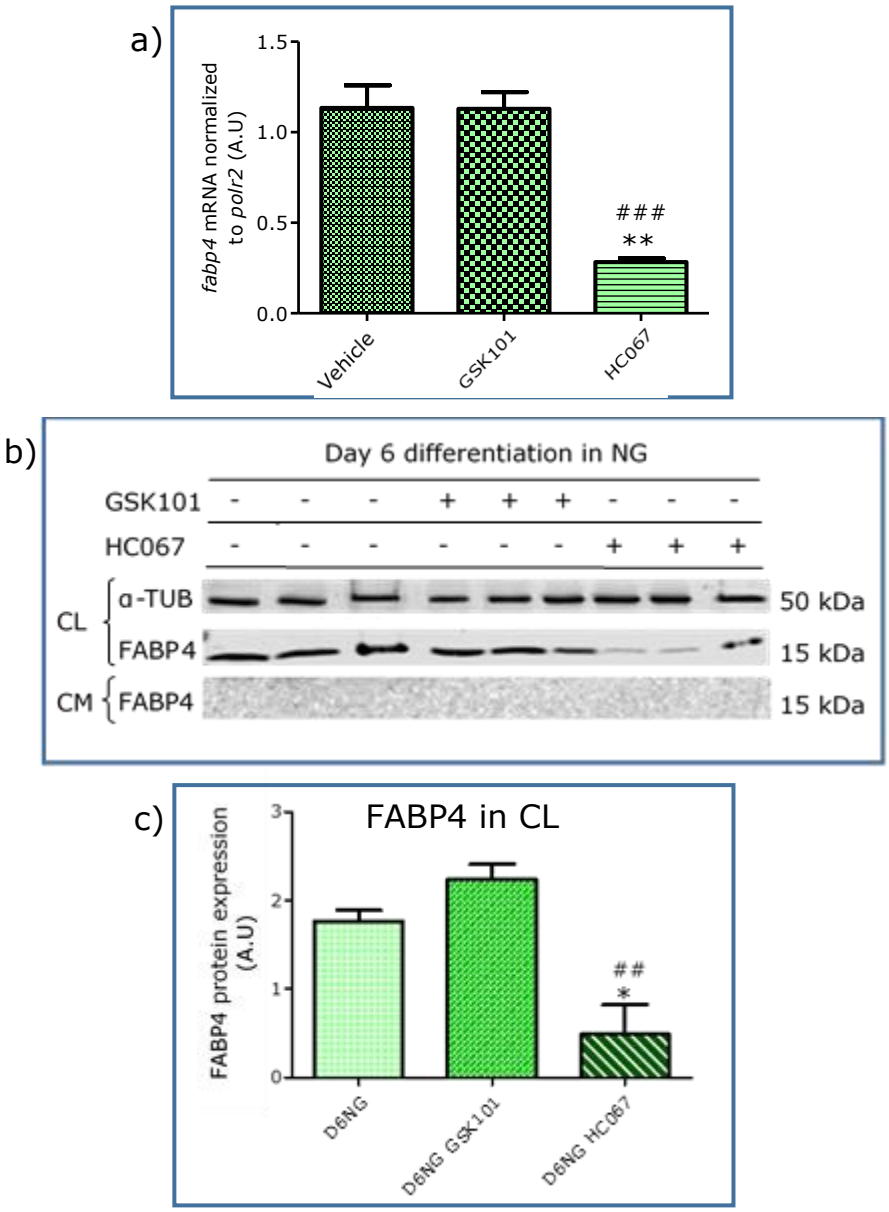

Figure 4.12: FABP4 mRNA expression, protein expression and secretion at day 6 adipocytes differentiation treated with TRPV4 ligands in NG media. (a) qRT-PCR analysis of *fabp4* mRNA expression, (b) WB results for FABP4 protein expression from CL and protein secretion from CM. The results were obtained from at least three independent experiments; n=3 or 4 in each preparation. (c) Statistical analysis of FABP4 protein expression using Image J. The data for gene and protein were analysed by using one-way ANOVA, followed by Bonferroni's post-hoc test and expressed as mean ± SEM; *p<0.05, **p<0.01, ***p<0.001; TRPV4 agonist (GSK101 100nM); TRPV4 antagonist (HC067 500nM); *=compare to control; #=compare to agonist.

ii. Day 6 HG

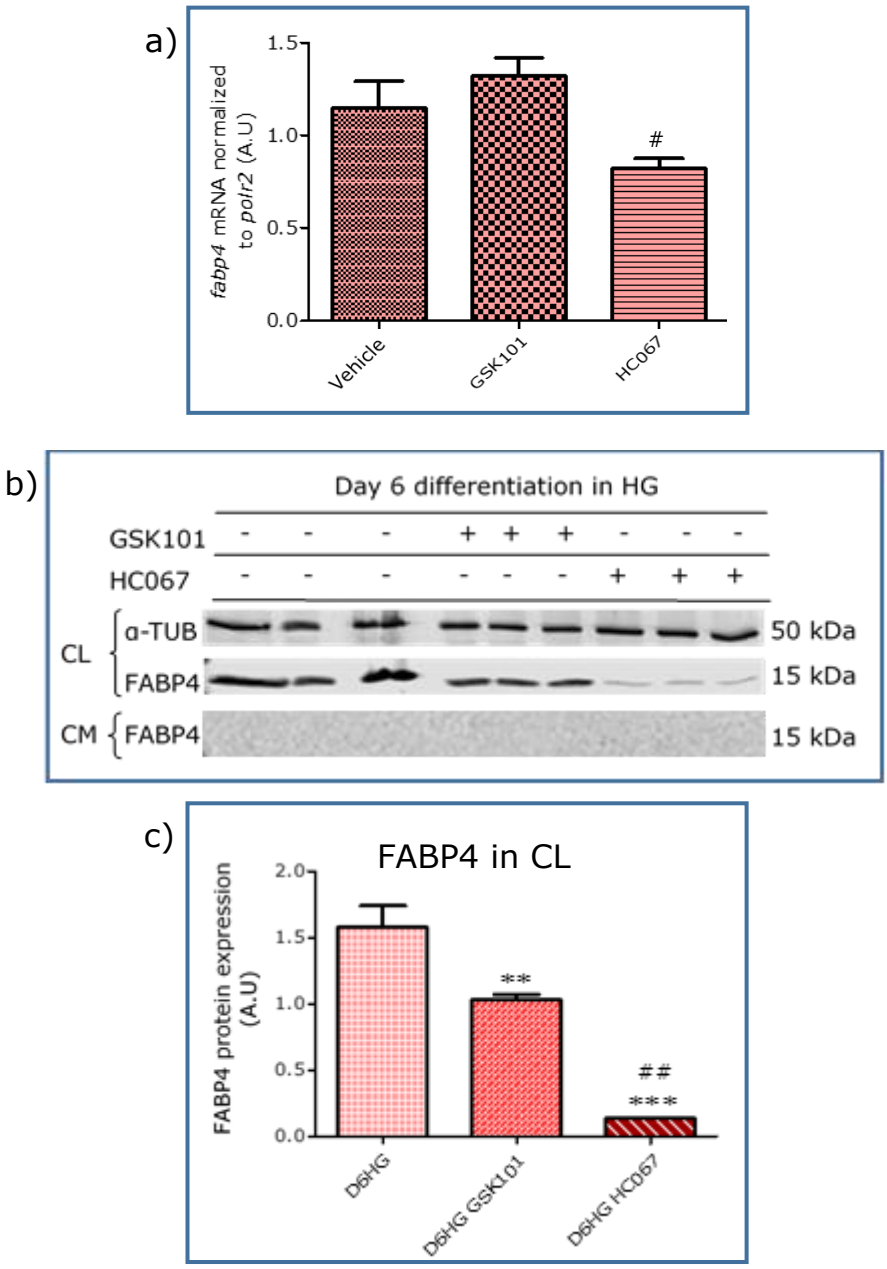

Figure 4.13: FABP4 mRNA expression, protein expression and secretion at day 6 adipocytes differentiation treated with TRPV4 ligands in HG media. (a) qRT-PCR analysis of *fabp4* mRNA expression, (b) WB results for FABP4 protein expression from CL and protein secretion from CM. The results were obtained from at least three independent experiments; *n*=3 or 4 in each preparation. (c) Statistical analysis of FABP4 protein expression using Image J. The data for gene and protein were analysed by using one-way ANOVA, followed by Bonferroni's post-hoc test and expressed as mean ± SEM; *p<0.05, **p<0.01, ***p<0.001; TRPV4 agonist (GSK101 100nM); TRPV4 antagonist (HC067 500nM); *=compare to control; #=compare to agonist.

iii. Day 10 NG

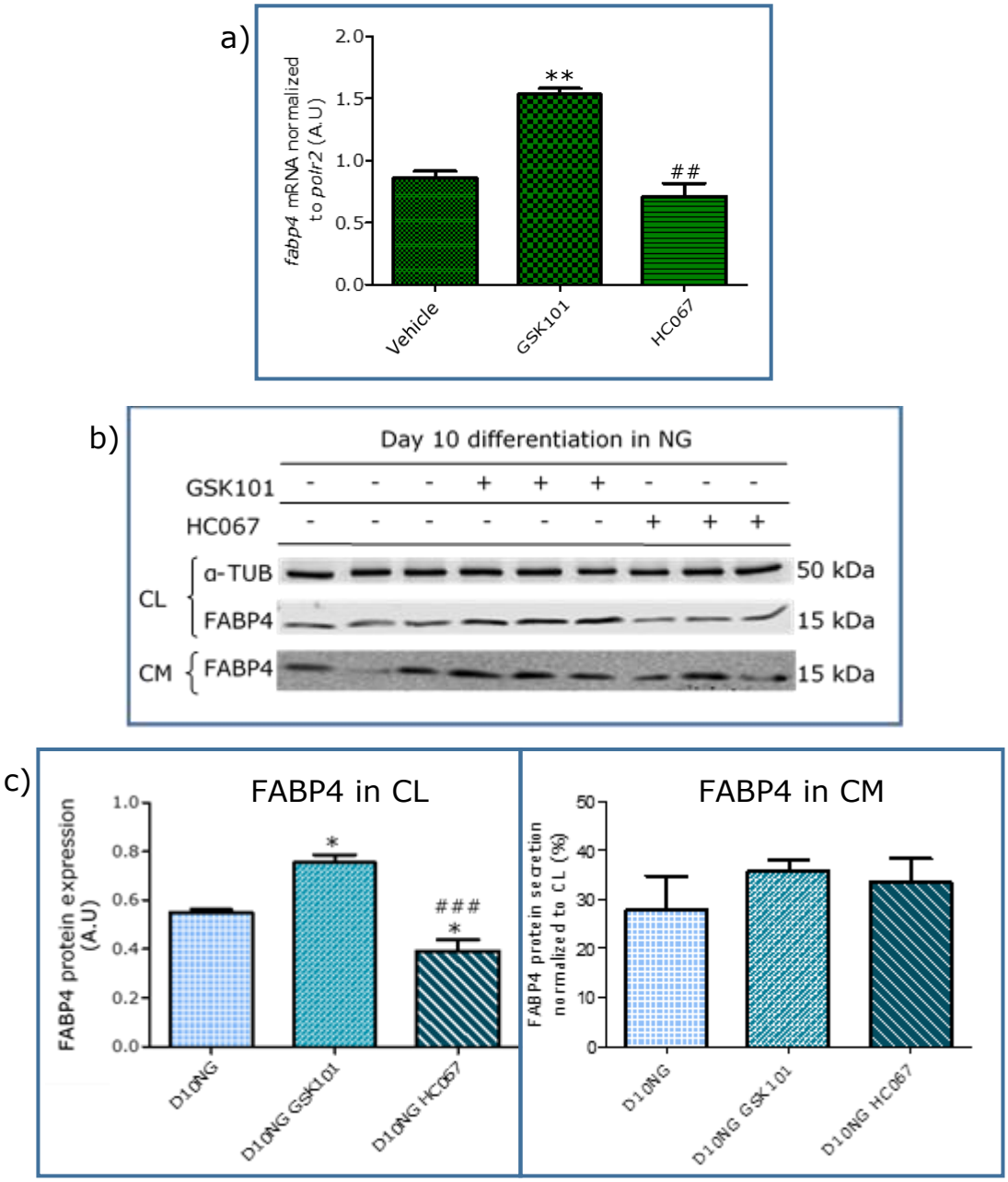

Figure 4.14: FABP4 mRNA expression, protein expression and secretion at day 10 adipocytes differentiation treated with TRPV4 ligands in NG media. (a) qRT-PCR analysis of *fabp4* mRNA expression, (b) WB results for FABP4 protein expression from CL and protein secretion from CM. The results were obtained from at least three independent experiments; *n*=3 or 4 in each preparation. (c) Statistical analysis of FABP4 protein expression and secretion using Image J. The data for gene and protein were analysed by using one-way ANOVA, followed by Bonferroni's post-hoc test and expressed as mean ± SEM; **p*<0.05, ***p*<0.01, ****p*<0.001; TRPV4 agonist (GSK101 100nM); TRPV4 antagonist (HC067 500nM); *=compare to control; #=compare to agonist.

iv. Day 10 HG

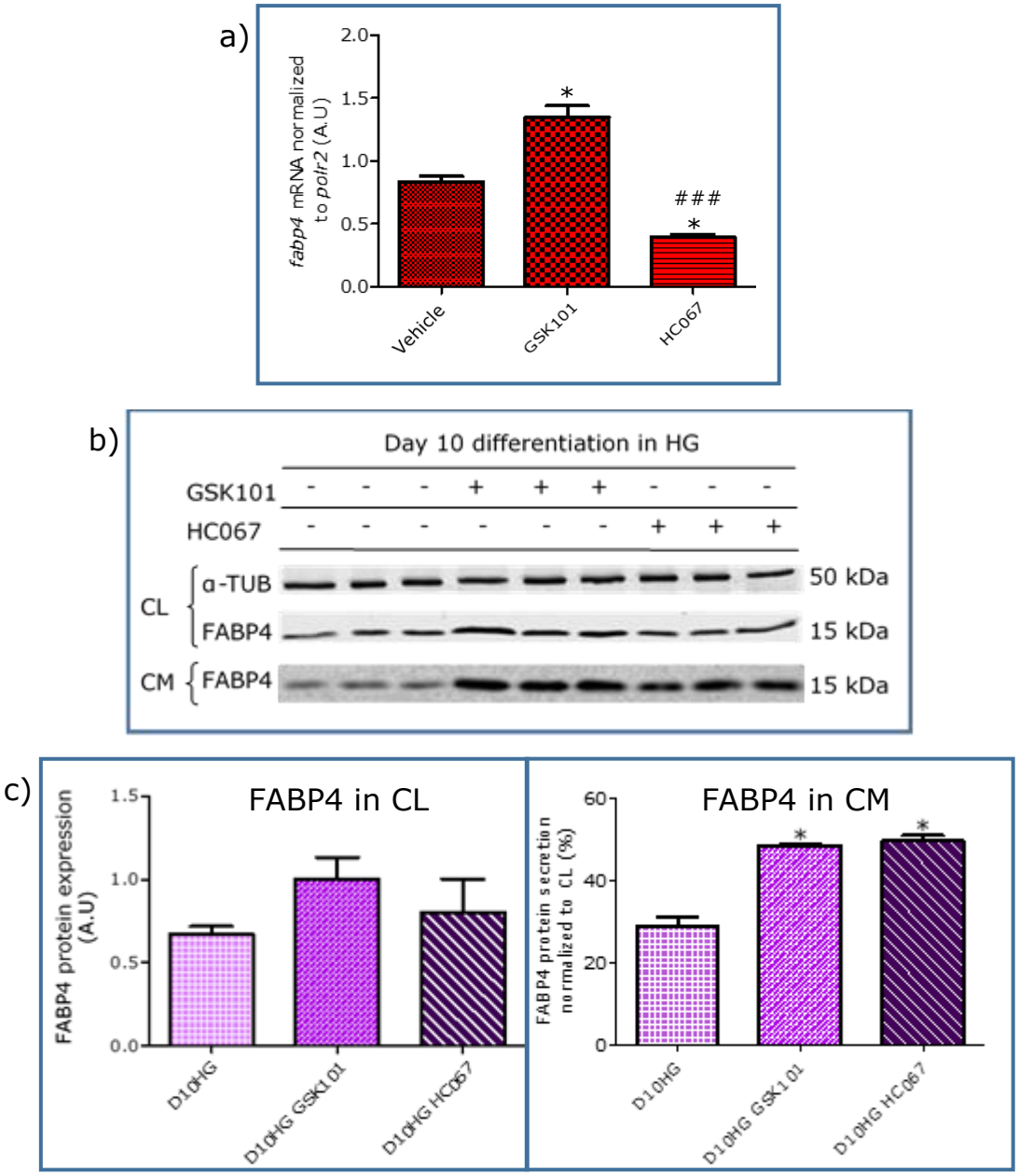

Figure 4.15: FABP4 mRNA expression, protein expression and secretion at day 10 adipocytes differentiation treated with TRPV4 ligands in HG media. (a) qRT-PCR analysis of *fabp4* mRNA expression, (b) WB results for FABP4 protein expression from CL and protein secretion from CM. The results were obtained from at least three independent experiments; n=3 or 4 in each preparation. (c) Statistical analysis of FABP4 protein expression and secretion using Image J. The data for gene and protein were analysed by using one-way ANOVA, followed by Bonferroni's post-hoc test and expressed as mean ± SEM; *p<0.05, **p<0.01, ***p<0.001; TRPV4 agonist (GSK101 100nM); TRPV4 antagonist (HC067 500nM); *=compare to control; #=compare to agonist.

Stimulation of the channel with TRPV4 agonist did not show significant increment on *fabp4* gene expression except for day 10 groups, whereas cells treated with TRPV4 antagonist showed reduced expression.

Inhibition by HC067 was observed as it downregulated FABP4 protein expression. However, this effect was not reflected in its secretion as FABP4 protein band was not seen among day 6 CM samples; whereas day 10 FABP4 protein secretion was not corresponded to its gene and protein expression.

Since Figure 4.7 showed that *trpv4* gene expression was significantly different between day 6 and day 10 differentiation; this study intended to determine the interaction between glucose concentration media and TRPV4 ligands towards genes expression in primary rat adipocyte. A two-way ANOVA was conducted to analyse the influence of two independent variables (glucose, TRPV4 treatments) on adipocytes' genes expression (*lcn2, fabp4, pparγ, pgc1α and ccl2*). Glucose concentration media included two levels (NG, HG), while TRPV4 treatment consisted of three levels (untreated/vehicle, GSK101, HC067).

4.3.6) Interation of factors that affect regulation of *lcn2* gene expression

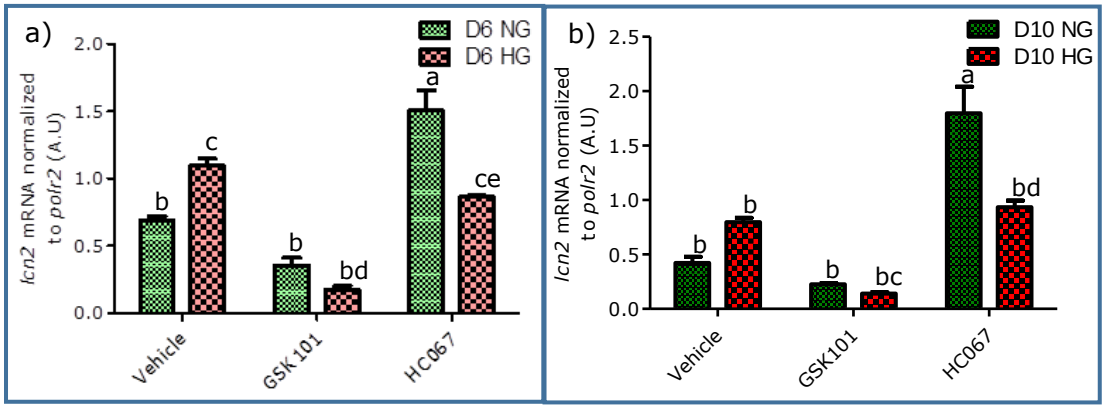

Figure 4.16: Interaction among glucose concentration and TRPV4 agonist and antagonist, which influence *lcn2* gene expression from primary rat adipocytes. (a) Day 6 differentiated cells in NG and HG and (b) day 10 differentiated cells in NG and HG. The data were repeated thrice and analysed by using two-way ANOVA, followed by Bonferroni's post-hoc test and expressed as mean ± SEM, n=3; *p<0.05, **p<0.01, ***p<0.001; TRPV4 agonist (GSK101 100nM); TRPV4 antagonist (HC067 500nM).

The main effect of glucose concentration on *lcn2* gene expression was significant at day 6 ($F(1,12) = 5.41$, $p = 0.038$) and day 10 ($F(1,12) = 4.83$, $p = 0.048$). Besides, the main effect of TRPV4 treatments on *lcn2* gene expression among day 6 ($F(2,12) = 84.14$, $p < 0.0001$), as well as day 10 ($F(2,12) = 63.27$, $p < 0.0001$) was also significant.

Both the above graphs showed significant interaction between glucose concentration and TRPV4 treatment, [day 6: $F(2,12) = 26.40$, $p = < 0.0001$; day 10: $F(2,12) = 17.33$, $p = 0.0003$].

For day 6 (Figure 4.16 a), GSK101 led to significant reduction in *lcn2* gene expression in HG as compared to vehicle [$F(2,12) = 9.0$, $p < 0.001$] and HC067 [$F(2,12) = 6.741$, $p < 0.001$]. The remarkable increment of *lcn2* gene level caused by HC067 was seen in NG, but not in HG ($F(2,12) = 2.259$, $p > 0.05$).

Figure 4.16 (b) showed similar negative effect of GSK101 towards *lcn2* gene expression in HG at day 10 adipocytes differentiation. Similar to day 6, day 10 HG also revealed insignificant increment of *lcn2* gene expression caused by HC067 $F(2,12) = 0.9003$, $p > 0.05$).

4.3.7) Interation of factors that affect regulation of *fabp4* gene expression

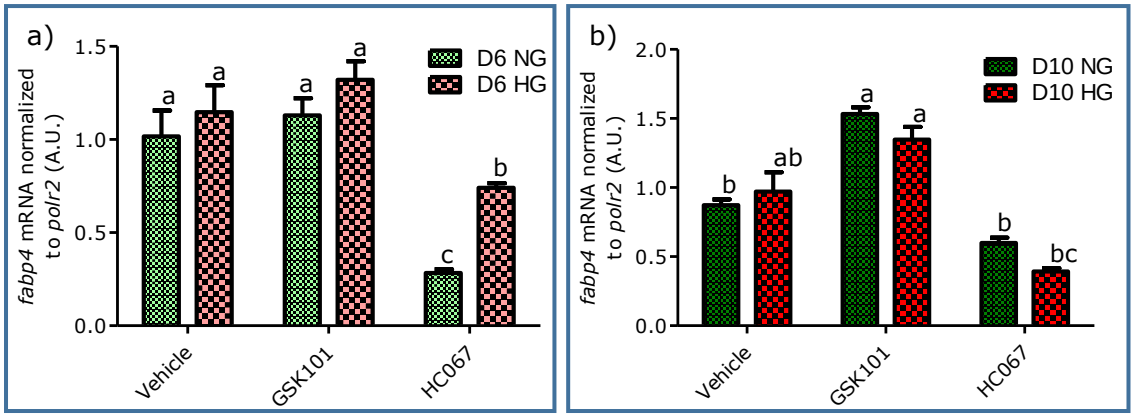

Figure 4.17: Interaction among glucose concentration and TRPV4 agonist and antagonist, which influence *fabp4* gene expression from primary rat adipocytes. (a) Day 6 differentiated cells in NG and HG and (b) day 10 differentiated cells in NG and HG. The data were repeated thrice and analysed by using two-way ANOVA, followed by Bonferroni's post-hoc test and expressed as mean ± SEM, n=3; *p<0.05, **p<0.01, ***p<0.001; TRPV4 agonist (GSK101 100nM); TRPV4 antagonist (HC067 500nM).

Figure 4.17 (a) showed both main effects; glucose concentration (F(1,12) = 10.07, p = 0.008) and TRPV4 treatments (F(2,12) = 28.49, p < 0.0001) significantly affect the level of *fabp4* gene. Whilst in day 10 groups (see Figure 4.17 b), *fabp4* gene expression of NG and HG were not significantly different (F(1,12) = 2.56, p = 0.1358); but TRPV4 treatments significantly affect *fabp4* gene level (F(1,12) = 2.56, p = 0.1358).

The interaction of these independent variables was insignificant in both day 6 (F(2,12) = 1.51, p = 0.2596) and day 10 (F(2,12) = 2.61, p = 0.1143), signifying the independent effect of TRPV4 treatments and glucose concentration on *fabp4* gene expression.

4.3.8) Genes involved in adipogenesis and inflammation

i. pparγ

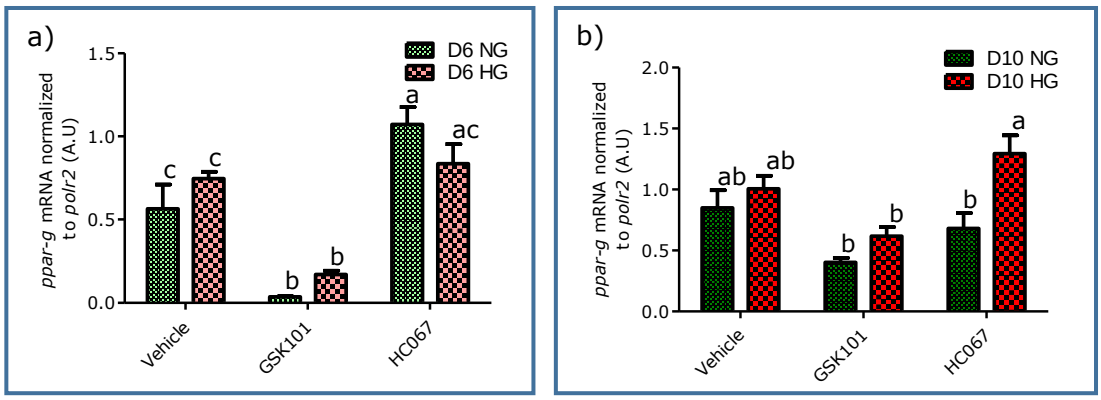

Figure 4.18: Interaction among glucose concentration and TRPV4 agonist and antagonist, which influence *pparγ* gene expression from primary rat adipocytes. (a) Day 6 differentiated cells in NG and HG and (b) day 10 differentiated cells in NG and HG. The data were repeated thrice and analysed by using two-way ANOVA, followed by Bonferroni's post-hoc test and expressed as mean ± SEM, n=3; *p<0.05, **p<0.01, ***p<0.001; TRPV4 agonist (GSK101 100nM); TRPV4 antagonist (HC067 500nM).

The main effect of glucose concentration on *pparγ* gene level among day 6 was not significant ($F(1,12) = 0.14$, $p = 0.7141$), in contrast to the main effect TRPV4 treatments ($F(2,12) = 46.40$, $p < 0.0001$) (see Figure 4.18 a). Whereas day 10 showed both main effects significantly affects *pparγ* gene expression [glucose: $F(1,12) = 12.49$, $p = 0.0041$; TRPV4: $F(2,12) = 10.43$, $p = 0.0024$].

Nevertheless, the interaction of these two independent variables was insignificant in both day 6 ($F(2,12) = 3.23$, $p = 0.0752$) and day 10 ($F(2,12) = 2.38$, $p = 0.1347$.

ii. pgc1a

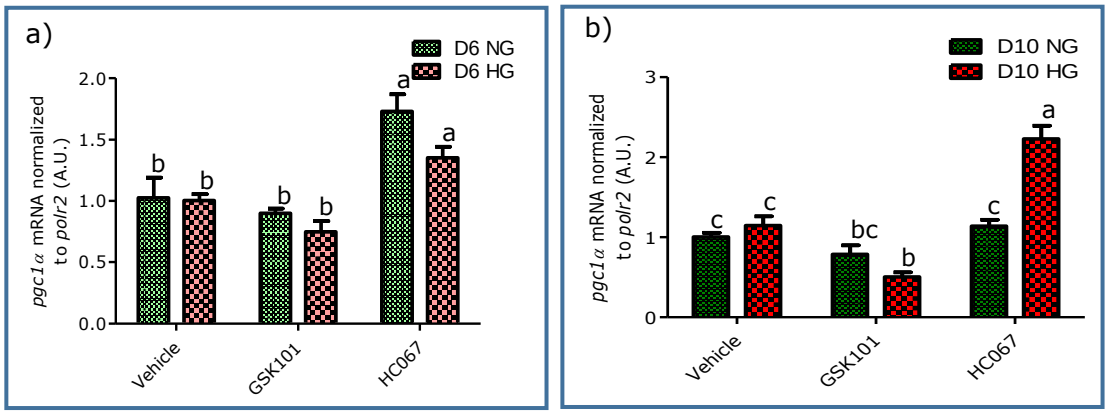

Figure 4.19: Interaction among glucose concentration and TRPV4 agonist and antagonist, which influence *pgc1a* gene expression from primary rat adipocytes. (a) Day 6 differentiated cells in NG and HG and (b) day 10 differentiated cells in NG and HG. The data were repeated thrice and analysed by using two-way ANOVA, followed by Bonferroni's post-hoc test and expressed as mean ± SEM, n=3; *p<0.05, **p<0.01, ***p<0.001; TRPV4 agonist (GSK101 100nM); TRPV4 antagonist (HC067 500nM).

For differentiating adipocytes as in day 6 (see Figure 4.19 a), the main effect of glucose concentration on *pgc1a* gene expression was not significant ($F(2,12) = 4.71$, $p = 0.0507$), but the main effect of TRPV4 treatments was significant, ($F(2,12) = 25.12$, $p < 0.0001$); such that cells treated with HC067 had raised level of *pgc1a* gene compared to vehicle and GSK101. However, the interaction of these two independent variables was insignificant ($F(2,12) = 1.49$, $p = 0.2651$).

As for mature adipocytes depicted by day 10 (see Figure 4.19 b), both main effects; glucose concentration ($F(1,12) = 13.54$, $p = 0.0032$) and TRPV4 treatments ($F(2,12) = 49.26$, $p < 0.0001$)

significantly affect the level of *pgc1a* gene. Hence, the interaction of main effects was significant ($F(2,12) = 22.26$, $p < 0.0001$). For day 10 HG, HC067 led to significant increment of *pgc1a* gene expression than day 10 NG (M = 2.228, SD = 0.544).

iii. ccl2

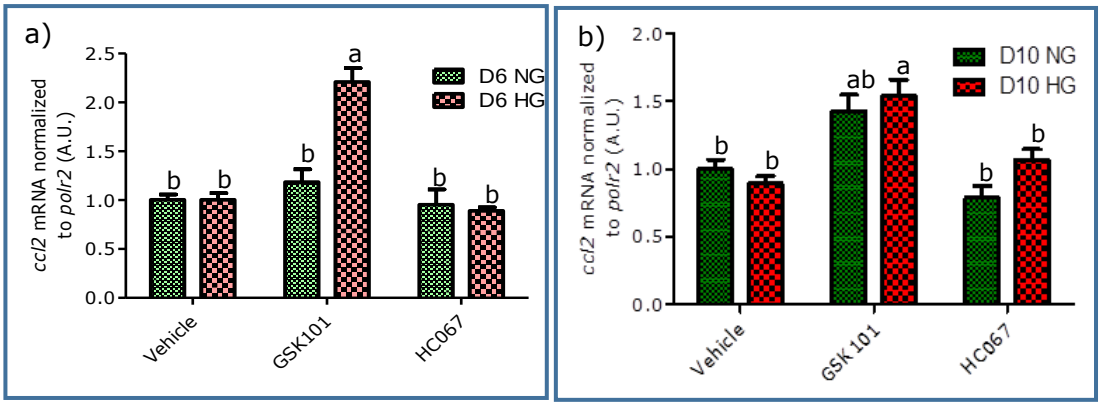

Figure 4.20: Interaction among glucose concentration and TRPV4 agonist and antagonist, which influence *ccl2* gene expression from primary rat adipocytes. (a) Day 6 differentiated cells in NG and HG and (b) day 10 differentiated cells in NG and HG. The data were repeated thrice and analysed by using two-way ANOVA, followed by Bonferroni's post-hoc test and expressed as mean ± SEM, $n=3$; *$p<0.05$, **$p<0.01$, ***$p<0.001$; TRPV4 agonist (GSK101 100nM); TRPV4 antagonist (HC067 500nM).

In Figure 4.20 (a), the data revealed significant main effects [glucose: $F(1,12) = 13.07$, $p = 0.0035$; TRPV4: $F(2,12) = 30.64$, $p < 0.0001$] and interaction effect ($F(2,12) = 15.82$, $p = 0.0004$). It appears that GSK101 (M = 2.21, SD = 0.51) led to significant increment of *ccl2* gene expression in HG as compared to vehicle (M = 0.97, SD = 0.0167) and HC067 (M = 0.89, SD = 0.0317). However, TRPV4 treatments had no effect in NG condition.

Figure 4.20 (b) showed main effect of TRPV4 treatments yielded an F ratio of $F(2,12) = 24.46$, $p < 0.0001$, whereas main effect of glucose was not significant ($F(1,12) = 1.16$, $p = 0.2288$). The interaction effect was also insignificant ($F(2,12) = 2.35$, $p = 0.1374$).

4.4) **Discussion**

Many researchers interested in studying TRPV4, not only due to its role in thermogenesis and mechanosensation, but also because of its association with various diseases (Nilius & Voets, 2013). This has highlighted the importance of the channel in normal physiology. Hence, the effects of TRPV4 agonist and antagonist in NG and HG media on LCN2 and FABP4 signalling in primary cultured rat adipocyte were presented in this chapter.

4.4.1) The effect of concomitant TRPV4 agonist-antagonist upon adipocytes calcium signalling

GSK1016790A (GSK101) is a novel activator for TRPV4 and has the efficacy of much greater than 4α-phorbol 12,13-didecanoate (4α−PDD) (Willette et al., 2008). It appears that GSK101 can cause calcium influx in HEK cells, thus activates whole-cell currents 300-fold more potent than 4α−PDD (Thorneloe et al., 2008; Willette et al., 2008). While other TRPV4 agonist, RN-1747, is noted to be

selective to TRPV3 and able to induce hTRPV1 activation simultaneously at 100μM of dosage (Vincent & AJ Duncton, 2011).

Whereas HC-067047 (HC067), a potent TRPV4 antagonist of human, rat and mouse, able to reverse the activation of TRPV4 regardless of its stimuli. Interestingly, its usage in *in vivo* setting did not affect core body temperature, water intake, heart rate, locomotion or motor coordination (Vincent & AJ Duncton, 2011). Other TRPV4 antagonist such as ruthenium red and gadolinium are reported as lack of specificity towards the channel and known as inhibiting inward, but not outward currents (Garcia-Elias Heras, 2011).

Using calcium imaging, this study employed various concentrations of GSK101 and perfused the cells simultaneously with HC067. Despite of duration of adipogenesis or glucose concentration, HC067 failed to inhibit further rise of calcium flux when GSK101 concentration was increased up to 100nM (see Figure 4.2); as compared to inhibition of GSK101 action by HC067 in cells treated with lower concentration of agonist (refer Appendix D: Figure 6.4 to 6.7). This helped to determine the working concentration in this experiment, similar to as what has been used by Ye *et al* (Ye et al., 2012).

4.4.2) Calcium response in the presence of TRPV4 agonist using calcium and calcium-free media in NG/HG

Next, calcium and calcium-free buffer were employed to further understand the effect of TRPV4 ligands on their receptor in adipocyte. As expected, presence of $[Ca^{2+}]e$ and GSK101 in the buffer induced calcium influx. Interestingly, calcium signalling was still generated, although minimally, by GSK101 in the absence of $[Ca^{2+}]e$ (see Figure 4.3). This was possibly due to release of calcium internal store from organelle, such as ER or mitochondria when cytosolic calcium was depleted (Choi et al., 2011; M. Jin et al., 2011).

4.4.3) *trpv1* and *trpv4* gene expression at day 6 and day 10 differentiation in NG and HG media

In order to determine the effects of these ligands on primary rat adipocyte culture, *trpv1* and *trpv4* mRNA expression were detected and highly expressed at day 6 differentiation, when compared to that at day 10 (see Figure 4.7).

The expression of TRPVs in adipocytes was inconsistently documented, as *trpv4* was observed to be abundantly present together with *trpv2* and *trpm7*, but not *trpv1* (Che, Yue, Tse, & Li, 2014). *trpv1* was reported to be downregulated as the cells aged and

adipogenesis advanced. On the contrary, *trpv4* was lowly expressed in the early phase of adipogenesis and subsequently increased as they turned into mature cells (Baboota et al., 2014). The discrepancy has never been highlighted before since it may be closely related to variances in method, duration and tissues employed in each study. It is believed that expression of TRPVs are most likely high in the early phase of adipogenesis since high level of calcium supresses the progression of adipocyte differentiation, but induces adipogenesis process at a later phase (Bishnoi, Kondepudi, Gupta, Karmase, & Boparai, 2013). This is supported by Shi *et al.* who revealed 60 to 70% reduction of TGs content among day 2 differentiated adipocyte treated with thapsigargin (H. Shi, HALVORSEN, ELLIS, WILKISON, & ZEMEL, 2000).

Although it is tempting to conclude the correlation between TRPVs expression and calcium regulation, as well as its effect on adipogenesis; the role of calcium in signal transduction pathway is intricate as its activation involved numerous mechanisms, such as voltage-operated, store-operated and mechanically-activated channels, among others (Bootman et al., 2001).

4.4.4) The effect of TRPV4 agonist/antagonist upon LCN2 and FABP4 signalling in primary rat adipocytes cultured

i. LCN2

The preliminary results showed that GSK101 diminished *lcn2* expression, while HC076 did not affect *lcn2* gene level in HG but raised the expression significantly among NG. Apparently, LCN2 protein expression and secretion showed that GSK101 diminished LCN2 protein, unlike HC067 that had no profound effect (see Figure 4.8 to 4.11).

To further evaluate the effect of glucose and TRPV4 treatments on LCN2 signalling, the action of these main effects was analysed simultaneously using two-way ANOVA (see Figure 4.16). The result showed that both glucose and TRPV4 treatments affects its expression and the interaction was significant.

In HG media, GSK101 effectively reduced *lcn2* gene expression, but the antagonistic effect of HC067 was not observed. In contrast to NG media, stimulation of the channel showed insignificant effect on *lcn2* expression, but inhibition by HC067 remarkably induced *lcn2* gene level. It can be concluded that the interplay between HG and GSK101 significantly suppressed the expression, but presence of HC067 in NG positively affect the level of *lcn2* gene. This was similarly observed either at day 6 or day 10 differentiation.

ii. FABP4

Stimulation of the channel did not affect FABP4 signalling, unlike antagonist treatment that was able to reduce its expression and secretion (see Figure 4.12 to 4.15). However, FABP4 secretion was not observed at day 6, only can be visualized among day 10 groups. This finding is similar to other reports that FABP4 is being secreted by mature cells (Kralisch et al., 2014; Schlottmann et al., 2014).

Intracellular and extracellular calcium are said to be involved in cell proliferation, differentiation and survival in 3T3-L1 cells (Jensen, Farach-Carson, Kenaley, & Akanbi, 2004; Ochieng, Tahin, Booth, & Russo, 1991). Thus, induction of calcium signalling by GSK101 at day 10 differentiation could possibly lead to secretion of FABP4 as part of paracrine/endocrine signalling. This finding is supported by others that linked FABP4 secretion with raised [Ca2+]*i* induced by ionomycin (Kralisch et al., 2014; Schlottmann et al., 2014). To date, no report has explained FABP4 protein expression or secretion at early phase of differentiation.

As the interaction effect was insignificant between glucose concentration and TRPV4 treatments in both day 6 and day 10 groups, the latter factor was noted to be significantly affect *fabp4* expression. Correspondingly, inhibition of the channel by HC067 caused reduction of *fabp4* gene expression, and the response was

equally similar in NG and HG media. Whereas glucose only affect its expression among day 6 groups, such that reduction of *fabp4* gene level in HC067-NG was significantly lower than HC067-HG (see Figure 4.17).

4.4.5) The effects of TRPV4 agonist/antagonist upon genes involved in adipogenesis and inflammation

In relation to response of these adipocyte LCPs with TRPV4 ligands, the interaction of main effects (glucose concentration and TRPV4 treatments) towards genes involved in adipogenesis and inflammation were also analysed.

i. *pparγ* and *pgc1α*

PPARγ is an important transcription factor which also known as key regulator in adipogenesis. While PGC1α is a transcription co-activator that engages with many transcription factors responsible for glucose/fatty acid metabolism, thermogenesis and mitochondrial biogenesis (Liang & Ward, 2006). It acts as a co-activator for PPARγ and regulates uncoupling protein 1 (UCP1) promoter in BAT (Ye et al., 2012).

This study output showed that both *pparγ* and *pgc1α* mRNA expressions significantly decreased following GSK101 treatment, as

compared to HC067. This suggests that increased $[Ca^{2+}]i$ negatively affect adipogenic process. This finding is supported by the inverse relationship between *pparγ* and calreticulin, an ER luminal protein that binds to calcium ion. They found that increased $[Ca^{2+}]e$ caused reduction in expression of adipogenic genes, such as *pparγ* and CCAAT enhancer binding protein alpha (*CEBP/α*), while upregulating calreticulin mRNA and protein expression (Vergara, Dela Cruz, Kim, & Hwang, 2016). Whereas *pgc1α* is negatively regulated by TRPV4 since it is able to promote expression of genes responsible for phosphorylation of mitochondrial oxidation in *trpv4* knockdown adipocyte (Ye, 2013; Ye et al., 2012).

ii. ccl2

Monocyte chemoattractant protein 1 (MCP-1), also known as CCL2, is responsible for infiltration of monocytes and memory T lymphocytes into tissues. It is known as adipokine that involved in initiating insulin resistance, hence noted to be increased in obese animals and humans (Bruun, Lihn, Pedersen, & Richelsen, 2005). Among inflammatory genes studied by Xu *et al.*, *ccl2* expression increased as early as 3 weeks post-induction of obesity and insulin-resistance in mice by HFD, when compared to other cytokines (H. Xu et al., 2003).

Based on the outcomes, both day 6 and day 10 HG groups treated with GSK101, showed at least one-fold higher *ccl2* mRNA expression as compared to control. It is remarkably significant, in comparison to NG groups. This suggests that high $[Ca^{2+}]i$ initiates inflammatory cytokines expression with the presence of HG condition, but not in NG.

In summary, this study has demonstrated that TRPV4 ligands are able to induce calcium mobilisation, either in calcium or calcium-free buffer. *trpv1* and *trpv4* mRNA expressions also have been successfully identified in primary cultured rat adipocytes grown in NG and HG media at day 6 and day 10 differentiation. The study outcomes suggest that presence of inflammatory state, such as raised cytosolic calcium, in concurrent hyperglycaemia, suppresses the expression of *lcn2,* but induce *ccl2*. While HG together with GSK101 did not have much effect towards *fabp4* as compared to HC067, that is capable of negatively regulates *fabp4*. Activation of TRPV4 caused reduction in *pparγ* and *pgc1α* expressions, and inhibition of the channel showed contradictory outcome.

CHAPTER 5: GENERAL DISCUSSION

5) Discussion

Previously known as an inert nutrient storage, AT has begun receiving great attention as an essential organ responsible in development of metabolic diseases. Initiation of metainflammation in AT is caused by interplay of various mediators that involve several extracellular factors, such as FFAs and cytokines, as well as intracellular factors, such as ER stress and ROS overproduction by mitochondria. Such signalling mediates inflammatory cascade in the cell and activates various kinases pathways, for example, IKK and JNK. These metabolic changes seemed to induce development of insulin resistance, as illustrated in Figure 5.1.

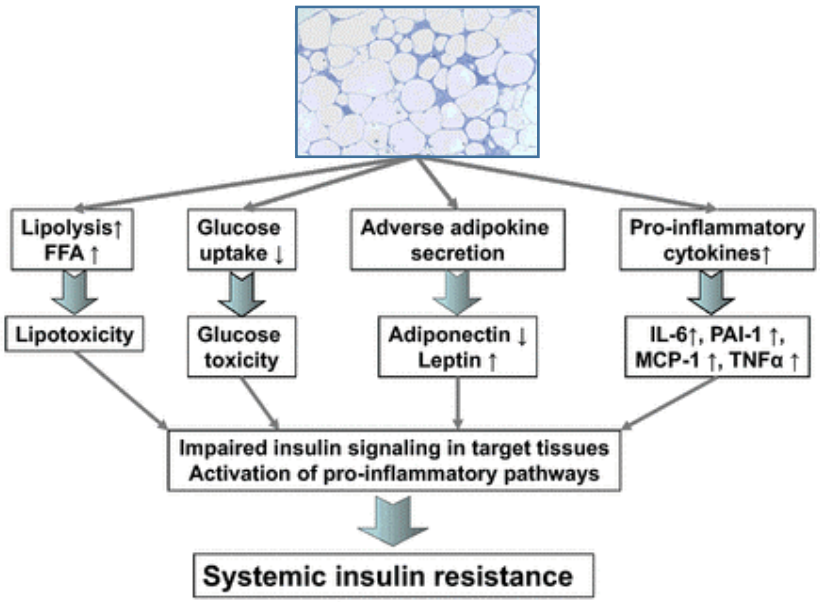

Figure 5.1: Mechanistic model for the link between adipose tissue inflammation and insulin resistance [adapted from (Blüher, 2016)].

In relation to the above, this study addressed three main areas, which are: 1) the effect of concurrent obesogenic factors on LCPs expression and secretion in adipocyte, 2) changes in LCPs signalling in the presence of TRPV4 ligands, particularly GSK101, which manifests as pro-inflammatory mediator, and lastly 3) the interaction effects of various inflammatory factors upon adipocyte genes expression.

First, as presented in Chapter 3, the regulation of *lcn2* gene expression, protein expression and secretion were affected significantly by glucose concentration and oxygenation (see Figure 3.7). These findings were most likely mediated by different insulin concentration supplemented in NG and HG, as insulin, together with glucose, is crucial in regulating metabolic homeostasis (Y. Zhang et al., 2014). Since glucose mediates LCN2 regulation, it was expected that hypoxia supressed LCN2 since the latter inhibited insulin-stimulated glucose uptake, as evidence by decreased IRβ and IRS-1 protein expression in 3T3-L1 adipocytes (Yin et al., 2009).

Whereas FABP4 signalling was only influenced by oxygenation (see Figure 3.8). This study outcomes showed insignificant variances between FABP4 mRNA, protein expression and protein secretion among NG and HG groups although Qin *et al.* reported that HG can induce *fabp4* expression (B. Qin & Anderson, 2011). This supports

the notion that insulin is capable of suppressing FABP4 signalling from adipocytes since HG was given higher concentration of insulin than NG (Cao et al., 2013; Mita et al., 2015). Apart from that, hypoxia, which upregulates lipolysis and FFAs efflux (Chan, Hsieh, & Understanding, 2017), appears to increase circulating FABP4, which was demonstrated in the empirical outcomes (see Figure 3.8 b and c). Hence, increase plasma FABP4 is suggestive as a metabolic biomarker for obesity (Wu et al., 2014; A. Xu et al., 2006).

These results also demonstrated conflicting outcome as hypoxia caused downregulation of *fabp4* mRNA expression but upregulated its protein secretion. To date, evidence of adipokine gene transcription up to its protein signalling is scarce, as most studies mainly focused on gene expression analysis. Trayhurn *et al.* in his review, reported decreased adipocyte key genes expression, including *fabp4* and *fabp5*, in response to hypoxia (Trayhurn, 2013). Wu *et al*. discovered elevated FABP4 secretion in hypoxia; similar to that obtained in this study (Wu et al., 2014). Hence, it is rather challenging to explain FABP4 regulation in adipocytes due to lack of signalling peptide, either nuclear or secretory (Furuhashi & Hotamisligil, 2008; Furuhashi et al., 2014). The intricacy of this notion is also shared by Dusserre *et al*., since AT, which yielded very low total RNA concentration, expressed gene coding for adipokines that did not necessarily translated into protein via direct manner

(Dusserre, Moulin, & Vidal, 2000). This discrepancy could be due to several assumptions, namely synthesized protein half-life, which is responsible in determining protein turnover, thus further regulates mRNA-protein synthesis (Maier, Güell, & Serrano, 2009), recycling of tRNAs that enhances the efficiency of translational elongation, and dynamically changing tRNAs supply in response to various cellular milieu (Gingold & Pilpel, 2011).

In Chapter 4 , GSK101 was applied; a potent TRPV4 agonist that induces $[Ca^{2+}]i$ response, which is capable of mediating inflammatory response and affect adipocyte LCPs signalling (Ye et al., 2012). Calcium is required in glucose metabolism within its optimal range since it can exert dual function in affecting insulin sensitivity. Reduction in $[Ca^{2+}]i$ due to chelation by BAPTA-AM, results in diminished GLUT4 vesicle translocation to plasma membrane (Worrall & Olefsky, 2002). Whilst adipocyte treated with ionomycin, a calcium ionophore, showed impaired insulin-stimulated glucose uptake (BORIS DRAZNIN et al., 1989; B Draznin et al., 1988). This is because, the ideal calcium concentration to stimulate glucose transport by insulin in rat adipocyte is between 1 to 2nM (B Draznin, Sussman, Kao, Lewis, & Sherman, 1987) and any level beyond optimal range may affect cellular signalling and metabolism.

As evidence by calcium imaging (see Figure 4.3 to 4.6), pharmacological approach of TRPV4 showed that stimulation by GSK101 can act as negative regulator of LCN2, so does inhibition by HC067 towards FABP4 (see Figure 4.8 to 4.11). It has been reported that inhibition of TRPV4 in cultured adipocyte also reduced the expression of multiple proinflammatory genes such as *tnfa, Rantes* and *Vcam* (Ye, 2013).

Activation of TRPV4 suppressed *pparγ* and *pgc1α* expression but increased *ccl2* gene level. Conversely, chemical inhibition of TRPV4 channel antagonised these outcomes. It appears that stimulation of TRPV4 by its ligand may compromise adipogenesis and presumably induce inflammatory response.

Finally, throughout the analysis, adipocyte LCPs signalling is expressed differently at day 6 and day 10 adipogenesis. The interaction effect of increased $[Ca^{2+}]i$ significantly associated with HG in suppressing *lcn2* expression and inducing *ccl2* gene level. However, the former factor acted independently in affecting the expression of *fabp4.* The main effect of TRPV4 treatments also significantly affect the expression of *pparγ* and *pgc1α* as compared to the main effect of glucose concentration.

These study outcomes extend a small but growing body of literature as it appeared to be the first report that document regulation of adipocyte-derived LCPs gene expression, protein expression and secretion post concurrent obesogenic and TRPV4 treatments. Therefore, understanding the regulation of adipocyte molecular signalling exerted by interaction of multiple factors helps to initiate an appropriate approach in underpinning mechanism towards development and progression of metabolic diseases. For example, when these two main effects (glucose concentration and TRPV4 treatments) were investigated in this study, it seems that the interplay between glucose and chemical manipulation of TRPV4 channel is essential in regulating adipogenic genes that are responsible in adipogenesis and inflammation.

5.1) **Limitation to the study**

One of the main limitations in this study is its cross-sectional design, which does not permit determination of cause-and-effect relationships between various factors; nonetheless enough to make inferences about possible interplay of the variables that influenced the outcome. Thus, the obtained results should be interpreted with caution.

Additionally, three-way ANOVA could be conducted to explore interrelation of various physiological and pathological factors

towards adipocyte LCPs signalling. However, this current study focused on the effect of obesogenic and inflammatory factors in LCN2 and FABP4 signalling. Thus, inclusion of physiological factors such as differentiation duration may diverge from the research objective.

Besides, *trpv4* gene expression at day 6 and day 10 adipocytes differentiation were significantly different (see Figure 4.7 b). Therefore, comparing the outcome of TRPV4 activation and inhibition towards adipocytes' LCPs in these two durations would be unparalleled.

In order to make a comparable assessment, analysis of another receptor that is consistently expressed throughout adipogenesis could be done. For instance, expression of vitamin D receptor (VDR) was very low in 3T3-L1 preadipocyte stage, and constantly expressed minimally from day 2 differentiation onwards (Ji, Doumit, & Hill, 2015). It appears that activation of VDR by its natural ligand, 1α,25-dihydroxyvitamin D_3 ($1,25(OH)_2D_3$, or calcitriol) inhibits 3T3-L1 preadipocyte differentiation. This is supported as evidence by suppression of adipogenic transcription factors (such as *C/EBPβ, pparγ and srebp1*) and adipocyte markers (such as LPL and FAS) (Ding, Gao, Wilding, Trayhurn, & Bing, 2012).

5.2) **Further study of interest**

Perhaps, if further experiment is designed to extend the scope of the study, preadipocyte stage could be included to elicit differences in molecular signalling from initially undifferentiated cells up to mature cells. Higher glucose concentration media (e.g: 25-30mmol/L) could be included in order to observe possible detrimental effect to the cells as compared to what has been observed in this study.

Nonetheless, further study can be extended by investigating role of Ca^{2+}/calmodulin-dependent protein kinase II (CaMKK2) in adipocytes metabolism. Increased in $[Ca^{2+}]i$ leads to activation of calmodulin, and subsequently CaMKK2 (Hurley et al., 2005). It appears that expression of *camkk2* reduced as adipocyte differentiation advances. The inverse correlation between *camkk2* and adipogenic transcription factor, such as *C/EBP*, indicates its inhibitory effect on adipogenesis (Lin, Ribar, & Means, 2011). CaMKK2 and its substrate, 5' adenosine monophosphate-activated protein kinase (AMPK), maintain the expression of *Pref-1* as it acts as transcriptional repressor towards *C/EBP*β and *C/EBP*δ. These two genes are known as positive regulator of preadipocyte differentiation to adipocyte (Kim, Kim, Wang, Sul, & biology, 2007). It seems that activation of CamKK2 in undifferentiated state suppresses adipogenesis and is associated with low adipogenic marker such as

fabp4. It would be interesting to investigate the role of *lcn2* since it is found to be highly expressed in early stage of adipogenesis.

Other intracellular calcium signalling molecules that may be involved in regulating adipocyte LCPs is nuclear factor of activated T cell (NFAT), a transcription factor modulated by calcium/calcineurin regulation. NFAT has been thought to bind and activate FABP4 promoter; while treatment with cyclosporine A (CsA), an immunosuppressive drug that is known to inhibit NFAT pathway in lymphocytes, showed poor oil red 'O' staining in differentiating 3T3-L1 adipocyte, as well as reduction in *C/EBPα* and *fabp4* (Ho, Kim, Rooney, Spiegelman, & Glimcher, 1998). Meanwhile, Kang *et al*. demonstrated the ability of CsA and FK506, which are calcineurin inhibitors, in promoting NF-κB signalling; suggesting that activation of calcineurin may suppress NF-κB activity (Kang et al., 2007). These suggests the role of NFAT in upregulating *fabp4* and downregulating *lcn2* in the presence of high $[Ca^{2+}]i$ via increment in calcineurin activity.

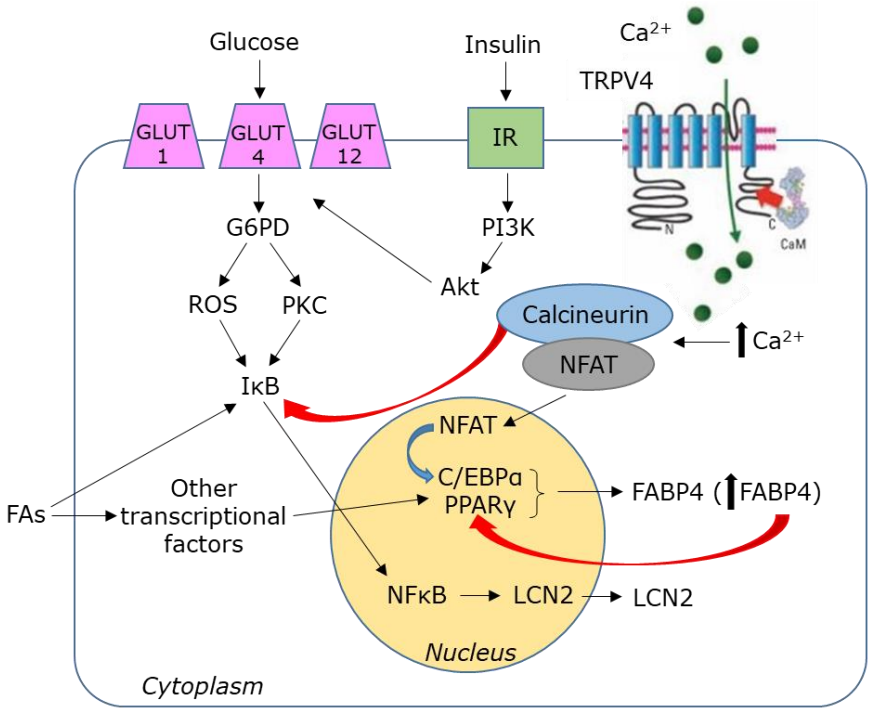

Figure 5.2: A model of insulin-mediated glucose uptake, FAs and calcium influx in regulating transcription factors, thus further influences the production of LCPs. Blue arrow=induce, red arrow=suppress.

6) Appendices

6.1) **Appendix A: Cell viability post-GSK101 treatment**

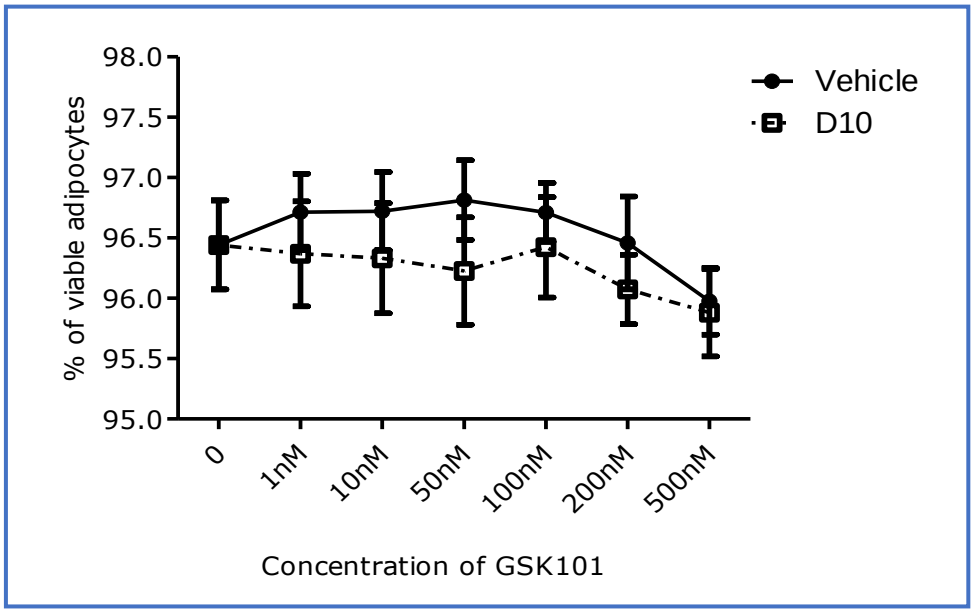

Figure 6.1: Dose response analysis using various concentrations of GSK101 upon viability of primary cultured rat adipocytes incubated for 24 hours. Trypan blue assay was used to assess the cells at day 10 differentiation. The data were analysed by using two-way ANOVA, followed by Bonferroni's post-hoc test and expressed as mean ± SEM, n=4. This experiment was repeated three times using samples from 3 different preparations.

To verify the viability of cells treated with GSK101, two-way ANOVA was performed to assess the impact of various GSK101 concentrations in media, when compared to vehicle, upon number of live cells in percentage. There was a statistically insignificant interaction between the effect of GSK101 dosages up to 500nM in media and vehicle groups on the viability of cells, $F(6, 42)=0.15$, $p=0.99$.

6.2) **Appendix B: Determining gene as internal reference**

a) *polr2*

slope	3.47003146
intercept	25.86153831
r2	0.99891037

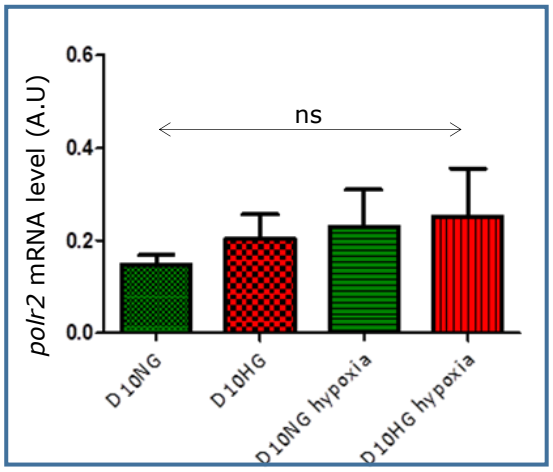

b) *β-actin*

slope	3.658020655
intercept	23.18753146
r2	0.995094601

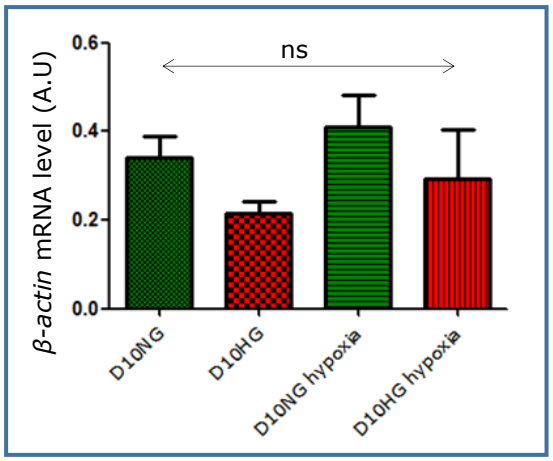

c) *gapdh*

slope	3.706807108
intercept	20.6158626
r2	0.998831883

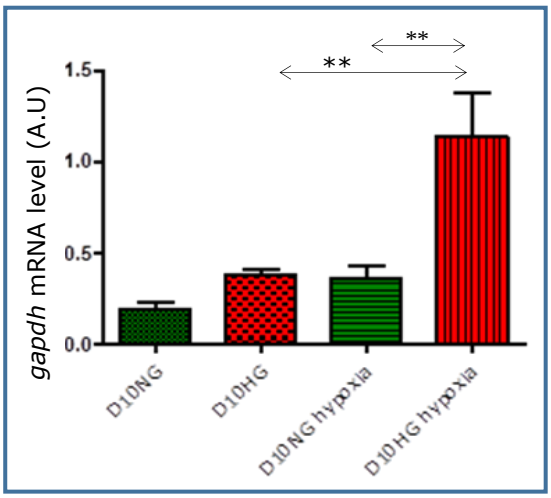

Figure 6.2: Tables at the left panel showed data for (a) *polr2*, (b) *β-actin* and (c) *gapdh* mRNA that was statistically analysed using Excel. Right panel showed qRT-PCR analysis of each reference genes in rat primary adipocytes. Data presented as mean ± SEM (one-way ANOVA with Bonferroni's post-hoc, n=6, $^{**}p<0.01$, ns=not significant). This experiment was repeated three times using samples from 3 different preparations.

gapdh is noted to be unreliable since hypoxia can induce its expression, as a consequence of increased glycolytic activity, to make up for decreased level of ATP in the cells (Yamaji et al., 2003). Whilst *β-actin* is not recommended to be used in experiment involving the growth of primary cultures since it is a structural protein; and in a condition where the cell differentiates, its involvement in cytoskeletal modulation often changes (Fink et al., 2008; Selvey et al., 2001). Among different reference genes, *polr2* displayed low RNA transcriptional variability. Although no significant differences were noted between *polr2* (0.227±0.05) and *β-actin* (0.31±0.05), but the former has better standard curve slope and co-efficient (r^2) value than the latter (see Figure 6.1 a and b).

6.3) **Appendix C: Detection of *fetA* expression from primary rat adipocytes cDNA**

a)

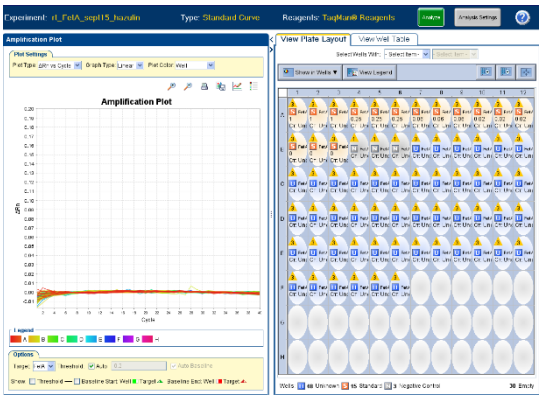

b)

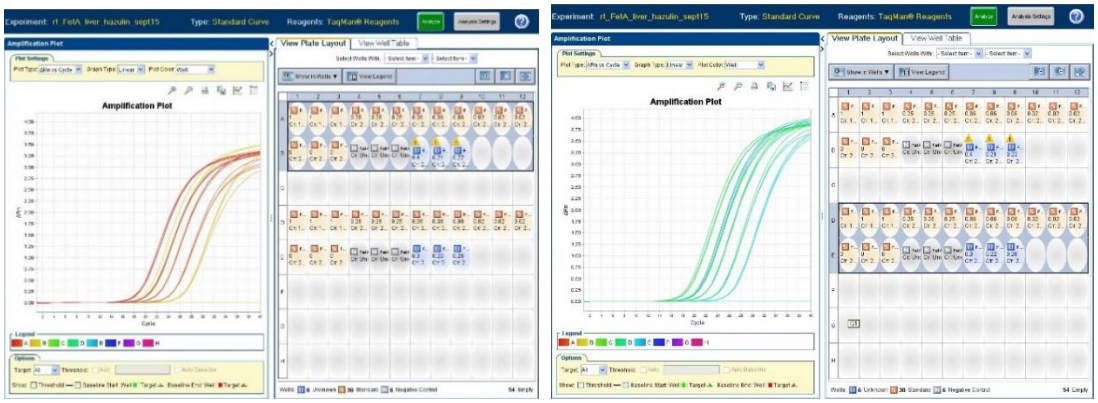

Figure 6.3: Upper panel graph showed (a) undetectable expression of *fetA* in rat primary adipocytes cDNA. New primers and probe set was designed and both (the former and the new set) was used to assess *fetA* amplification in primary rat hepatocytes cDNA that acts as positive control sample. (b) The left figure with red graph lines (former primers and probe) and the right figure with green graph line (new primers and probe) showed expression of *fetA* in rat primary hepatocytes cDNA.

Interestingly, mRNA expression for *fetA* was undetected in primary cultured rat adipocytes. Chatterjee *et al.* has reported the presence of *fetA* expression within adipocytes and indicated a role of *fetA* in macrophage infiltration and polarisation (Chatterjee et al., 2013). More recently *fetA* mRNA expression and protein secretion were described in mouse adipocytes treated with palmitate, wherein the

effects were attributed to activation of NF-κB (Trepanowski, Mey, & Varady, 2015). Thus, the expression of *fetA* in adipocytes may be dependent on precise culture condition used.

6.4) **Appendix D: Various dosages of GSK101 used to determine its working concentration**

6.4.1) Day 6 NG

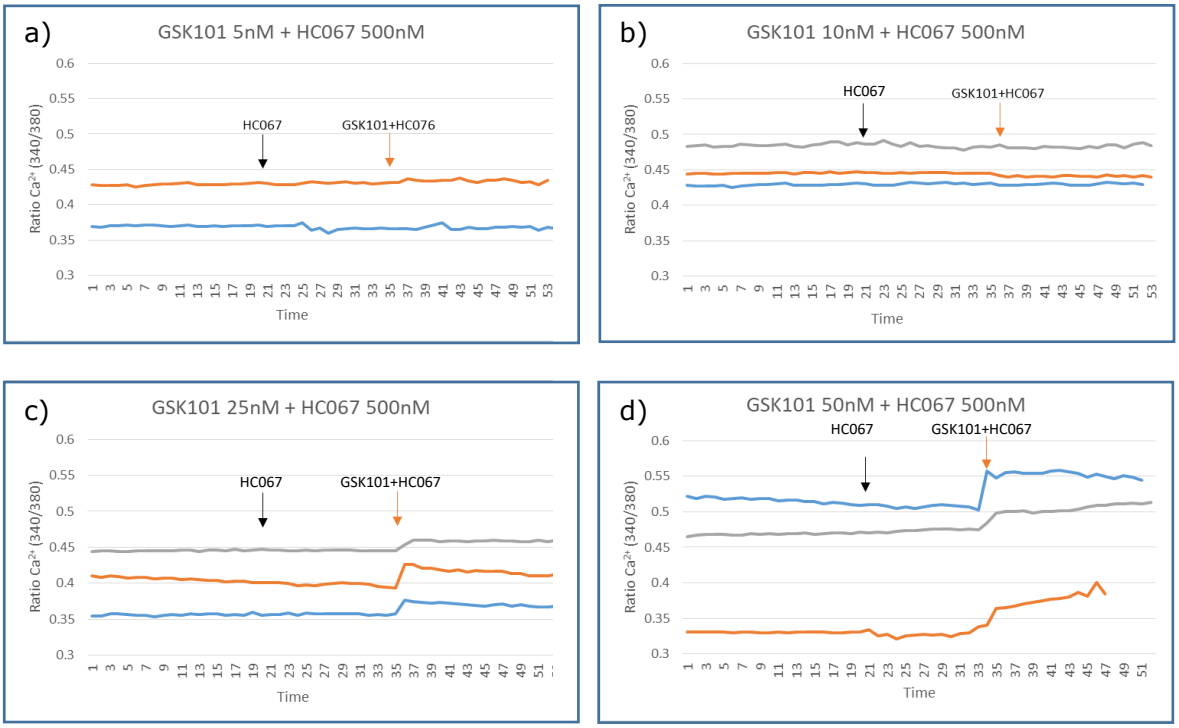

Figure 6.4: The effect of increasing concentration of GSK101 upon HC067 in adipocytes calcium signalling at day 6 differentiation in NG media. The cells were perfused with calcium buffer prior to addition of HC067 500nM. Next, the cells were treated with either (a) 5nM, (b) 10nM, (c) 25nM or (d) 50nM GSK101 in the presence of HC067. The experiments were repeated two to three times using samples from different preparations, represented by different coloured lines, with a minimum of 25 cells each.

6.4.2) Day 6 HG

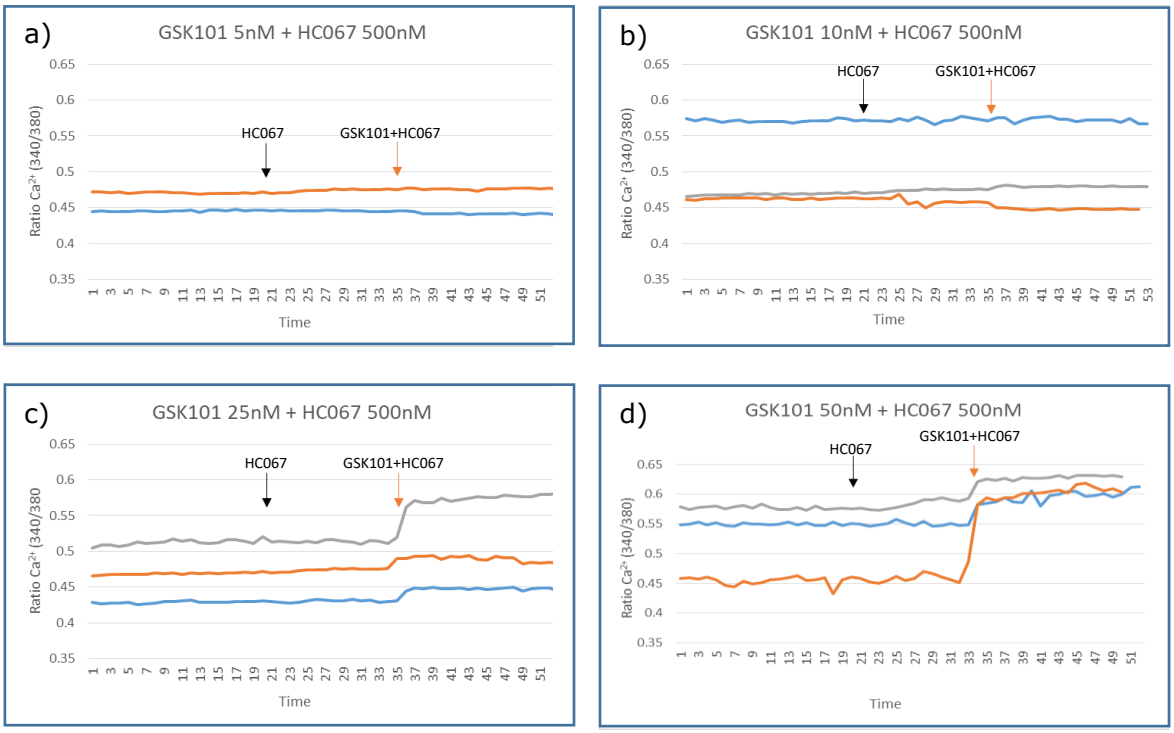

Figure 6.5: The effect of increasing concentration of GSK101 upon HC067 in adipocytes calcium signalling at day 6 differentiation in HG media. The cells were perfused with calcium buffer prior to addition of HC067 500nM. Next, the cells were treated with either (a) 5nM, (b) 10nM, (c) 25nM or (d) 50nM GSK101 in the presence of HC067. The experiments were repeated two to three times using samples from different preparations, represented by different coloured lines, with a minimum of 25 cells each.

6.4.3) Day 10 NG

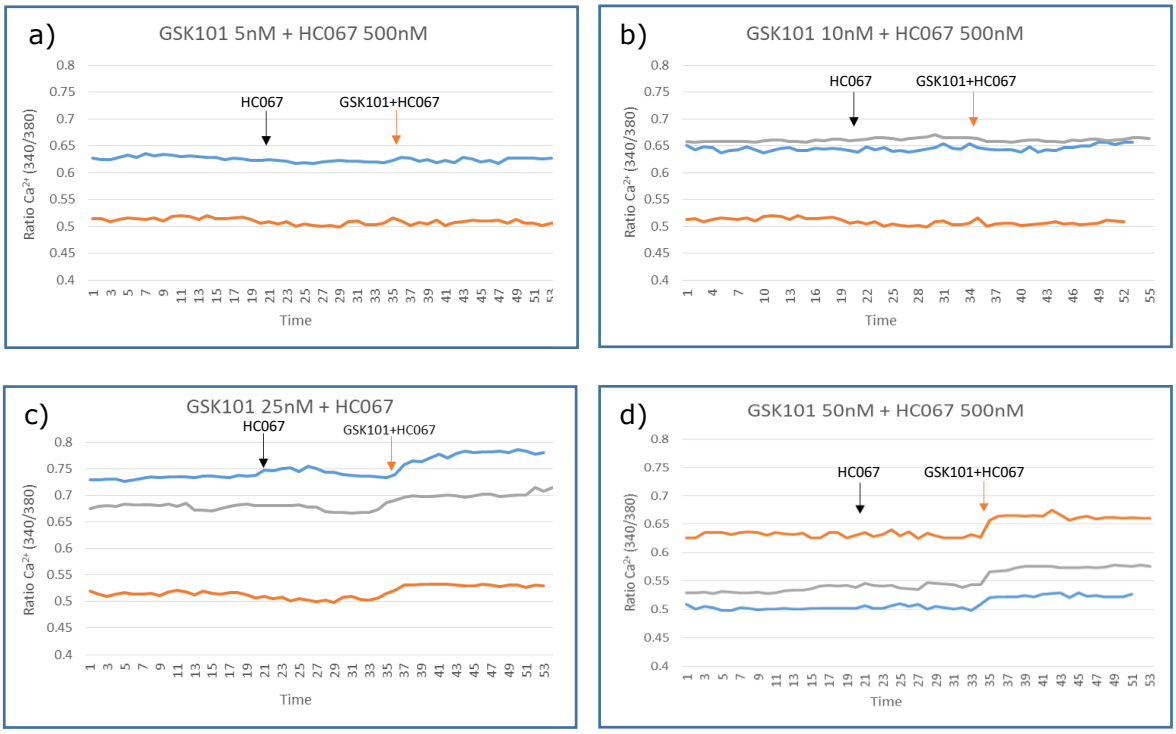

Figure 6.6: The effect of increasing concentration of GSK101 upon HC067 in adipocytes calcium signalling at day 10 differentiation in NG media. The cells were perfused with calcium buffer prior to addition of HC067 500nM. Next, the cells were treated with either (a) 5nM, (b) 10nM, (c) 25nM or (d) 50nM GSK101 in the presence of HC067. The experiments were repeated two to three times using samples from different preparations, represented by different coloured lines, with a minimum of 25 cells each.

6.4.4) Day 10 HG

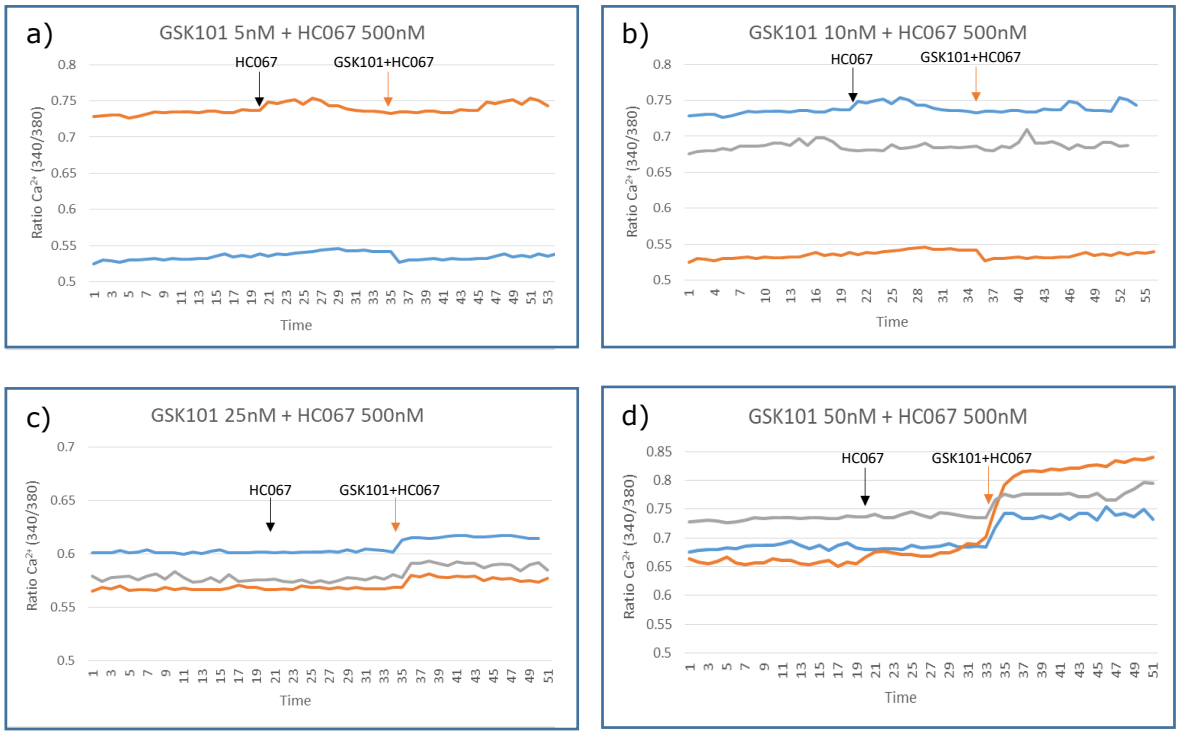

Figure 6.7: The effect of increasing concentration of GSK101 upon HC067 in adipocytes calcium signalling at day 10 differentiation in HG media. The cells were perfused with calcium buffer prior to addition of HC067 500nM. Next, the cells were treated with either (a) 5nM, (b) 10nM, (c) 25nM or (d) 50nM GSK101 in the presence of HC067. The experiments were repeated two to three times using samples from different preparations, represented by different coloured lines, with a minimum of 25 cells each.

It had been demonstrated that HC067 could blocked GSK101 activity, only in low GSK101 dose concentration (see Figure 6.4 to 6.7). Cells treated with HC067 500nM displayed inhibition of GSK101 effect in dosage as low as 5 and 10nM. The effect of HC067 was slightly reduced by treating the cells with GSK101 25nM. The antagonistic action of HC067 was further diminished after GSK101 50nM and 100nM were given to the cells.

7) References

Alvarez, S., Suazo, C., Boltansky, A., Ursu, M., Carvajal, D., Innocenti, G., . . . Irarrazabal, C. E. (2013). Urinary Exosomes as a Source of Kidney Dysfunction Biomarker in Renal Transplantation. *Transplantation Proceedings, 45*(10), 3719-3723. doi:https://doi.org/10.1016/j.transproceed.2013.08.079

Ambele, M. A., Dessels, C., Durandt, C., & Pepper, M. S. (2016). Genome-wide analysis of gene expression during adipogenesis in human adipose-derived stromal cells reveals novel patterns of gene expression during adipocyte differentiation. *Stem cell research, 16*(3), 725-734.

Arner, P. (2001). Free fatty acids–do they play a central role in type 2 diabetes? *Diabetes, Obesity and Metabolism, 3*, 11-19.

Baar, R. A., Dingfelder, C. S., Smith, L. A., Bernlohr, D. A., Wu, C., Lange, A. J., & Parks, E. J. (2005). Investigation of in vivo fatty acid metabolism in AFABP/aP2−/− mice. *American Journal of Physiology-Endocrinology and Metabolism, 288*(1), E187-E193.

Baboota, R. K., Singh, D. P., Sarma, S. M., Kaur, J., Sandhir, R., Boparai, R. K., . . . Bishnoi, M. (2014). Capsaicin induces "brite" phenotype in differentiating 3T3-L1 preadipocytes. *PloS one, 9*(7), e103093.

Baranyai, T., Herczeg, K., Onódi, Z., Voszka, I., Módos, K., Marton, N., . . . El Andaloussi, S. J. P. o. (2015). Isolation of exosomes from blood plasma: qualitative and quantitative comparison of ultracentrifugation and size exclusion chromatography methods. *10*(12), e0145686.

Beach, A., Zhang, H.-G., Ratajczak, M. Z., & Kakar, S. S. J. J. o. o. r. (2014). Exosomes: an overview of biogenesis, composition and role in ovarian cancer. *7*(1), 14.

Berry, D. C., Stenesen, D., Zeve, D., & Graff, J. M. (2013). The developmental origins of adipose tissue. *Development, 140*(19), 3939-3949.

Beylot, M. (2014). Metabolism of White Adipose Tissue. In *Adipose Tissue and Adipokines in Health and Disease* (pp. 33-52): Springer.

Bhattacharya, S., Kundu, R., Dasgupta, S., & Bhattacharya, S. (2012). Mechanism of Lipid Induced Insulin Resistance: An Overview. *Endocrinology and Metabolism, 27*(1), 12-19.

Bishnoi, M., Kondepudi, K. K., Gupta, A., Karmase, A., & Boparai, R. K. (2013). Expression of multiple Transient Receptor Potential channel genes in murine 3T3-L1 cell lines and adipose tissue. *Pharmacological Reports, 65*(3), 751-755.

Blüher, M. (2016). Adipose tissue inflammation: a cause or consequence of obesity-related insulin resistance? *Clinical Science, 130*(18), 1603-1614. doi:10.1042/cs20160005

Bootman, M. D., Rietdorf, K., Hardy, H., Dautova, Y., Corps, E., Pierro, C., . . . Proudfoot, D. (2001). Calcium signalling and regulation of cell function. *e LS*.

Brasaemle, D. L. (2007). Thematic review series: adipocyte biology. The perilipin family of structural lipid droplet proteins: stabilization of lipid droplets and control of lipolysis. *J Lipid Res, 48*(12), 2547-2559. doi:10.1194/jlr.R700014-JLR200

Bricambert, J., Favre, D., Brajkovic, S., Bonnefond, A., Boutry, R., Salvi, R., . . . Abderrahmani, A. (2016). Impaired histone deacetylases 5 and 6 expression mimics the effects of obesity and hypoxia on adipocyte function. *Molecular metabolism, 5*(12), 1200-1207. doi:https://doi.org/10.1016/j.molmet.2016.09.011

Bruun, J. M., Lihn, A. S., Pedersen, S. B., & Richelsen, B. (2005). Monocyte chemoattractant protein-1 release is higher in visceral than subcutaneous

human adipose tissue (AT): implication of macrophages resident in the AT. *The Journal of clinical endocrinology & metabolism, 90*(4), 2282-2289.
Cao, H., Sekiya, M., Ertunc, M. E., Burak, M. F., Mayers, J. R., White, A., . . . Furuhashi, M. (2013). Adipocyte lipid chaperone AP2 is a secreted adipokine regulating hepatic glucose production. *Cell metabolism, 17*(5), 768-778.
Casas, S., Novials, A., Reimann, F., Gomis, R., & Gribble, F. J. D. (2008). Calcium elevation in mouse pancreatic beta cells evoked by extracellular human islet amyloid polypeptide involves activation of the mechanosensitive ion channel TRPV4. *51*(12), 2252-2262.
Catalan, V., Gomez-Ambrosi, J., Rodriguez, A., Ramirez, B., Silva, C., Rotellar, F., . . . Fruhbeck, G. (2009). Increased adipose tissue expression of lipocalin-2 in obesity is related to inflammation and matrix metalloproteinase-2 and metalloproteinase-9 activities in humans. *J Mol Med (Berl), 87*(8), 803-813. doi:10.1007/s00109-009-0486-8
Catalán, V., Gómez-Ambrosi, J., Rodriguez, A., Ramírez, B., Silva, C., Rotellar, F., . . . Frühbeck, G. (2009). Increased adipose tissue expression of lipocalin-2 in obesity is related to inflammation and matrix metalloproteinase-2 and metalloproteinase-9 activities in humans. *Journal of molecular medicine, 87*(8), 803.
Chakraborty, S., Kaur, S., Guha, S., & Batra, S. K. (2012). The multifaceted roles of neutrophil gelatinase associated lipocalin (NGAL) in inflammation and cancer. *Biochimica et Biophysica Acta (BBA) - Reviews on Cancer, 1826*(1), 129-169. doi:https://doi.org/10.1016/j.bbcan.2012.03.008
Chakraborty, S., Kaur, S., Tong, Z., Batra, S. K., & Guha, S. (2011). Neutrophil Gelatinase Associated Lipocalin: Structure, Function and Role in Human Pathogenesis.
Chan, P.-C., Hsieh, P.-S. J. A. O., & Understanding, M. (2017). The Role of Adipocyte Hypertrophy and Hypoxia in the Development of Obesity-Associated Adipose Tissue Inflammation and Insulin Resistance. 127.
Chatterjee, P., Seal, S., Mukherjee, S., Kundu, R., Mukherjee, S., Ray, S., . . . Bhattacharya, S. (2013). Adipocyte fetuin-a contributes to macrophage migration into adipose tissue and polarization of macrophages. *Journal of Biological Chemistry, 288*(39), 28324-28330.
Che, H., Yue, J., Tse, H.-F., & Li, G.-R. (2014). Functional TRPV and TRPM channels in human preadipocytes. *Pflügers Archiv-European Journal of Physiology, 466*(5), 947-959.
Cheng, N.-C., Hsieh, T.-Y., Lai, H.-S., & Young, T.-H. (2016). High glucose-induced reactive oxygen species generation promotes stemness in human adipose-derived stem cells. *Cytotherapy, 18*(3), 371-383.
Chivet, M., Hemming, F., Fraboulet, S., & Sadoul, R. J. F. i. p. (2012). Emerging role of neuronal exosomes in the central nervous system. *3*, 145.
Choi, K. J., Cho, D. S., Kim, J. Y., Kim, B. J., Lee, K. M., Kim, S. H., . . . Park, H. S. (2011). Ca2+-induced Ca2+ release from internal stores in INS-1 rat insulinoma cells. *The Korean Journal of Physiology & Pharmacology, 15*(1), 53-59.
Cinti, S. (2005). The adipose organ. *Prostaglandins, Leukotrienes and Essential Fatty Acids, 73*(1), 9-15. doi:https://doi.org/10.1016/j.plefa.2005.04.010
Clapham, D. E. (2007). Calcium signaling. *Cell, 131*(6), 1047-1058.
Coe, N. R., Simpson, M. A., & Bernlohr, D. A. (1999). Targeted disruption of the adipocyte lipid-binding protein (aP2 protein) gene impairs fat cell lipolysis and increases cellular fatty acid levels. *Journal of lipid research, 40*(5), 967-972.
Coelho, M., Oliveira, T., & Fernandes, R. (2013). State of the art paper Biochemistry of adipose tissue: an endocrine organ. *Archives of Medical Science, 9*(2), 191-200.

Collins, J. M., Neville, M. J., Pinnick, K. E., Hodson, L., Ruyter, B., van Dijk, T. H., . . . Frayn, K. N. (2011). De novo lipogenesis in the differentiating human adipocyte can provide all fatty acids necessary for maturation. *Journal of Lipid Research*, jlr. M012195.

Colsoul, B., Nilius, B., Vennekens, R. J. C., & Allergy, E. (2009). On the putative role of transient receptor potential cation channels in asthma. *39*(10), 1456-1466.

Connolly, K. D., Guschina, I. A., Yeung, V., Clayton, A., Draman, M. S., Von Ruhland, C., . . . Rees, D. A. J. J. o. e. v. (2015). Characterisation of adipocyte-derived extracellular vesicles released pre-and post-adipogenesis. *4*(1), 29159.

Cowland, J. B., Muta, T., & Borregaard, N. (2006). IL-1β-specific up-regulation of neutrophil gelatinase-associated lipocalin is controlled by IκB-ζ. *The Journal of Immunology, 176*(9), 5559-5566.

Cui, L. Y., Yang, S., & Zhang, J. (2011). Protective Effects of Neutrophil Gelatinase–Associated Lipocalin on Hypoxia/Reoxygenation Injury of HK-2 Cells. *Transplantation Proceedings, 43*(10), 3622-3627. doi:https://doi.org/10.1016/j.transproceed.2011.08.090

Czech, M. P. (2002). Fat Targets for Insulin Signaling. *Molecular cell, 9*(4), 695-696. doi:https://doi.org/10.1016/S1097-2765(02)00509-9

D'Aldebert, E., Cenac, N., Rousset, P., Martin, L., Rolland, C., Chapman, K., . . . Vergnolle, N. J. G. (2011). Transient receptor potential vanilloid 4 activated inflammatory signals by intestinal epithelial cells and colitis in mice. *140*(1), 275-285. e273.

Dalen, K. T., Ulven, S. M., Bamberg, K., Gustafsson, J.-Å., & Nebb, H. I. (2003). Expression of the insulin-responsive glucose transporter GLUT4 in adipocytes is dependent on liver X receptor α. *Journal of Biological Chemistry, 278*(48), 48283-48291.

Dasgupta, S., Bhattacharya, S., Biswas, A., Majumdar, S., Mukhopadhyay, S., & Ray, S. (2010). NF-kappaB mediates lipid-induced fetuin-A expression in hepatocytes that impairs adipocyte function effecting insulin resistance. *Biochem. J, 429*, 451-462.

Denecke, B., Graber, S., Schafer, C., Heiss, A., Woltje, M., & Jahnen-Dechent, W. (2003). Tissue distribution and activity testing suggest a similar but not identical function of fetuin-B and fetuin-A. *Biochem. J, 376*, 135-145.

Deng, H.-X., Klein, C. J., Yan, J., Shi, Y., Wu, Y., Fecto, F., . . . Siddique, N. J. N. g. (2010). Scapuloperoneal spinal muscular atrophy and CMT2C are allelic disorders caused by alterations in TRPV4. *42*(2), 165.

Deng, Z.-b., Poliakov, A., Hardy, R. W., Clements, R., Liu, C., Liu, Y., . . . Zhuang, X. (2009). Adipose tissue exosome-like vesicles mediate activation of macrophage-induced insulin resistance. *Diabetes, 58*(11), 2498-2505.

Deng, Z.-b., Poliakov, A., Hardy, R. W., Clements, R., Liu, C., Liu, Y., . . . Zhang, H.-G. (2009). Adipose Tissue Exosome-Like Vesicles Mediate Activation of Macrophage-Induced Insulin Resistance. *58*(11), 2498-2505. doi:10.2337/db09-0216 %J Diabetes

Dinel, A., Kolditz, C., & Langin, D. (2010). Metabolism of fatty acids in adipocytes. In *Novel Insights into Adipose Cell Functions* (pp. 21-43): Springer.

Ding, C., Gao, D., Wilding, J., Trayhurn, P., & Bing, C. J. B. J. o. N. (2012). Vitamin D signalling in adipose tissue. *108*(11), 1915-1923.

DRAZNIN, B., LEWIS, D., HOULDER, N., SHERMAN, N., ADAMO, M., GARVEY, W. T., . . . SUSSMAN, K. (1989). Mechanism of insulin resistance induced by sustained levels of cytosolic free calcium in rat adipocytes. *Endocrinology, 125*(5), 2341-2349.

Draznin, B., Sussman, K., Eckel, R., Kao, M., Yost, T., & Sherman, N. (1988). Possible role of cytosolic free calcium concentrations in mediating insulin

resistance of obesity and hyperinsulinemia. *The Journal of clinical investigation, 82*(6), 1848-1852.
Draznin, B., Sussman, K., Kao, M., Lewis, D., & Sherman, N. (1987). The existence of an optimal range of cytosolic free calcium for insulin-stimulated glucose transport in rat adipocytes. *Journal of Biological Chemistry, 262*(30), 14385-14388.
Duncan, R. E., Sarkadi-Nagy, E., Jaworski, K., Ahmadian, M., & Sul, H. S. (2008). Identification and functional characterization of adipose-specific phospholipase A2 (AdPLA). *The Journal of biological chemistry, 283*(37), 25428-25436. doi:10.1074/jbc.M804146200
Dunn, K. M., Hill-Eubanks, D. C., Liedtke, W. B., & Nelson, M. T. (2013). TRPV4 channels stimulate Ca2+-induced Ca2+ release in astrocytic endfeet and amplify neurovascular coupling responses. *Proceedings of the National Academy of Sciences, 110*(15), 6157-6162.
Durcin, M., Fleury, A., Taillebois, E., Hilairet, G., Krupova, Z., Henry, C., . . . Mabilleau, G. (2017). Characterisation of adipocyte-derived extracellular vesicle subtypes identifies distinct protein and lipid signatures for large and small extracellular vesicles. *Journal of Extracellular Vesicles, 6*(1), 1305677.
Dusserre, E., Moulin, P., & Vidal, H. (2000). Differences in mRNA expression of the proteins secreted by the adipocytes in human subcutaneous and visceral adipose tissues. *Biochimica et Biophysica Acta (BBA)-Molecular Basis of Disease, 1500*(1), 88-96.
Erikci Ertunc, M., Sikkeland, J., Fenaroli, F., Griffiths, G., Daniels, M. P., Cao, H., . . . Hotamisligil, G. S. (2014). Secretion of fatty acid binding protein aP2 from adipocytes through a non-classical pathway in response to adipocyte lipase activity. *Journal of Lipid Research*. doi:10.1194/jlr.M055798
Everaerts, W., Zhen, X., Ghosh, D., Vriens, J., Gevaert, T., Gilbert, J. P., . . . Moran, M. M. J. P. o. t. N. A. o. S. (2010). Inhibition of the cation channel TRPV4 improves bladder function in mice and rats with cyclophosphamide-induced cystitis. *107*(44), 19084-19089.
F., A., T., M. H., G., S. H., A., W. E., A., A., P., O., . . . J., T. (2007). Lipocalin-2 Regulates the Inflammatory Response During Ischemia and Reperfusion of the Transplanted Heart. *American Journal of Transplantation, 7*(4), 779-788. doi:doi:10.1111/j.1600-6143.2006.01723.x
Fain, J. N. (2010). Release of inflammatory mediators by human adipose tissue is enhanced in obesity and primarily by the nonfat cells: a review. *Mediators of inflammation, 2010*.
Fantuzzi, G. (2005). Adipose tissue, adipokines, and inflammation. *Journal of Allergy and Clinical Immunology, 115*(5), 911-919.
Fehrer, C., Brunauer, R., Laschober, G., Unterluggauer, H., Reitinger, S., Kloss, F., . . . Lepperdinger, G. (2007). Reduced oxygen tension attenuates differentiation capacity of human mesenchymal stem cells and prolongs their lifespan. *Aging Cell, 6*. doi:10.1111/j.1474-9726.2007.00336.x
Ferrante, S. C., Nadler, E. P., Pillai, D. K., Hubal, M. J., Wang, Z., Wang, J. M., . . . Wiles, A. A. (2015). Adipocyte-derived exosomal miRNAs: a novel mechanism for obesity-related disease. *Pediatric research, 77*(3), 447.
Ferrante, S. C., Nadler, E. P., Pillai, D. K., Hubal, M. J., Wang, Z., Wang, J. M., . . . Freishtat, R. J. (2014). Adipocyte-derived exosomal miRNAs: a novel mechanism for obesity-related disease. *Pediatric Research, 77*, 447. doi:10.1038/pr.2014.202
https://www.nature.com/articles/pr2014202#supplementary-information
Fink, T., Lund, P., Pilgaard, L., Rasmussen, J., Duroux, M., & Zachar, V. (2008). Instability of standard PCR reference genes in adipose-derived stem cells during propagation, differentiation and hypoxic exposure. *BMC molecular biology, 9*(1), 98.

Fischer, H., Gustafsson, T., Sundberg, C. J., Norrbom, J., Ekman, M., Johansson, O., & Jansson, E. (2006). Fatty acid binding protein 4 in human skeletal muscle. *Biochemical and biophysical research communications, 346*(1), 125-130.

Fontana, L., Eagon, J. C., Trujillo, M. E., Scherer, P. E., & Klein, S. (2007). Visceral fat adipokine secretion is associated with systemic inflammation in obese humans. *Diabetes, 56*(4), 1010-1013.

Foucaud, L., Grillasca, J., Niot, I., Domingo, N., Lafont, H., Planells, R., & Besnard, P. (1999). Output of liver fatty acid-binding protein (L-FABP) in bile. *Biochimica et Biophysica Acta (BBA)-Molecular and Cell Biology of Lipids, 1436*(3), 593-599.

Frayn, K., Karpe, F., Fielding, B., Macdonald, I., & Coppack, S. (2003). Integrative physiology of human adipose tissue. *International Journal Of Obesity, 27*(8), 875.

Frühbeck, G. (2007). Vasoactive factors and inflammatory mediators produced in adipose tissue. In *Adipose tissue and adipokines in health and disease* (pp. 63-77): Springer.

Furuhashi, M., Fucho, R., Görgün, C. Z., Tuncman, G., Cao, H., & Hotamisligil, G. S. (2008). Adipocyte/macrophage fatty acid–binding proteins contribute to metabolic deterioration through actions in both macrophages and adipocytes in mice. *The Journal of clinical investigation, 118*(7), 2640.

Furuhashi, M., & Hotamisligil, G. S. (2008). Fatty acid-binding proteins: role in metabolic diseases and potential as drug targets. *Nature reviews Drug discovery, 7*(6), 489.

Furuhashi, M., Ishimura, S., Ota, H., & Miura, T. (2011). Lipid chaperones and metabolic inflammation. *International journal of inflammation, 2011*.

Furuhashi, M., Saitoh, S., Shimamoto, K., & Miura, T. (2014). Fatty acid-binding protein 4 (FABP4): pathophysiological insights and potent clinical biomarker of metabolic and cardiovascular diseases. *Clinical Medicine Insights: Cardiology, 8*, CMC. S17067.

Furuhashi, M., Tuncman, G., Görgün, C. Z., Makowski, L., Atsumi, G., Vaillancourt, E., . . . Linton, M. F. (2007). Treatment of diabetes and atherosclerosis by inhibiting fatty-acid-binding protein aP2. *Nature, 447*(7147), 959.

Gallo, A., Tandon, M., Alevizos, I., & Illei, G. G. J. P. o. (2012). The majority of microRNAs detectable in serum and saliva is concentrated in exosomes. *7*(3), e30679.

Gao, X., Salomon, C., & Freeman, D. J. (2017). extracellular vesicles from Adipose Tissue—A Potential Role in Obesity and Type 2 Diabetes? *Frontiers in endocrinology, 8*, 202.

Garay-Rojas, E., Harper, M., Hraba-Renevey, S., & Kress, M. (1996). An apparent autocrine mechanism amplifies the dexamethasone- and retinoic acid-induced expression of mouse lipocalin-encoding gene 24p3. *Gene, 170*(2), 173-180. doi:https://doi.org/10.1016/0378-1119(95)00896-9

Garcia-Elias Heras, A. (2011). *Molecular determinants of TRPV4 channel regulation.* Universitat Pompeu Fabra,

Garin-Shkolnik, T., Rudich, A., Hotamisligil, G. S., & Rubinstein, M. (2014). FABP4 Attenuates PPARγ and Adipogenesis and Is Inversely Correlated With PPARγ in Adipose Tissues. *Diabetes, 63*(3), 900-911. doi:10.2337/db13-0436

Gingold, H., & Pilpel, Y. (2011). Determinants of translation efficiency and accuracy. *Molecular systems biology, 7*(1), 481.

Giordano, A., Frontini, A., & Cinti, S. (2016). Convertible visceral fat as a therapeutic target to curb obesity. *Nature Reviews Drug Discovery, 15*(6), 405.

Glatz, J. F., Luiken, J. J., Van Bilsen, M., & Van Der Vusse, G. J. (2002). Cellular lipid binding proteins as facilitators and regulators of lipid metabolism. *Molecular and cellular biochemistry, 239*(1-2), 3-7.

Glatz, J. F. C. (2015). Lipids and lipid binding proteins: A perfect match. *Prostaglandins, Leukotrienes and Essential Fatty Acids (PLEFA), 93*, 45-49. doi:https://doi.org/10.1016/j.plefa.2014.07.011

Gough, N. R. (2012). Targeting TRPV4 to Treat Metabolic Disease. *Sci. Signal., 5*(244), ec253-ec253.

Greenberg, A. S., & Obin, M. S. (2006). Obesity and the role of adipose tissue in inflammation and metabolism–. *The American journal of clinical nutrition, 83*(2), 461S-465S.

Guo, H., Jin, D., & Chen, X. (2014). Lipocalin 2 is a Regulator Of Macrophage Polarization and NF-κB/STAT3 Pathway Activation. *Molecular Endocrinology, 28*(10), 1616-1628. doi:doi:10.1210/me.2014-1092

Guo, H., Jin, D., Zhang, Y., Wright, W., Bazuine, M., Brockman, D. A., . . . Chen, X. (2010). Lipocalin 2 deficiency impairs thermogenesis and potentiates diet-induced insulin resistance in mice. *Diabetes*.

Hartmannsgruber, V., Heyken, W.-T., Kacik, M., Kaistha, A., Grgic, I., Harteneck, C., . . . Köhler, R. (2007). Arterial response to shear stress critically depends on endothelial TRPV4 expression. *PloS one, 2*(9), e827.

Hatanaka, M., Shimba, S., Sakaue, M., Kondo, Y., Kagechika, H., Kokame, K., . . . Hara, S. (2009). Hypoxia-Inducible Factor-3. ALPHA. Functions as an Accelerator of 3T3-L1 Adipose Differentiation. *Biological and Pharmaceutical Bulletin, 32*(7), 1166-1172.

Hausman, D. B., Park, H. J., & Hausman, G. J. (2008). Isolation and Culture of Preadipocytes from Rodent White Adipose Tissue. In K. Yang (Ed.), *Adipose Tissue Protocols* (pp. 201-219). Totowa, NJ: Humana Press.

He, Z., Jiang, T., Wang, Z., Levi, M., & Li, J. (2004). Modulation of carbohydrate response element-binding protein ChREBP gene expression in 3T3-L1 adipocyte and rat adipose tissue. *American Journal of Physiology-Endocrinology and Metabolism*.

Ho, I.-C., Kim, J. H.-J., Rooney, J. W., Spiegelman, B. M., & Glimcher, L. H. (1998). A potential role for the nuclear factor of activated T cells family of transcriptional regulatory proteins in adipogenesis. *Proceedings of the National Academy of Sciences, 95*(26), 15537-15541.

Hogan, P. G., & Rao, A. (2015). Store-operated calcium entry: Mechanisms and modulation. *Biochemical and biophysical research communications, 460*(1), 40-49.

Holden, V. I., Lenio, S., Kuick, R., Ramakrishnan, S. K., Shah, Y. M., & Bachman, M. A. (2014). Bacterial Siderophores That Evade or Overwhelm Lipocalin 2 Induce Hypoxia Inducible Factor 1α and Proinflammatory Cytokine Secretion in Cultured Respiratory Epithelial Cells. *Infection and Immunity, 82*(9), 3826-3836. doi:10.1128/iai.01849-14

Horowitz, L. F., Hirdes, W., Suh, B.-C., Hilgemann, D. W., Mackie, K., & Hille, B. (2005). Phospholipase C in living cells: activation, inhibition, Ca2+ requirement, and regulation of M current. *The Journal of general physiology, 126*(3), 243-262.

Hotamisligil, G. S., Johnson, R. S., Distel, R. J., Ellis, R., Papaioannou, V. E., & Spiegelman, B. M. (1996). Uncoupling of obesity from insulin resistance through a targeted mutation in aP2, the adipocyte fatty acid binding protein. *Science, 274*. doi:10.1126/science.274.5291.1377

Hotamisligil, G. S., Murray, D. L., Choy, L. N., & Spiegelman, B. M. (1994). Tumor necrosis factor alpha inhibits signaling from the insulin receptor. *Proceedings of the National Academy of Sciences, 91*(11), 4854-4858.

Hu, L., Wang, J., Zhou, X., Xiong, Z., Zhao, J., Yu, R., . . . Chen, L. (2016). Exosomes derived from human adipose mensenchymal stem cells

accelerates cutaneous wound healing via optimizing the characteristics of fibroblasts. *Scientific reports, 6*, 32993.

Hui, X., Li, H., Zhou, Z., Lam, K. S., Xiao, Y., Wu, D., . . . Xu, A. (2010). Adipocyte fatty acid-binding protein modulates inflammatory responses in macrophages through a positive feedback loop involving c-Jun NH2-terminal kinases and activator protein-1. *Journal of Biological Chemistry, 285*(14), 10273-10280.

Hurley, R. L., Anderson, K. A., Franzone, J. M., Kemp, B. E., Means, A. R., & Witters, L. A. J. J. o. B. C. (2005). The Ca2+/calmodulin-dependent protein kinase kinases are AMP-activated protein kinase kinases. *280*(32), 29060-29066.

Ichiro, S., L, L. B., T, V. J., Jian-Guo, C., & J, P. D. (2004). Adipogenic Differentiation of Human Adult Stem Cells From Bone Marrow Stroma (MSCs). *Journal of Bone and Mineral Research, 19*(2), 256-264. doi:doi:10.1359/JBMR.0301220

Jaworski, K., Ahmadian, M., Duncan, R. E., Sarkadi-Nagy, E., Varady, K. A., Hellerstein, M. K., . . . Sul, H. S. (2009). AdPLA ablation increases lipolysis and prevents obesity induced by high-fat feeding or leptin deficiency. *Nature medicine, 15*(2), 159-168. doi:10.1038/nm.1904

Jensen, B., Farach-Carson, M. C., Kenaley, E., & Akanbi, K. A. (2004). High extracellular calcium attenuates adipogenesis in 3T3-L1 preadipocytes. *Experimental cell research, 301*(2), 280-292.

Jessen, B. A., & Stevens, G. J. (2002). Expression profiling during adipocyte differentiation of 3T3-L1 fibroblasts. *Gene, 299*(1), 95-100.

Ji, S., Doumit, M. E., & Hill, R. A. (2015). Regulation of adipogenesis and key adipogenic gene expression by 1, 25-dihydroxyvitamin D in 3T3-L1 cells. *PloS one, 10*(6), e0126142.

Jin, J., Shi, Y., Gong, J., Zhao, L., Li, Y., He, Q., . . . therapy. (2019). Exosome secreted from adipose-derived stem cells attenuates diabetic nephropathy by promoting autophagy flux and inhibiting apoptosis in podocyte. *10*(1), 95.

Jin, M., Wu, Z., Chen, L., Jaimes, J., Collins, D., Walters, E. T., & O'Neil, R. G. (2011). Determinants of TRPV4 activity following selective activation by small molecule agonist GSK1016790A. *PloS one, 6*(2), e16713.

Jørgensen, M., Bæk, R., Pedersen, S., Søndergaard, E. K., Kristensen, S. R., & Varming, K. (2013). Extracellular Vesicle (EV) Array: microarray capturing of exosomes and other extracellular vesicles for multiplexed phenotyping. *Journal of Extracellular Vesicles, 2*(1), 20920.

Jun, L. S., Siddall, C. P., & Rosen, E. D. (2011). *A minor role for lipocalin 2 in high-fat diet-induced glucose intolerance* (Vol. 301).

Kadowaki, T., & Yamauchi, T. (2005). Adiponectin and adiponectin receptors. *Endocrine reviews, 26*(3), 439-451.

Kaestner, K. H., Christy, R. J., & Lane, M. D. (1990). Mouse insulin-responsive glucose transporter gene: characterization of the gene and trans-activation by the CCAAT/enhancer binding protein. *Proceedings of the National Academy of Sciences, 87*(1), 251-255. doi:10.1073/pnas.87.1.251

Kang, Y. J., Kusler, B., Otsuka, M., Hughes, M., Suzuki, N., Suzuki, S., . . . Jones, P. P. (2007). Calcineurin negatively regulates TLR-mediated activation pathways. *The Journal of Immunology, 179*(7), 4598-4607.

Kastelowitz, N., & Yin, H. (2014). Exosomes and microvesicles: identification and targeting by particle size and lipid chemical probes. *Chembiochem, 15*(7), 923-928.

Katsuda, T., Tsuchiya, R., Kosaka, N., Yoshioka, Y., Takagaki, K., Oki, K., . . . Ochiya, T. (2013). Human adipose tissue-derived mesenchymal stem cells secrete functional neprilysin-bound exosomes. *Scientific reports, 3*, 1197.

Kern, P. A., Di Gregorio, G. B., Lu, T., Rassouli, N., & Ranganathan, G. (2003). Adiponectin expression from human adipose tissue: relation to obesity, insulin resistance, and tumor necrosis factor-α expression. *Diabetes, 52*(7), 1779-1785.

Kershaw, E. E., & Flier, J. S. (2004). Adipose tissue as an endocrine organ. *The Journal of Clinical Endocrinology & Metabolism, 89*(6), 2548-2556.

Kim, K.-A., Kim, J.-H., Wang, Y., Sul, H. S. J. M., & biology, c. (2007). Pref-1 (preadipocyte factor 1) activates the MEK/extracellular signal-regulated kinase pathway to inhibit adipocyte differentiation. *27*(6), 2294-2308.

Kiskac, M., Zorlu, M., Akkoyunlu, M. E., Kilic, E., Karatoprak, C., Cakirca, M., . . . Cikrikcioglu, M. (2014). Vaspin and lipocalin-2 levels in severe obsructive sleep apnea. *Journal of thoracic disease, 6*(6), 720.

Kleine, A. H., Glatz, J. F., Van Nieuwenhoven, F. A., & Van der Vusse, G. J. (1992). Release of heart fatty acid-binding protein into plasma after acute myocardial infarction in man. In *Lipid Metabolism in the Healthy and Disease Heart* (pp. 155-162): Springer.

Kleiner, S., Douris, N., Fox, E. C., Mepani, R. J., Verdeguer, F., Wu, J., . . . Spiegelman, B. M. (2012). FGF21 regulates PGC-1α and browning of white adipose tissues in adaptive thermogenesis. *Genes & development, 26*(3), 271-281.

Kowal, J., Arras, G., Colombo, M., Jouve, M., Morath, J. P., Primdal-Bengtson, B., . . . Théry, C. (2016). Proteomic comparison defines novel markers to characterize heterogeneous populations of extracellular vesicle subtypes. *Proceedings of the National Academy of Sciences*, 201521230.

Kralisch, S., Ebert, T., Lossner, U., Jessnitzer, B., Stumvoll, M., & Fasshauer, M. (2014). Adipocyte fatty acid-binding protein is released from adipocytes by a non-conventional mechanism. *International Journal Of Obesity, 38*(9), 1251.

Kralisch, S., & Fasshauer, M. (2013). Adipocyte fatty acid binding protein: a novel adipokine involved in the pathogenesis of metabolic and vascular disease? *Diabetologia, 56*(1), 10-21.

Krušinová, E., & Pelikánová, T. (2008). Fatty acid binding proteins in adipose tissue: A promising link between metabolic syndrome and atherosclerosis? *Diabetes research and clinical practice, 82*, S127-S134.

Kuo, I. Y., & Ehrlich, B. E. (2015). Signaling in muscle contraction. *Cold Spring Harbor perspectives in biology, 7*(2), a006023.

L., B. J., G., Z. J., Nathalie, A., Alexandre, P., Wee, Y. V., H., J. F., . . . Samuel, D. (2012). Lipocalin 2 is a novel immune mediator of experimental autoimmune encephalomyelitis pathogenesis and is modulated in multiple sclerosis. *Glia, 60*(7), 1145-1159. doi:doi:10.1002/glia.22342

Lai, R. C., Yeo, R. W. Y., Tan, K. H., & Lim, S. K. J. B. a. (2013). Exosomes for drug delivery—a novel application for the mesenchymal stem cell. *31*(5), 543-551.

Lamounier-Zepter, V., Look, C., Alvarez, J., Christ, T., Ravens, U., Schunck, W.-H., . . . Morano, I. (2009). Adipocyte Fatty Acid–Binding Protein Suppresses Cardiomyocyte Contraction. *A New Link Between Obesity and Heart Disease, 105*(4), 326-334. doi:10.1161/circresaha.109.200501

Laulagnier, K., Motta, C., Hamdi, S., Sébastien, R., Fauvelle, F., Pageaux, J.-F., . . . Bonnerot, C. J. B. J. (2004). Mast cell-and dendritic cell-derived exosomes display a specific lipid composition and an unusual membrane organization. *380*(1), 161-171.

Laviola, L., Perrini, S., Cignarelli, A., & Giorgino, F. (2006). Insulin signalling in human adipose tissue. *Archives of physiology and biochemistry, 112*(2), 82-88.

Law, I. K., Xu, A., Lam, K. S., Berger, T., Mak, T. W., Vanhoutte, P. M., . . . Yang, B. (2010). Lipocalin-2 deficiency attenuates insulin resistance associated with ageing and obesity. *Diabetes*.

Law, I. K. M., Xu, A., Lam, K. S. L., Berger, T., Mak, T. W., Vanhoutte, P. M., . . . Wang, Y. (2010). Lipocalin-2 Deficiency Attenuates Insulin Resistance Associated With Aging and Obesity. *Diabetes, 59*(4), 872-882. doi:10.2337/db09-1541

Lee, D.-F., Kuo, H.-P., Chen, C.-T., Wei, Y., Chou, C.-K., Hung, J.-Y., . . . Hung, M.-C. (2008). IKKβ suppression of TSC1 function links the mTOR pathway with insulin resistance. *International journal of molecular medicine, 22*(5), 633-638.

Lefterova, M. I., & Lazar, M. A. (2009). New developments in adipogenesis. *Trends in Endocrinology & Metabolism, 20*(3), 107-114. doi:https://doi.org/10.1016/j.tem.2008.11.005

Li, H., Luo, H.-Y., Liu, Q., Xiao, Y., Tang, L., Zhong, F., . . . Dai, R.-P. (2018). Intermittent High Glucose Exacerbates A-FABP Activation and Inflammatory Response through TLR4-JNK Signaling in THP-1 Cells. *Journal of Immunology Research, 2018*, 1319272. doi:10.1155/2018/1319272

Li, J., Kanju, P., Patterson, M., Chew, W.-L., Cho, S.-H., Gilmour, I., . . . Simon, S. A. J. E. h. p. (2011). TRPV4-mediated calcium influx into human bronchial epithelia upon exposure to diesel exhaust particles. *119*(6), 784-793.

Liang, H., & Ward, W. F. (2006). PGC-1α: a key regulator of energy metabolism. *Advances in physiology education, 30*(4), 145-151.

Lin, F., Ribar, T. J., & Means, A. R. J. E. (2011). The Ca2+/calmodulin-dependent protein kinase kinase, CaMKK2, inhibits preadipocyte differentiation. *152*(10), 3668-3679.

Lindberg, S., Jensen, J. S., Mogelvang, R., Pedersen, S. H., Galatius, S., Flyvbjerg, A., & Magnusson, N. E. (2014). Plasma Neutrophil Gelatinase-Associated Lipocalinin the General Population. *Association With Inflammation and Prognosis*. doi:10.1161/atvbaha.114.303950

Lindstad, T. (2010). Molecular Mechanisms of Adipogenesis and Adipocyte Biology: Possible role of MKPs and STAMPs.

Lobb, R. J., Becker, M., Wen Wen, S., Wong, C. S., Wiegmans, A. P., Leimgruber, A., & Möller, A. (2015). Optimized exosome isolation protocol for cell culture supernatant and human plasma. *Journal of Extracellular Vesicles, 4*(1), 27031.

Lolmede, K., de Saint Front, V. D., Galitzky, J., Lafontan, M., & Bouloumie, A. (2003). Effects of hypoxia on the expression of proangiogenic factors in differentiated 3T3-F442A adipocytes. *International Journal Of Obesity, 27*(10), 1187.

Maeda, K., Cao, H., Kono, K., Gorgun, C. Z., Furuhashi, M., Uysal, K. T., . . . Hotamisligil, G. S. (2005). Adipocyte/macrophage fatty acid binding proteins control integrated metabolic responses in obesity and diabetes. *Cell Metabolism, 1*(2), 107-119. doi:https://doi.org/10.1016/j.cmet.2004.12.008

Maeda, K., Uysal, K. T., Makowski, L., Görgün, C. Z., Atsumi, G., Parker, R. A., . . . Hotamisligil, G. S. (2003). Role of the fatty acid binding protein mal1 in obesity and insulin resistance. *Diabetes, 52*(2), 300-307.

Maier, T., Güell, M., & Serrano, L. (2009). Correlation of mRNA and protein in complex biological samples. *FEBS letters, 583*(24), 3966-3973.

Makowski, L., Boord, J. B., Maeda, K., Babaev, V. R., Uysal, K. T., Morgan, M. A., . . . Hotamisligil, G. S. (2001). Lack of macrophage fatty-acid–binding protein aP2 protects mice deficient in apolipoprotein E against atherosclerosis. *Nature medicine, 7*(6), 699.

Martin, S., & Parton, R. G. (2006). Opinion: Lipid droplets: a unified view of a dynamic organelle. *Nature reviews Molecular cell biology, 7*(5), 373.

Masuyama, R., Vriens, J., Voets, T., Karashima, Y., Owsianik, G., Vennekens, R., . . . Bosch, A. V. J. C. m. (2008). TRPV4-mediated calcium influx regulates terminal differentiation of osteoclasts. *8*(3), 257-265.

Mita, T., Furuhashi, M., Hiramitsu, S., Ishii, J., Hoshina, K., Ishimura, S., . . . Ohno, K. (2015). FABP4 is secreted from adipocytes by adenyl cyclase-PKA- and guanylyl cyclase-PKG-dependent lipolytic mechanisms. *Obesity, 23*(2), 359-367.

Mori, K., Emoto, M., & Inaba, M. (2011). Fetuin-A: a multifunctional protein. *Recent patents on endocrine, metabolic & immune drug discovery, 5*(2), 124-146.

Moseti, D., Regassa, A., & Kim, W.-K. (2016). Molecular regulation of adipogenesis and potential anti-adipogenic bioactive molecules. *International journal of molecular sciences, 17*(1), 124.

Murase, K., Mori, K., Yoshimura, C., Aihara, K., Chihara, Y., Azuma, M., . . . Handa, T. (2013). Association between plasma neutrophil gelatinase associated lipocalin level and obstructive sleep apnea or nocturnal intermittent hypoxia. *PloS one, 8*(1), e54184.

Nguyen, M. A., Favelyukis, S., Nguyen, A.-K., Reichart, D., Scott, P. A., Jenn, A., . . . Olefsky, J. M. (2007). A subpopulation of macrophages infiltrates hypertrophic adipose tissue and is activated by free fatty acids via Toll-like receptors 2 and 4 and JNK-dependent pathways. *Journal of Biological Chemistry, 282*(48), 35279-35292.

Nilius, B., & Voets, T. (2013). The puzzle of TRPV4 channelopathies. *EMBO reports, 14*(2), 152-163.

Ochieng, J., Tahin, Q. S., Booth, C. C., & Russo, J. (1991). Buffering of intracellular calcium in response to increased extracellular levels in mortal, immortal, and transformed human breast epithelial cells. *Journal of cellular biochemistry, 46*(3), 250-254.

Osborn, O., & Olefsky, J. M. (2012). The cellular and signaling networks linking the immune system and metabolism in disease. *Nature medicine, 18*(3), 363.

Pal, D., Dasgupta, S., Kundu, R., Maitra, S., Das, G., Mukhopadhyay, S., . . . Bhattacharya, S. (2012). Fetuin-A acts as an endogenous ligand of TLR4 to promote lipid-induced insulin resistance. *Nature medicine, 18*(8), 1279-1285.

Pan, Y., Hui, X., Hoo, R. L. C., Ye, D., Chan, C. Y. C., Feng, T., . . . Xu, A. J. T. J. o. c. i. (2019). Adipocyte-secreted exosomal microRNA-34a inhibits M2 macrophage polarization to promote obesity-induced adipose inflammation. *129*(2).

Pavlova, G. D. (2016). *Isolation and Characterization of Cancer-Derived Exosomes.*

Peshdary, V., Gagnon, A., & Sorisky, A. (2016). Effect of high glucose concentration on human preadipocytes and their response to macrophage-conditioned medium. *Canadian journal of diabetes, 40*(5), 411-418.

Prax, M., Vatani Shahmirzadi, S., & Götz, F. (2015). Sodium polyanethol sulfonate (SPS) falsifies protein staining and quantification and how to solve this problem. *Journal of Microbiological Methods, 118*, 176-181. doi:https://doi.org/10.1016/j.mimet.2015.10.002

Qin, B., & Anderson, R. A. (2011). An extract of chokeberry attenuates weight gain and modulates insulin, adipogenic and inflammatory signalling pathways in epididymal adipose tissue of rats fed a fructose-rich diet. *British Journal of Nutrition, 108*(4), 581-587. doi:10.1017/S000711451100599X

Qin, W., Tsukasaki, Y., Dasgupta, S., Mukhopadhyay, N., Ikebe, M., & Sauter, E. R. J. C. C. R. (2016). Exosomes in human breast milk promote EMT. *22*(17), 4517-4524.

Raposo, G., & Stoorvogel, W. (2013). Extracellular vesicles: Exosomes, microvesicles, and friends. *The Journal of Cell Biology, 200*(4), 373-383. doi:10.1083/jcb.201211138

Ravussin, E., & Smith, S. R. (2002). Increased fat intake, impaired fat oxidation, and failure of fat cell proliferation result in ectopic fat storage, insulin resistance, and type 2 diabetes mellitus. *Annals of the New York Academy of Sciences, 967*(1), 363-378.

Regazzetti, C., Peraldi, P., Grémeaux, T., Najem-Lendom, R., Ben-Sahra, I., Cormont, M., . . . Giorgetti-Peraldi, S. (2009). Hypoxia Decreases Insulin Signaling Pathways in Adipocytes. *Diabetes, 58*(1), 95-103. doi:10.2337/db08-0457

Rezaee, F., & Dashty, M. (2013). Role of adipose tissue in metabolic system disorders adipose tissue is the initiator of metabolic diseases. *J Diabetes Metab, 13*, 2.

Rock, M. J., Prenen, J., Funari, V. A., Funari, T. L., Merriman, B., Nelson, S. F., . . . Quadrelli, R. J. N. g. (2008). Gain-of-function mutations in TRPV4 cause autosomal dominant brachyolmia. *40*(8), 999.

Rodvold, J. J., Mahadevan, N. R., & Zanetti, M. (2012). Lipocalin 2 in cancer: When good immunity goes bad. *Cancer Letters, 316*(2), 132-138. doi:https://doi.org/10.1016/j.canlet.2011.11.002

Rønningen, T., Shah, A., Reiner, A. H., Collas, P., & Moskaug, J. Ø. (2015). Epigenetic priming of inflammatory response genes by high glucose in adipose progenitor cells. *Biochemical and biophysical research communications, 467*(4), 979-986.

Sadovska, L., Eglitis, J., & Line, A. (2015). Extracellular Vesicles as Biomarkers and Therapeutic Targets in Breast Cancer. *Anticancer Res, 35*(12), 6379-6390.

Sano, H., Kane, S., Sano, E., Mıˆinea, C. P., Asara, J. M., Lane, W. S., . . . Lienhard, G. E. (2003). Insulin-stimulated phosphorylation of a Rab GTPase-activating protein regulates GLUT4 translocation. *Journal of Biological Chemistry, 278*(17), 14599-14602.

Satish, L., Krill-Burger, J. M., Gallo, P. H., Des Etages, S., Liu, F., Philips, B. J., . . . Kathju, S. (2015). Expression analysis of human adipose-derived stem cells during in vitro differentiation to an adipocyte lineage. *BMC medical genomics, 8*(1), 41.

Scheja, L., Makowski, L., Uysal, K. T., Wiesbrock, S. M., Shimshek, D. R., Meyers, D. S., . . . Hotamisligil, G. S. (1999). Altered insulin secretion associated with reduced lipolytic efficiency in aP2-/-mice. *Diabetes, 48*(10), 1987-1994.

Schenk, S., Saberi, M., & Olefsky, J. M. (2008). Insulin sensitivity: modulation by nutrients and inflammation. *The Journal of clinical investigation, 118*(9), 2992-3002.

Schiller, Z. A., Schiele, N. R., Sims, J. K., Lee, K., & Kuo, C. K. (2013). Adipogenesis of adipose-derived stem cells may be regulated via the cytoskeleton at physiological oxygen levels in vitro. *Stem Cell Research & Therapy, 4*(4), 79. doi:10.1186/scrt230

Schlottmann, I., Ehrhart-Bornstein, M., Wabitsch, M., Bornstein, S., & Lamounier-Zepter, V. (2014). Calcium-dependent release of adipocyte fatty acid binding protein from human adipocytes. *International Journal Of Obesity, 38*(9), 1221.

Selvey, S., Thompson, E., Matthaei, K., Lea, R., Irving, M., & Griffiths, L. (2001). Beta-actin - an unsuitable internal control for RT-PCR. *Mol Cell Probes, 15*(5), 307 - 311.

Sethi, J. K., & Vidal-Puig, A. J. (2007). Thematic review series: adipocyte biology. Adipose tissue function and plasticity orchestrate nutritional adaptation. *Journal of Lipid Research, 48*(6), 1253-1262. doi:10.1194/jlr.R700005-JLR200

Shabalina, I. G., Petrovic, N., de Jong, J. M., Kalinovich, A. V., Cannon, B., & Nedergaard, J. (2013). UCP1 in brite/beige adipose tissue mitochondria is functionally thermogenic. *Cell reports, 5*(5), 1196-1203.

Shi, H., HALVORSEN, Y.-D., ELLIS, P. N., WILKISON, W. O., & ZEMEL, M. B. (2000). Role of intracellular calcium in human adipocyte differentiation. *Physiological genomics, 3*(2), 75-82.

Shi, J., & Kandror, K. V. (2005). Sortilin is essential and sufficient for the formation of Glut4 storage vesicles in 3T3-L1 adipocytes. *Developmental cell, 9*(1), 99-108.

Sokabe, T., Fukumi-Tominaga, T., Yonemura, S., Mizuno, A., & Tominaga, M. J. J. o. B. C. (2010). The TRPV4 channel contributes to intercellular junction formation in keratinocytes. *285*(24), 18749-18758.

Stahl, A., Evans, J. G., Pattel, S., Hirsch, D., & Lodish, H. F. (2002). Insulin causes fatty acid transport protein translocation and enhanced fatty acid uptake in adipocytes. *Developmental cell, 2*(4), 477-488.

Stahl, A., Gimeno, R. E., Tartaglia, L. A., & Lodish, H. F. (2001). Fatty acid transport proteins: a current view of a growing family. *Trends in Endocrinology & Metabolism, 12*(6), 266-273.

Stefan, N., Fritsche, A., Weikert, C., Boeing, H., Joost, H.-G., Häring, H.-U., & Schulze, M. B. (2008). Plasma fetuin-A levels and the risk of type 2 diabetes. *Diabetes, 57*(10), 2762-2767.

Stefan, N., & Häring, H.-U. (2013). The role of hepatokines in metabolism. *Nature Reviews Endocrinology, 9*(3), 144-152.

Storch, J., & Corsico, B. (2008). The emerging functions and mechanisms of mammalian fatty acid-binding proteins. *Annu. Rev. Nutr., 28*, 73-95.

Storch, J., & McDermott, L. (2009). Structural and functional analysis of fatty acid-binding proteins. *Journal of Lipid Research, 50*(Supplement), S126-S131.

Storch, J., & Thumser, A. E. (2010). Tissue-specific functions in the FABP (fatty acid-binding protein) family. *Journal of Biological Chemistry*, jbc. R110. 135210.

Stuart Wood, I., Wang, B., Lorente-Cebrián, S., & Trayhurn, P. (2007). Hypoxia increases expression of selective facilitative glucose transporters (GLUT) and 2-deoxy-d-glucose uptake in human adipocytes. *Biochemical and biophysical research communications, 361*(2), 468-473. doi:https://doi.org/10.1016/j.bbrc.2007.07.032

Sun, K., Kusminski, C. M., & Scherer, P. E. (2011). Adipose tissue remodeling and obesity. *The Journal of clinical investigation, 121*(6), 2094-2101.

Tan, C. Y., & Vidal-Puig, A. (2008). Adipose tissue expandability: the metabolic problems of obesity may arise from the inability to become more obese. In: Portland Press Limited.

Tanaka, T., Hirota, Y., Sohmiya, K.-I., Nishimura, S., & Kawamura, K. (1991). Serum and urinary human heart fatty acid-binding protein in acute myocardial infarction. *Clinical biochemistry, 24*(2), 195-201.

Thery, C., Amigorena, S., Raposo, G., & Clayton, A. (2006). Isolation and characterization of exosomes from cell culture supernatants and biological fluids. *Curr Protoc Cell Biol, Chapter 3*, Unit 3.22. doi:10.1002/0471143030.cb0322s30

Thorneloe, K., Sulpizio, A., Lin, Z., Figueroa, D., Clouse, A., McCafferty, G., . . . Evans, L. (2008). GSK1016790A, a novel and potent TRPV4 channel agonist induces urinary bladder contraction and hyperactivity: part I. *J Pharmacol Exp Ther, 326*, 432-442.

Trayhurn, P. (2007). Adipocyte biology. *Obesity reviews, 8*, 41-44.

Trayhurn, P. (2013). Hypoxia and adipose tissue function and dysfunction in obesity. *Physiological reviews, 93*(1), 1-21.
Trayhurn, P., Wang, B., & Wood, I. S. (2008). Hypoxia in adipose tissue: a basis for the dysregulation of tissue function in obesity? *British Journal of Nutrition, 100*(2), 227-235.
Trayhurn, P., & Wood, I. S. (2004). Adipokines: inflammation and the pleiotropic role of white adipose tissue. *British Journal of Nutrition, 92*(3), 347-355.
Trepanowski, J., Mey, J., & Varady, K. (2015). Fetuin-A: a novel link between obesity and related complications. *International journal of obesity, 39*(5), 734.
Ullah, M., Stich, S., Häupl, T., Eucker, J., Sittinger, M., & Ringe, J. (2013). Reverse differentiation as a gene filtering tool in genome expression profiling of adipogenesis for fat marker gene selection and their analysis. *PloS one, 8*(7), e69754.
Uyeda, K., Yamashita, H., & Kawaguchi, T. (2002). Carbohydrate responsive element-binding protein (ChREBP): a key regulator of glucose metabolism and fat storage. *Biochemical pharmacology, 63*(12), 2075-2080.
van Dam, R. M., & Hu, F. B. (2007). Lipocalins and insulin resistance: etiological role of retinol-binding protein 4 and lipocalin-2? *Clinical chemistry, 53*(1), 5-7.
van der Eerden, B. C., Koek, W. N. H., Roschger, P., Zillikens, M. C., Waarsing, J. H., van der Kemp, A., . . . Hoenderop, J. G. (2016). Lifelong challenge of calcium homeostasis in male mice lacking TRPV5 leads to changes in bone and calcium metabolism. *Oncotarget, 7*(18), 24928.
Vergara, E. J. S., Dela Cruz, J., Kim, C. M., & Hwang, S. G. (2016). Increased adipocyte differentiation may be mediated by extracellular calcium levels through effects on calreticulin and peroxisome proliferator activated receptor gamma expression in intramuscular stromal vascular cells isolated from Hanwoo beef cattle. *Italian Journal of Animal Science, 15*(2), 256-263.
Vigouroux, C., Caron-Debarle, M., Le Dour, C., Magré, J., & Capeau, J. (2011). Molecular mechanisms of human lipodystrophies: from adipocyte lipid droplet to oxidative stress and lipotoxicity. *The international journal of biochemistry & cell biology, 43*(6), 862-876.
Villeneuve, J., Bassaganyas, L., Lepreux, S., Chiritoiu, M., Costet, P., Ripoche, J., . . . Schekman, R. (2017). Unconventional secretion of FABP4 by endosomes and secretory lysosomes. *The Journal of Cell Biology*. doi:10.1083/jcb.201705047
Vincent, F., & AJ Duncton, M. (2011). TRPV4 agonists and antagonists. *Current topics in medicinal chemistry, 11*(17), 2216-2226.
Voets, T., Prenen, J., Vriens, J., Watanabe, H., Janssens, A., Wissenbach, U., . . . Nilius, B. (2002). Molecular determinants of permeation through the cation channel TRPV4. *Journal of Biological Chemistry, 277*(37), 33704-33710.
Wajchenberg, B. L. (2000). Subcutaneous and visceral adipose tissue: their relation to the metabolic syndrome. *Endocrine reviews, 21*(6), 697-738.
Wang, B., Wood, I. S., & Trayhurn, P. (2008). Hypoxia induces leptin gene expression and secretion in human preadipocytes: differential effects of hypoxia on adipokine expression by preadipocytes. *Journal of Endocrinology, 198*(1), 127-134.
Wang, Y., Lam, K. S., Kraegen, E. W., Sweeney, G., Zhang, J., Tso, A. W., . . . Hoo, R. L. (2007). Lipocalin-2 is an inflammatory marker closely associated with obesity, insulin resistance, and hyperglycemia in humans. *Clinical chemistry, 53*(1), 34-41.
Watson, R. T., Kanzaki, M., & Pessin, J. E. (2004). Regulated membrane trafficking of the insulin-responsive glucose transporter 4 in adipocytes. *Endocrine reviews, 25*(2), 177-204.

Weisberg, S. P., McCann, D., Desai, M., Rosenbaum, M., Leibel, R. L., & Ferrante, A. W., Jr. (2003). Obesity is associated with macrophage accumulation in adipose tissue. *The Journal of clinical investigation, 112*(12), 1796-1808. doi:10.1172/jci19246

White, U. A., & Stephens, J. M. (2010). Transcriptional factors that promote formation of white adipose tissue. *Molecular and cellular endocrinology, 318*(1-2), 10-14.

Willette, R. N., Bao, W., Nerurkar, S., Yue, T.-l., Doe, C. P., Stankus, G., . . . Fishman, C. E. (2008). Systemic activation of the transient receptor potential vanilloid subtype 4 channel causes endothelial failure and circulatory collapse: Part 2. *Journal of Pharmacology and Experimental Therapeutics, 326*(2), 443-452.

Worrall, D. S., & Olefsky, J. M. (2002). The effects of intracellular calcium depletion on insulin signaling in 3T3-L1 adipocytes. *Molecular endocrinology, 16*(2), 378-389.

Wu-Wong, J. R., Berg, C. E., Wang, J., Chiou, W. J., & Fissel, B. (1999). Endothelin stimulates glucose uptake and GLUT4 translocation via activation of endothelin ETA receptor in 3T3-L1 adipocytes. *Journal of Biological Chemistry, 274*(12), 8103-8110.

Wu, L. E., Samocha-Bonet, D., Whitworth, P. T., Fazakerley, D. J., Turner, N., Biden, T. J., . . . Cantley, J. (2014). Identification of fatty acid binding protein 4 as an adipokine that regulates insulin secretion during obesity. *Molecular metabolism, 3*(4), 465-473.

Xu, A., Wang, Y., Xu, J. Y., Stejskal, D., Tam, S., Zhang, J., . . . Lam, K. S. (2006). Adipocyte fatty acid–binding protein is a plasma biomarker closely associated with obesity and metabolic syndrome. *Clinical chemistry, 52*(3), 405-413.

Xu, H., Barnes, G. T., Yang, Q., Tan, G., Yang, D., Chou, C. J., . . . Chen, H. (2003). Chronic inflammation in fat plays a crucial role in the development of obesity-related insulin resistance. *The Journal of clinical investigation, 112*(12), 1821-1830. doi:10.1172/jci19451

Yamaji, R., Fujita, K., Takahashi, S., Yoneda, H., Nagao, K., Masuda, W., . . . Nakano, Y. (2003). Hypoxia up-regulates glyceraldehyde-3-phosphate dehydrogenase in mouse brain capillary endothelial cells: involvement of Na+/Ca2+ exchanger. *Biochimica et Biophysica Acta (BBA) - Molecular Cell Research, 1593*(2), 269-276. doi:https://doi.org/10.1016/S0167-4889(02)00397-X

Yan, Q.-W., Yang, Q., Mody, N., Graham, T. E., Hsu, C.-H., Xu, Z., . . . Rosen, E. D. (2007). The adipokine lipocalin 2 is regulated by obesity and promotes insulin resistance. *Diabetes, 56*(10), 2533-2540.

Yang, Y., Chen, Y., Zhang, F., Zhao, Q., & Zhong, H. J. I. J. o. H. (2015). Increased anti-tumour activity by exosomes derived from doxorubicin-treated tumour cells via heat stress. *31*(5), 498-506.

Ye, L. (2013). *Identification of TRPV4 as a Regulator of Adipose Oxidative Metabolism, Inflammation and Energy Homeostasis by a Chemical Biology Approach.*

Ye, L., Kleiner, S., Wu, J., Sah, R., Gupta, R. K., Banks, A. S., . . . Mepani, R. J. (2012). TRPV4 is a regulator of adipose oxidative metabolism, inflammation, and energy homeostasis. *Cell, 151*(1), 96-110.

Yin, J., Gao, Z., He, Q., Zhou, D., Guo, Z., & Ye, J. (2009). Role of hypoxia in obesity-induced disorders of glucose and lipid metabolism in adipose tissue. *American Journal of Physiology-Endocrinology and Metabolism, 296*(2), E333-E342.

Zhang, J., Wu, Y., Zhang, Y., LeRoith, D., Bernlohr, D. A., & Chen, X. (2008). The role of lipocalin 2 in the regulation of inflammation in adipocytes and macrophages. *Molecular endocrinology, 22*(6), 1416-1426.

Zhang, L. L., Yan Liu, D., Ma, L. Q., Luo, Z. D., Cao, T. B., Zhong, J., . . . Tepel, M. (2007). Activation of Transient Receptor Potential Vanilloid Type-1 Channel Prevents Adipogenesis and Obesity. *Circulation Research, 100*(7), 1063-1070. doi:10.1161/01.RES.0000262653.84850.8b

Zhang, Y.-Y., Li, X., Qian, S.-W., Guo, L., Huang, H.-Y., He, Q., . . . Tang, Q.-Q. (2011). Transcriptional activation of histone H4 by C/EBPβ during the mitotic clonal expansion of 3T3-L1 adipocyte differentiation. *Molecular biology of the cell, 22*(13), 2165-2174.

Zhang, Y., Foncea, R., Deis, J. A., Guo, H., Bernlohr, D. A., & Chen, X. (2014). Lipocalin 2 expression and secretion is highly regulated by metabolic stress, cytokines, and nutrients in adipocytes. *PloS one, 9*(5), e96997.

Zhao, H., Shang, Q., Pan, Z., Bai, Y., Li, Z., Zhang, H., . . . Wang, Q. (2018). Exosomes From Adipose-Derived Stem Cells Attenuate Adipose Inflammation and Obesity Through Polarizing M2 Macrophages and Beiging in White Adipose Tissue. *67*(2), 235-247. doi:10.2337/db17-0356 %J Diabetes

Zhao, P., Elks, C. M., & Stephens, J. M. (2014). The induction of lipocalin-2 expression in vivo and in vitro. *Journal of Biological Chemistry*, jbc. M113. 532234.

Zhou, S., Lechpammer, S., Greenberger, J., & Glowacki, J. (2005). Hypoxia inhibition of adipocytogenesis in human bone marrow stromal cells requires TGFbeta/Smad3 signaling. *Journal of Biological Chemistry*.

Zhuang, X., Xiang, X., Grizzle, W., Sun, D., Zhang, S., Axtell, R. C., . . . Steinman, L. J. M. T. (2011). Treatment of brain inflammatory diseases by delivering exosome encapsulated anti-inflammatory drugs from the nasal region to the brain. *19*(10), 1769-1779.